

THESE TERMS GOVERN YOUR USE OF THIS DOCUMENT

Your use of this Ontario Geological Survey document (the “Content”) is governed by the terms set out on this page (“Terms of Use”). By downloading this Content, you (the “User”) have accepted, and have agreed to be bound by, the Terms of Use.

Content: This Content is offered by the Province of Ontario’s *Ministry of Northern Development and Mines* (MNDM) as a public service, on an “as-is” basis. Recommendations and statements of opinion expressed in the Content are those of the author or authors and are not to be construed as statement of government policy. You are solely responsible for your use of the Content. You should not rely on the Content for legal advice nor as authoritative in your particular circumstances. Users should verify the accuracy and applicability of any Content before acting on it. MNDM does not guarantee, or make any warranty express or implied, that the Content is current, accurate, complete or reliable. MNDM is not responsible for any damage however caused, which results, directly or indirectly, from your use of the Content. MNDM assumes no legal liability or responsibility for the Content whatsoever.

Links to Other Web Sites: This Content may contain links, to Web sites that are not operated by MNDM. Linked Web sites may not be available in French. MNDM neither endorses nor assumes any responsibility for the safety, accuracy or availability of linked Web sites or the information contained on them. The linked Web sites, their operation and content are the responsibility of the person or entity for which they were created or maintained (the “Owner”). Both your use of a linked Web site, and your right to use or reproduce information or materials from a linked Web site, are subject to the terms of use governing that particular Web site. Any comments or inquiries regarding a linked Web site must be directed to its Owner.

Copyright: Canadian and international intellectual property laws protect the Content. Unless otherwise indicated, copyright is held by the Queen’s Printer for Ontario.

It is recommended that reference to the Content be made in the following form:

Péloquin, A.S. and Piercey, S.J. 2005. Geology and base metal mineralization in Ben Nevis, Clifford and Katrine townships: Discover Abitibi Initiative; Ontario Geological Survey, Open File Report 6161, 86p.

Use and Reproduction of Content: The Content may be used and reproduced only in accordance with applicable intellectual property laws. *Non-commercial* use of unsubstantial excerpts of the Content is permitted provided that appropriate credit is given and Crown copyright is acknowledged. Any substantial reproduction of the Content or any *commercial* use of all or part of the Content is prohibited without the prior written permission of MNDM. Substantial reproduction includes the reproduction of any illustration or figure, such as, but not limited to graphs, charts and maps. Commercial use includes commercial distribution of the Content, the reproduction of multiple copies of the Content for any purpose whether or not commercial, use of the Content in commercial publications, and the creation of value-added products using the Content.

Contact:

FOR FURTHER INFORMATION ON	PLEASE CONTACT:	BY TELEPHONE:	BY E-MAIL:
The Reproduction of Content	MNDM Publication Services	Local: (705) 670-5691 Toll Free: 1-888-415-9845, ext. 5691 (inside Canada, United States)	Pubsales@ndm.gov.on.ca
The Purchase of MNDM Publications	MNDM Publication Sales	Local: (705) 670-5691 Toll Free: 1-888-415-9845, ext. 5691 (inside Canada, United States)	Pubsales@ndm.gov.on.ca
Crown Copyright	Queen’s Printer	Local: (416) 326-2678 Toll Free: 1-800-668-9938 (inside Canada, United States)	Copyright@gov.on.ca



**Ontario Geological Survey
Open File Report 6161**

**Geology and Base Metal
Mineralization in Ben Nevis,
Clifford and Katrine
Townships:
Discover Abitibi Initiative**

2005



ONTARIO GEOLOGICAL SURVEY

Open File Report 6161

Geology and Base Metal Mineralization in Ben Nevis, Clifford and Katrine Townships: Discover Abitibi Initiative

by

A.S. Péroquin and S.J. Piercey

2005

Parts of this publication may be quoted if credit is given. It is recommended that reference to this publication be made in the following form:

Péroquin, A.S. and Piercey, S.J. 2005. Geology and base metal mineralization in Ben Nevis, Clifford and Katrine townships: Discover Abitibi Initiative; Ontario Geological Survey, Open File Report 6161, 86p.



Discover Abitibi Initiative

The Discover Abitibi Initiative is a regional, cluster economic development project based on geoscientific investigations of the western Abitibi greenstone belt. The initiative, centred on the Kirkland Lake and Timmins mining camps, will complete 19 projects developed and directed by the local stakeholders. FedNor, Northern Ontario Heritage Fund Corporation, municipalities and private sector investors have provided the funding for the initiative.

Initiative Découvrons l'Abitibi

L'initiative Découvrons l'Abitibi est un projet de développement économique régional dans une grappe d'industries, projet fondé sur des études géoscientifiques de la ceinture de roches vertes de l'Abitibi occidental. Cette initiative, centrée sur les zones minières de Kirkland Lake et de Timmins, mènera à bien 19 projets élaborés et dirigés par des intervenants locaux. FedNor, la Société de gestion du Fonds du patrimoine du Nord de l'Ontario, municipalités et des investisseurs du secteur privé ont fourni les fonds de cette initiative.



Canada



Ontario

Northern Ontario
Heritage Fund

Fonds du patrimoine
du Nord de l'Ontario

© Queen's Printer for Ontario, 2005.

Open File Reports of the Ontario Geological Survey are available for viewing at the Mines Library in Sudbury, at the Mines and Minerals Information Centre in Toronto, and at the regional Mines and Minerals office whose district includes the area covered by the report (see below).

Copies can be purchased at Publication Sales and the office whose district includes the area covered by the report. Although a particular report may not be in stock at locations other than the Publication Sales office in Sudbury, they can generally be obtained within 3 working days. All telephone, fax, mail and e-mail orders should be directed to the Publication Sales office in Sudbury. Use of VISA or MasterCard ensures the fastest possible service. Cheques or money orders should be made payable to the *Minister of Finance*.

Mines and Minerals Information Centre (MMIC) Macdonald Block, Room M2-17 900 Bay St. Toronto, Ontario M7A 1C3	Tel: (416) 314-3800
Mines Library 933 Ramsey Lake Road, Level A3 Sudbury, Ontario P3E 6B5	Tel: (705) 670-5615
Publication Sales 933 Ramsey Lake Rd., Level A3 Sudbury, Ontario P3E 6B5	Tel: (705) 670-5691(local) 1-888-415-9845(toll-free) Fax: (705) 670-5770 E-mail: pubsales@ndm.gov.on.ca

Regional Mines and Minerals Offices:

Kenora - Suite 104, 810 Robertson St., Kenora P9N 4J2
Kirkland Lake - 10 Government Rd. E., Kirkland Lake P2N 1A8
Red Lake - Box 324, Ontario Government Building, Red Lake P0V 2M0
Sault Ste. Marie - 70 Foster Dr., Ste. 200, Sault Ste. Marie P6A 6V8
Southern Ontario - P.O. Bag Service 43, 126 Old Troy Rd., Tweed K0K 3J0
Sudbury - Level B3, 933 Ramsey Lake Rd., Sudbury P3E 6B5
Thunder Bay - Suite B002, 435 James St. S., Thunder Bay P7E 6S7
Timmins - Ontario Government Complex, P.O. Bag 3060, Hwy. 101 East, South Porcupine P0N 1H0
Toronto - MMIC, Macdonald Block, Room M2-17, 900 Bay St., Toronto M7A 1C3

This report has not received a technical edit. Discrepancies may occur for which the Ontario Ministry of Northern Development and Mines does not assume any liability. Source references are included in the report and users are urged to verify critical information. Recommendations and statements of opinions expressed are those of the author or authors and are not to be construed as statements of government policy.

If you wish to reproduce any of the text, tables or illustrations in this report, please write for permission to the Team Leader, Publication Services, Ministry of Northern Development and Mines, 933 Ramsey Lake Road, Level B4, Sudbury, Ontario P3E 6B5.

Cette publication est disponible en anglais seulement.

Parts of this report may be quoted if credit is given. It is recommended that reference be made in the following form:

Péloquin, A.S. and Piercey, S.J. 2005. Geology and base metal mineralization in Ben Nevis, Clifford and Katrine townships: Discover Abitibi Initiative; Ontario Geological Survey, Open File Report 6161, 86p.

Contents

Abstract	xi
Introduction	1
Location and Access	1
Acknowledgments.....	1
Previous Geological Work.....	3
Objectives and Methods.....	4
Geological Setting	5
Geology of Katrine, Ben Nevis and Clifford Townships.....	8
Katrine Township.....	8
Volcanic Rocks.....	8
Intrusive Rocks.....	9
Ben Nevis Township.....	11
Volcanic Rocks.....	11
Intrusive Rocks.....	13
Clifford Township.....	15
Volcanic Rocks.....	15
Intrusive Rocks.....	16
Geochemistry.....	18
Volcanic Rocks	18
Mafic to Intermediate Volcanic Rocks	23
Felsic Volcanic Rocks	31
Intrusive Rocks	36
High-Level Synvolcanic Intrusions	36
Intrusions.....	38
Summary	40
Alteration and Mineralization Styles	40
Summary	44
Discussion and Conclusion.....	46
References	48
Appendix 1: Major, trace and rare earth element data for Ben Nevis and Katrine townships.....	55
Appendix 2: Major, trace and rare earth element data for Clifford Township.....	75
Metric Conversion Table	86

FIGURES

1.	Location map for Clifford, Ben Nevis and Katrine townships.....	2
2.	Geological map of the Abitibi Subprovince of the Archean Superior Province, showing the Blake River Group and the bounding faults	3
3.	Geological assemblage map for the Abitibi Subprovince in Ontario.....	5
4.	Map of the Blake River Group subgroups and adjacent volcanic stratigraphy	6
5.	Geological map of the study area.....	7
6.	Grey-shaded second vertical derivative magnetic maps for Clifford, Ben Nevis and Katrine townships, showing major structures	10
7.	Grey-shaded gravity map of Clifford and Ben Nevis townships, showing the major structures and intrusions.....	14
8.	Geological map of Clifford Township	17
9.	SiO ₂ content of the volcanic rocks in the study area: a) SiO ₂ wt % histogram; b) linear plot of SiO ₂ wt %	19
10.	Rock classification diagram for a) the volcanic rocks; b) the high-level synvolcanic intrusions; c) the intrusive rocks	20
11.	AFM diagram for a) the volcanic rocks; b) the high-level synvolcanic intrusions; c) the intrusive rocks..	21
12.	Alteration box plot for a) the volcanic rocks; b) the high-level synvolcanic intrusions; c) the intrusive rocks.....	22
13.	MgO wt % versus FeO _{total} wt % for a) the volcanic rocks; b) the high-level synvolcanic intrusions; c) the intrusive rocks	24
14.	TiO ₂ wt % versus SiO ₂ wt % for a) the volcanic rocks; b) the high-level synvolcanic intrusions; c) the intrusive rocks	25
15.	Al ₂ O ₃ wt % versus SiO ₂ wt % for a) the volcanic rocks; b) the high-level synvolcanic intrusions; c) the intrusive rocks.....	26
16.	Zr/Y versus Y ppm for a) the volcanic rocks; b) the high-level synvolcanic intrusions; c) the intrusive rocks.....	27
17.	(La/Yb) _{cn} versus Yb _{cn} for a) the volcanic rocks; b) the high-level synvolcanic intrusions; c) the intrusive rocks.....	28
18.	Yb _{cn} versus a) SiO ₂ wt % and b) MgO wt % for the volcanic rocks	29
19.	Chondrite-normalized spider plots for the mafic-intermediate volcanic rocks	30
20.	a) (La/Yb) _{cn} versus Yb _{cn} diagram for the felsic volcanic rocks; b) Zr/Y versus (La/Yb) _{cn} diagram for the felsic volcanic rocks; c) La _{cn} versus Yb _{cn} diagram for the felsic volcanic rocks.....	32
21.	Chondrite-normalized spider plots for the felsic volcanic rocks.....	33
22.	Calculated Zr saturation temperature versus Zr/Y for a) the felsic volcanic rocks; b) the felsic high-level synvolcanic intrusions.....	35
23.	Chondrite-normalized spider plots for the high-level synvolcanic intrusions.....	37

24. Chondrite-normalized spider plots for the intrusive rocks	39
25. Schematic diagrams of the a) Ben Nevis–Clifford stratovolcano in relationship to the Misema mafic lava plain and the Noranda cauldron, b) the Ben Nevis–Clifford stratovolcano indicating the possible area of present exposure, and c) the Noranda cauldron indicating the possible area of present exposure ..	47

PHOTOS

1. Katrine Township volcanic and intrusive rocks: a) heterolithic andesite tuff breccia; b) jasper fragment in the heterolithic andesite tuff breccia; c) xenoliths in the multi-phase alkalic stock.....	8
2. Ben Nevis Township volcanic rocks: a) rhyolite dyke intruded into andesite, Interprovincial South showing; b) lapilli and bedded tuff, Canagau rhyolite; c) polygonally jointed rhyolite, Canagau rhyolite; d) tectonic overprinting of pyroclastic rhyolite producing pseudobreccia, Canagau rhyolite; e) epidotized and silicified andesite pillows, north of the Murdoch Creek–Kennedy Lake fault; f) pyroclastic rhyolite showing reaction rim on a fragment, north of the Murdoch Creek–Kennedy Lake fault.....	12
3. Ben Nevis Township intrusive and volcanic rocks: a) multiple injection borders in andesite dyke intruded into rhyolite; b) network silicification of andesite near synvolcanic rhyolite dykes; c) mafic fragment in deformed phase of QFP plug at the Ben Nevis–Katrine township boundary; d) monolithic carapace breccia of rhyolite with polygonally jointed, flow-banded rhyolite clasts	15
4. a) Typical recrystallized basaltic andesite of the Blake River Group; b) pillow lava with chlorite alteration, silicification of hyaloclastite, and pyrite-chalcopyrite; c) highly silicified pillows with pyrite in interpillow hyaloclastite, Interprovincial South showing; d) rhyolite breccia with pyrite in the breccia matrix, Interprovincial North showing; e) highly chloritized rhyolite, Interprovincial North showing; f) breccia pipe occurrence from the Brett-Tretheway (Croxall) prospect	41

TABLES

1. Geochemical criteria for the classification of rhyolites into F-types.....	31
2. Calculated Zr saturation temperature for the rhyolites.....	34
3. Calculated Zr saturation temperature for the high-level synvolcanic intrusions	38
4. Mineral prospects and occurrences in the study area	45

MAP

P.3543–Revised: Precambrian Geology of Ben Nevis and Katrine Townships	back pocket
--	-------------

Abstract

Katrine, Ben Nevis and Clifford townships are part of the Archean Blake River Group of the Abitibi Subprovince of the Superior Province of Canada. The Blake River Group hosts one of the most significant mining camps in Canada—the Noranda camp—where the origin, localization, and distribution of deposits are relatively well understood. In contrast, very little is known about the Blake River Group in Ontario; hence, this subproject of the Discover Abitibi Initiative was conceived to improve our knowledge of the Blake River Group in Ontario and to use that knowledge to assess its potential for VMS mineralization.

The Blake River Group is divided into three subgroups: the Garrison, the Misema and the Noranda. The volcanic rocks of Katrine, Ben Nevis and Clifford townships belong to the Misema subgroup, which in Ontario ranges in age from 2701 ± 2 Ma in Pontiac Township to 2696.6 ± 1.3 Ma in Ben Nevis Township. This spans the known ages for the Blake River Group in Québec (2701 ± 1 Ma to 2694 ± 2 Ma).

Subaqueous andesite flows are the dominant rock type in the study area. In Katrine Township, pyroclastic rocks are rare, and felsic volcanic rocks even rarer. In Ben Nevis and Clifford townships, there is a spectrum of subaqueous volcanic rocks from basalt to rhyolite. Both flow and pyroclastic facies occur in all rock types, but the felsic volcanic rocks are dominantly pyroclastic with rare flow or dome facies. The large pyroclastic component of the Ben Nevis–Clifford volcanic centre suggests that it may be a subaqueous composite stratovolcano constructed on a mafic to intermediate volcanic “floor” represented by the Misema mafic to intermediate volcanic rocks in Katrine Township. The increase in pyroclastic rocks, and the pumiceous and scoriaceous nature of some of the fragments, indicates shallow depth of emplacement for the Ben Nevis–Clifford volcano.

High-level synvolcanic dykes, which can only be distinguished from extrusive rocks by their cross-cutting relationships, occur in all rock types throughout the study area, as do mafic-intermediate dykes and irregular masses, which are comagmatic with the Blake River Group volcanism.

The volcanism in the study area is unimodal (andesite dominant), and there are no tholeiites in the area. Different populations of mafic-intermediate and felsic volcanic rocks are observed in the study area. Mafic-intermediate volcanic rocks with lower Yb_{cn} have SiO_2 and MgO wt % contents within the range of the higher Yb_{cn} population, and cannot be precursors to the magmas with higher Yb_{cn} . Felsic volcanic rocks with $Zr/Y > 5$ generally have higher calculated zircon saturation temperatures.

VMS-style alteration and mineralization occur in the study area, indicating that a synvolcanic hydrothermal system existed. However, the mineralization is concentrated in synvolcanic dykes as veins or in the multiple injection margins, suggesting that the fluids were channelized within the dykes. This indicates that the present exposure may represent the feeder zone of the hydrothermal system. The area is structurally complex and the influence of faults and deformation zones on the stratigraphy of the area must be determined, as should the effect of possible folding.

A porphyry system related to the Clifford stock is recognized in Clifford Township, opening up a new avenue for exploration. A gravity low in Ben Nevis Township, which is similar to that corresponding to the Clifford stock in Clifford Township, suggests a “Clifford-type” intrusion at depth, and the occurrence of Clifford-event porphyry dykes in Ben Nevis Township confirms that the Clifford intrusive event extends south of the Murdoch Creek–Kennedy Lake fault. These other occurrences of Clifford-type intrusive activity have not been fully evaluated for porphyry Cu-Mo-Au mineralization and thus represent a potential new target in Ben Nevis Township.

Geology and Base Metal Mineralization in Ben Nevis, Clifford and Katrine Townships: Discover Abitibi Initiative

A.S. Péroquin¹ and S.J. Piercey^{1,2}
Ontario Geological Survey
Open File Report 6161
2005

¹Mineral Exploration Research Centre, Laurentian University
speloquin@laurentian.ca

²Department of Earth Sciences, Laurentian University
spiercey@laurentian.ca

Introduction

Mapping and sampling transects were undertaken in Ben Nevis, Katrine and Clifford townships (Figure 1) as part of the Discover Abitibi Initiative under 2 subprojects: the Volcanogenic Massive Sulphide (VMS) Deposits 3 subproject; and the Intrusion subproject. The area is part of the Blake River Group (Figure 2), which hosts one of the most significant mining camps in Canada, the Noranda camp, and is one of the type localities for Cu-Zn VMS deposits (Sangster 1972; Hutchinson 1973; Franklin et al. 1981). In 1999, the cumulative production from the 25 past-producing and active Cu-Zn mines in the Noranda area was given by Hannington et al. (1999, their Table 1) as 263 million tonnes. Within the mining camp, the origin, localization, and distribution of deposits are relatively well understood. The Blake River Group in Ontario, and in Ben Nevis Township in particular, has been of interest to mineral exploration companies due to the presence of felsic volcanic centres in a dominantly andesitic regime and of known mineralized showings. However, little modern geological, geochemical, or isotopic studies have been undertaken in the area, in contrast to the Blake River Group in the Noranda camp in Québec. This subproject was conceived to improve our knowledge of the area and to relate that knowledge to the potential for VMS or other mineralization in the Blake River Group in Ontario.

LOCATION AND ACCESS

Ben Nevis and Clifford townships are located in the District of Cochrane; Katrine Township is in the District of Timiskaming. Ben Nevis and Katrine townships are 10 km north of the town of Larder Lake via the Larder Lake Station road, which intersects Highway 66 east of Larder Lake. Many logging roads in various states of repair and all-terrain-vehicle trails provide access from the Larder Lake Station road (Figure 1). Although watercrafts were not used in this project, some of the more remote areas could be accessed by river and/or lake. Clifford Township is located 20 km north of the town of Larder Lake and is accessible via logging roads off of the Esker Lakes Park Road (Highway 672) intersecting Highway 66 approximately 13 km west of Larder Lake (Figure 1).

The lowest elevation measured in the area, using a Garmin eTrex™ GPS, was 273 m; the highest elevation measured was 454 m. The highest point, Pushkin Hill, is approximately 490 m above sea level. In spite of the relief, outcrop is generally poor, due to forest cover. The exception to this are logged-out areas where outcrops are easily accessible and commonly mechanically stripped.

ACKNOWLEDGMENTS

The Discover Abitibi Initiative was funded by the Timmins Economic Development Corporation, which in turn received financial backing from FedNor, Northern Ontario Heritage Corporation and private sector investors. We thank the Discover Abitibi Research Group in its entirety, and particularly Drs. John Ayer and Phil Thurston for the conception of this project and their support logistically, scientifically and morally. The project was administered by the Mineral Exploration Research Centre at Laurentian University, and we thank Natalie Lafleur-Roy for handling all things administrative. Doug Hunter and the Wallbridge Mining Ltd. geological and technical staff are thanked for their assistance and support throughout this project. They have supplied property access, materials (specifically digitalized maps, air and satellite photos, and access to drill core), and scientific discussion and inspiration. S. Piercey is also supported by a Discovery Grant from the Natural Sciences and Engineering Research Council.

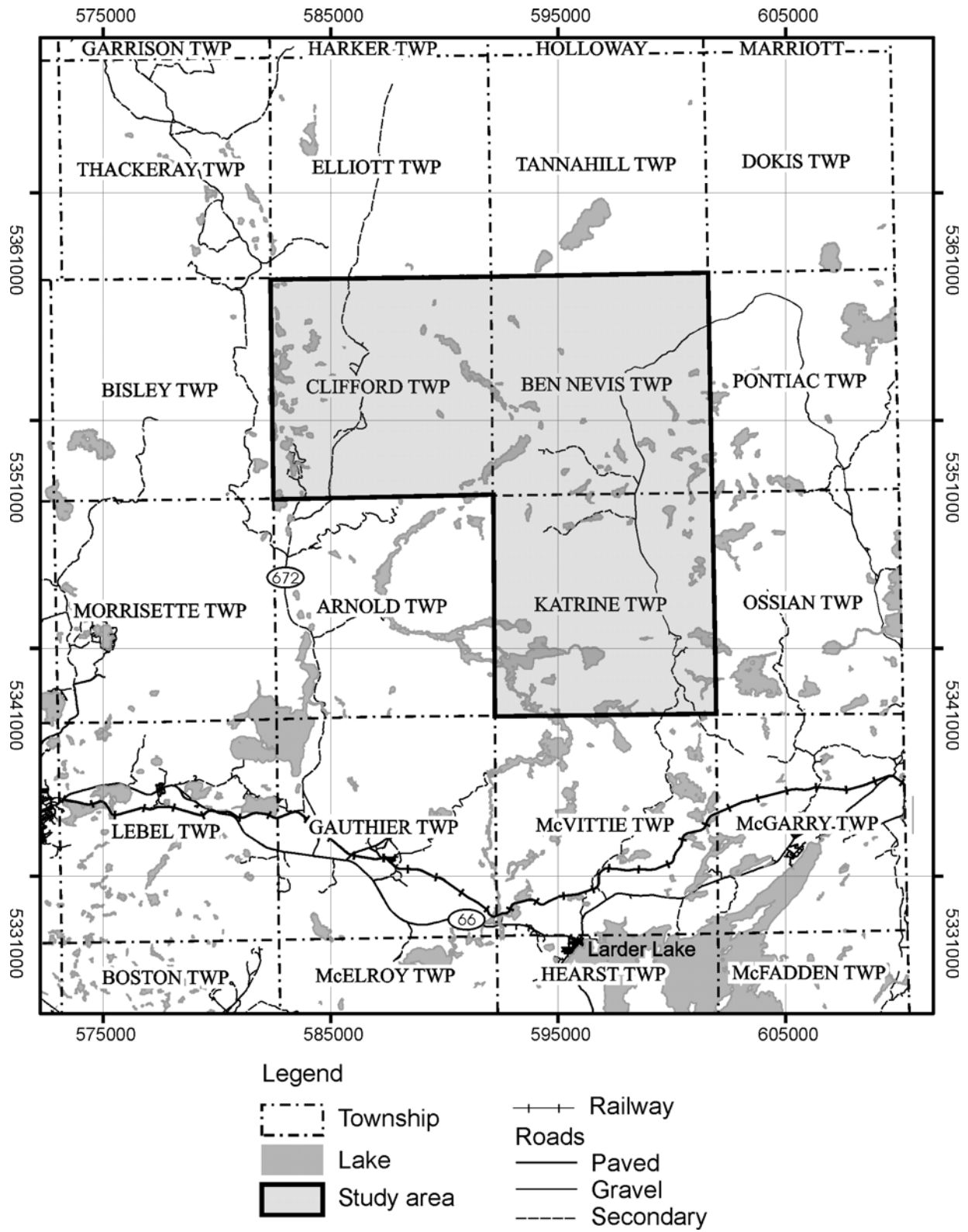


Figure 1. Location map for Clifford, Ben Nevis and Katrine townships.

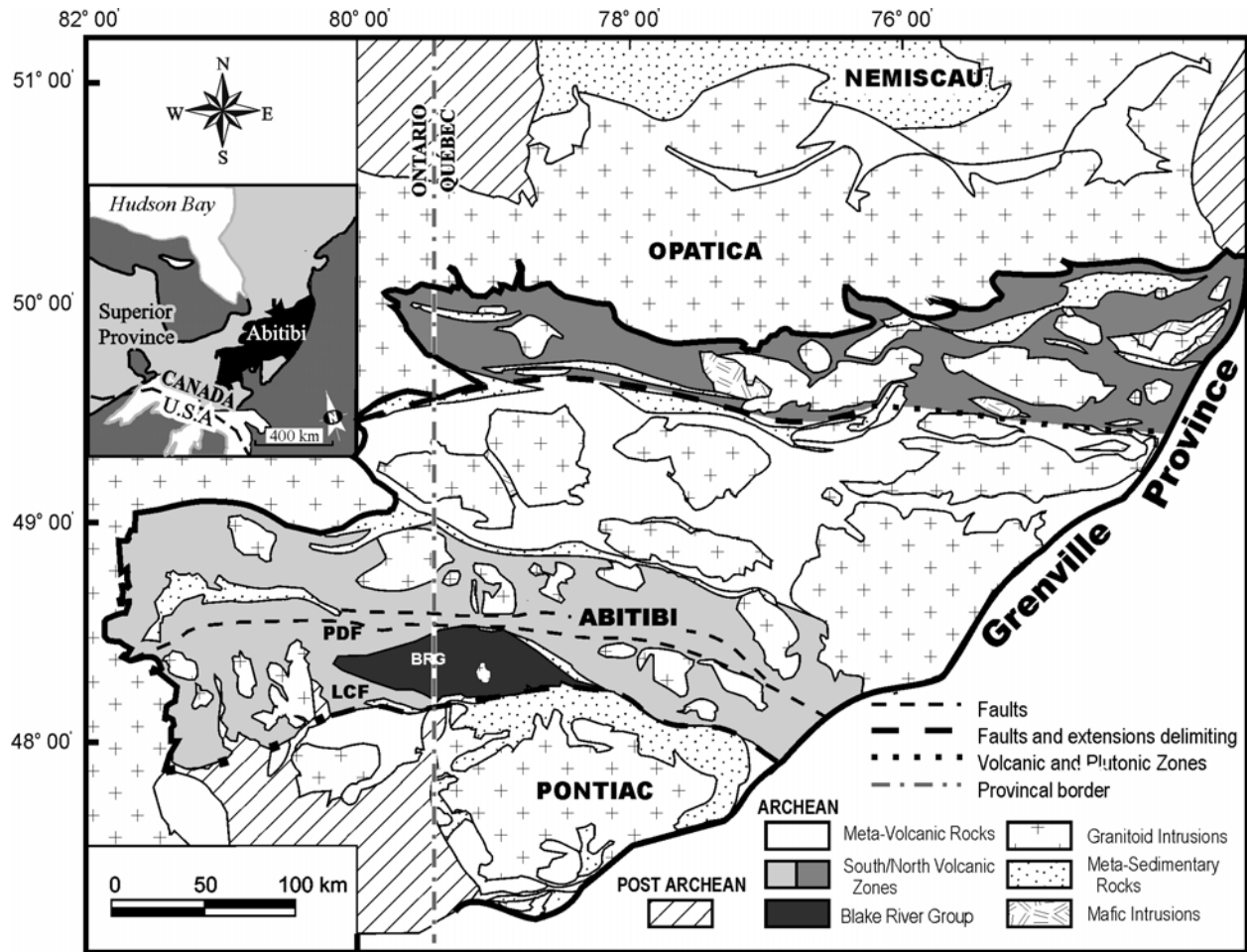


Figure 2. Geological map of the Abitibi Subprovince of the Archean Superior Province, showing the Blake River Group (BRG) and the bounding faults (LCF: Larder Lake–Cadillac fault; PDF: Porcupine–Destor fault).

Previous Geological Work

Katrine Township was first mapped in the 1920s by Knight (1920a, 1920b: map 29e) and Gledhill (1928a, 1928b: map 37g). Both of those maps were considered reconnaissance in nature and Katrine Township was systematically mapped for the Ontario Geological Survey by Hogg (1964a, 1964b: map 2061). The Ben Nevis–Clifford township area was first studied by Wilson (1901a, 1901b). The first reconnaissance mapping was undertaken by Knight (1920a, 1920b), with a second reconnaissance survey completed by Gledhill (1928). Early regional studies include the Goodwin (1977, 1979) and Baragar (1968) studies of the volcanology, stratigraphy and geochemistry, the Ridler (1970) study of the mineralization, and the Jolly (1977) study of the relationship between the volcanic and intrusive rocks. Systematic mapping of Ben Nevis and Clifford townships was performed by Jensen (1975a, 1975b: map 2283), and Wolfe (1977) studied the VMS metallogeny of Ben Nevis Township. Jensen and Langford (1985) produced a stratigraphic synthesis of the Kirkland Lake area, including Ben Nevis and Clifford townships, and Grunsky (1986, 1988) undertook a lithochemical study of Ben Nevis and Clifford townships. More recently, regional hydrothermal alteration studies including mineral chemical studies (Hannington and Kjarsgaard 1998), stable isotope (Taylor and Timbal 1998) studies, and a study of the

Clifford stock as a VMS-related synvolcanic intrusion (Galley 1998), were undertaken as part of the CAMIRO project: “The Use of Regional-scale Alteration Zones and Subvolcanic Intrusions in the Exploration for Volcanic-associated Massive Sulphide Deposits” (Bailes et al. 1998).

OBJECTIVES AND METHODS

The goal of the Blake River Group VMS Subproject of the Discover Abitibi Initiative is to reach a better understanding of the volcanic stratigraphy in Ben Nevis and Katrine townships, and relate this knowledge to the environment of formation of the volcanic sequence and the mineral potential of the Blake River Group. Mapping and sampling transects were undertaken across the stratigraphy. A concurrent study on the Clifford stock and the surrounding volcanic stratigraphy was undertaken as part of the Discover Abitibi Intrusion Subproject, and is reported in MacDonald et al. (2005). Data from the volcanic rocks examined in that study are, however, incorporated here.

Field work was conducted in Ben Nevis and Katrine townships by S. Péloquin over an 8 week period in the summer of 2003 and for 5 days during the summer of 2004. S. Piercey mapped the Clifford stock and surrounding volcanic rocks over 4 weeks in the summer of 2003, and examined and sampled drill core provided by Wallbridge Mining Ltd. during 2 weeks in 2004. Mapping of transects in Ben Nevis and Katrine townships was done at 1:20 000 scale, using the maps by Jensen (1975b) and Hogg (1964b) as base maps. The area of the Clifford stock in Clifford Township was mapped at a scale of 1:5000. Outcrop positioning on both projects was done with a Garmin eTrex™ GPS using NAD83.

Seventy-eight samples were collected for geochemical analysis from Ben Nevis and Katrine townships. Forty-two field samples were collected for analyses from Clifford Township and an additional 42 samples were collected from drill core. All samples were analysed for major, trace and rare earth elements following the methods outlined in MacDonald et al. (2005). Samples collected in 2003 were analysed at the Geoscience Laboratories, Willet Green Miller Centre, Sudbury, Ontario. Samples were crushed using an agate shatterbox. Major elements were analysed by X-ray fluorescence (XRF) on fused discs; the package also included loss on ignition (LOI). Chromium, Nb, Y and Zr were analysed by XRF using pressed-powder pellets. All other trace elements and the rare earth elements were analysed by inductively coupled plasma mass spectrometry (ICP-MS) and inductively coupled plasma atomic emission spectroscopy (ICP-AES) following a closed-beaker digestion (see Burnham and Schweyer 2004). Samples collected in 2004 were crushed at Activation Laboratories, Ancaster, Ontario, using a mild steel mill. Major elements were analyzed using fused-disc XRF, and Nb, V, Y, Zr, Cr and Ni were analysed using pressed-pellet XRF at Activation Laboratories. All other trace elements and the rare earth elements were analysed at the Ontario Geoscience Laboratories using the same methods as for the 2003 samples. All results are listed in Appendix 1; seven of the samples had poor major element closures and were rejected for use in this study. Data taken from MacDonald et al. (2005) is listed in Appendix 2. Details on the analytical methods, precision and accuracy can be found in MacDonald et al. (2005). Four samples of felsic rocks from the study area were radiometrically dated using U-Pb zircon methods at the Jack Satterly Geochronology Laboratory, University of Toronto. The samples included: 2 samples from Clifford Township (the Clifford stock and a felsic dyke near the stock), and 2 samples from Ben Nevis Township (a massive rhyolite flow from the Canagau Mine area and a QFP plug or dome near the Clifford–Ben Nevis township boundary). The results from these samples are reported in MacDonald et al. (2005) and Ayer et al. (2005). Details on the methodology for U-Pb geochronology at the Jack Satterly Geochronology Laboratory are provided by Hamilton in Ayer et al. (2005).

Under the Discover Abitibi umbrella, new airborne geophysical surveys were flown for Ben Nevis and Clifford townships (OGS 2003a). These data, along with surveys for Katrine Township (OGS 2003b), were used in producing the map P.3543–Revised, in the back pocket of this report.

Geological Setting

Ben Nevis, Katrine and Clifford townships are in the Blake River Group of the Abitibi Subprovince of the Archean Superior Province of Canada (Figure 2). The Blake River Group, along with the Kamiskotia gabbroic and volcanic complexes, is part of the larger Upper Blake River Assemblage (Figure 3; Ayer et al. 2005). The term “Assemblage” is used to refer to rocks of similar age and lithological character, in contrast to “Group”, which is a constrained stratigraphic entity. Goodwin (1977) divided the Blake River Group into four subgroups based on their lithological character: the Bowman, the Garrison, the Misema and the Noranda (Figure 4). The Bowman subgroup consisted of Mg-tholeiitic basalts (Goodwin 1977) and has since been re-interpreted as belonging to the Tisdale Assemblage (Figure 3; MERQ-OGS 1983). The Garrison subgroup is dominated by Fe-tholeiitic basalts with rare andesites (Goodwin 1977), and was interpreted on the Lithostratigraphic Map of the Abitibi (MERQ-OGS 1983) to belong to the Kinojevis Group. The Kinojevis Group in Ontario has been renamed the Lower Blake River Assemblage (Ayer et al. 2005; Figure 3). The Misema and Noranda subgroups belong to the Upper Blake River Assemblage (Figure 3; Ayer et al. 2005). The Misema subgroup is andesite dominated, with rare rhyolites; whereas the Noranda subgroup comprises bimodal, andesite-rhyolite volcanism (Goodwin 1977). The Blake River Group in Katrine, Ben Nevis and Clifford townships are within the Misema subgroup (Goodwin 1977); however, the contact between the Misema and Garrison subgroups has been interpreted by previous authors as occurring in the southern part of Katrine Township (Goodwin 1977, 1979; MERQ-OGS 1983; Ayer and Trowell 2000). Goodwin (1977, 1979) interpreted the contact to be conformable, and this interpretation appears on the Lithostratigraphic Map (MERQ-OGS 1983); on the most recent compilation map by Ayer and Trowell (2000) the contact is bound by a Proterozoic diabase dyke to the east and the Mulven Lake fault to the north.

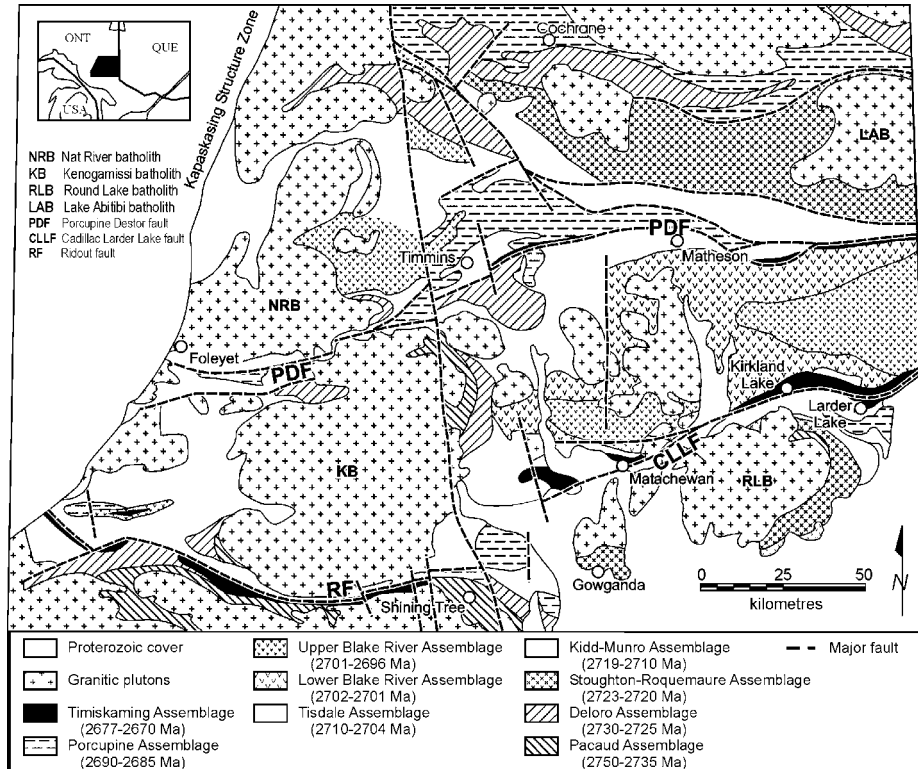


Figure 3. Geological assemblage map for the Abitibi Subprovince in Ontario (after Ayer et al. 2005).

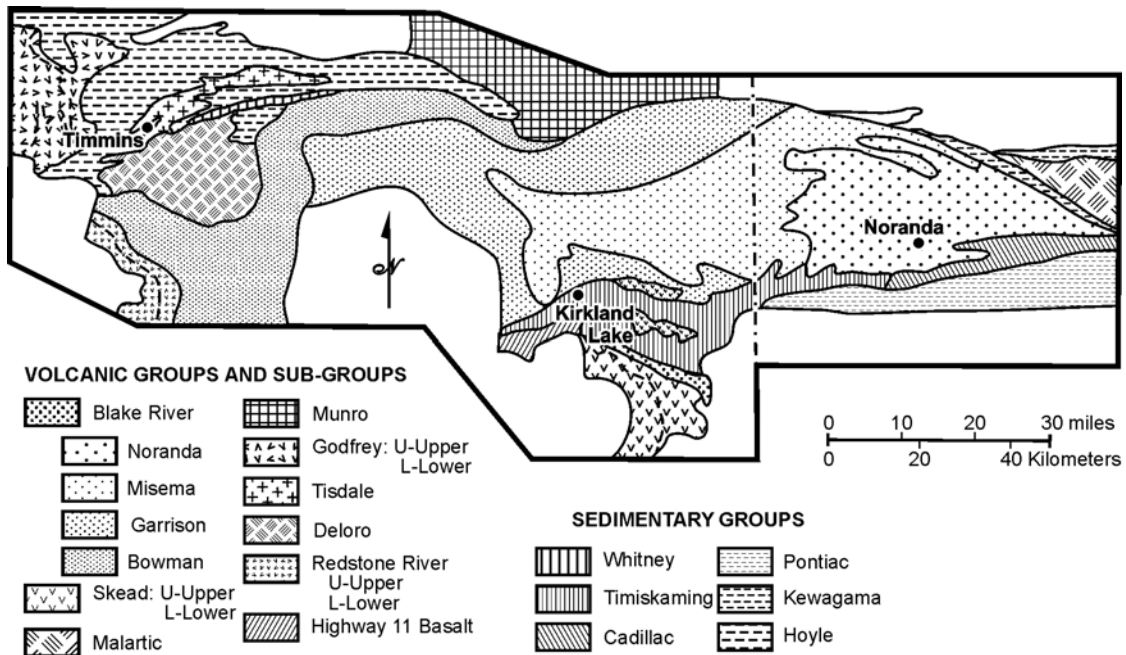


Figure 4. Map of the Blake River Group subgroups and adjacent volcanic stratigraphy, from Goodwin (1977).

In his classification, Goodwin (1977) proposed that the Blake River subgroups represented an age progression from the Garrison (the oldest) through the Misema to the Noranda (the youngest). The Misema and Noranda subgroups have since been re-interpreted as being contemporaneous (Péloquin et al. 1995; Péloquin 2000). The Noranda subgroup is considered to consist of 3 main phases of volcanism: pre-cauldron, cauldron and post-cauldron. The cauldron and post-cauldron phases have, in turn, been divided into formations (de Rosen-Spence 1976; Gibson 1989; Goutier 1997; Lafrance et al. 2003). Such detailed stratigraphy has not yet been done for the pre-cauldron phase of the Noranda subgroup or for the Misema subgroup. However, the Québec government is presently undertaking thematic mapping to better define the stratigraphy in the pre-cauldron Noranda and the Misema subgroups (Lafrance et al. 2004).

The Noranda subgroup was deposited between 2701 and 2694 Ma. The pre-cauldron phase was radiometrically dated at 2701 ± 1 Ma (the four-corners rhyolite; Mortensen 1993), and the post-cauldron phase has published U-Pb ages ranging from 2698.6 ± 1.5 Ma and 2694 ± 2 Ma (Lafrance et al. 2003; Mortensen 1993). The cauldron phase itself has never been accurately radiometrically dated, in spite of efforts to do so (Vaillancourt 1996). In Ontario, a Misema rhyolite in Pontiac Township, east of the study area, gave a radiometric age for the subgroup of 2701 ± 2 Ma (Corfu et al. 1989), and a rhyolite in an outlier of the Blake River Group in Gauthier Township, south of the study area, has an age of 2700 ± 3 Ma (Corfu 1993). These ages support the hypothesis that the Misema subgroup is contemporaneous with the Noranda subgroup. However, new zircon geochronology for a rhyolite in Ben Nevis Township yields a precise age of 2696.6 ± 1.3 Ma (Hamilton in Ayer et al. 2005), making it younger than the main volcanic phases of the Noranda and Misema subgroups, and a quartz-feldspar porphyritic dome in the Verna-Keith lakes area (Figure 5; P.3543-Revised, back pocket) has an age of 2695.6 ± 2.1 Ma (Hamilton in Ayer et al. 2005). These ages overlap published ages for the post-cauldron phase of the Noranda subgroup (the Renault-Dufresnoy formation: $2697.9 \pm 1.3/-0.7$ Ma (Mortensen 1993) and 2696 ± 1.1 Ma (Lafrance et al. 2003), and the Bousquet formation: 2698.6 ± 1.5 Ma, 2698.0 ± 1.5 Ma and 2694 ± 2 Ma (Lafrance et al. 2003)). The Garrison subgroup has a radiometric age of 2701 ± 3 Ma (Corfu and Noble 1992), and thus is the same age as the oldest rocks of the Noranda and Misema subgroups.

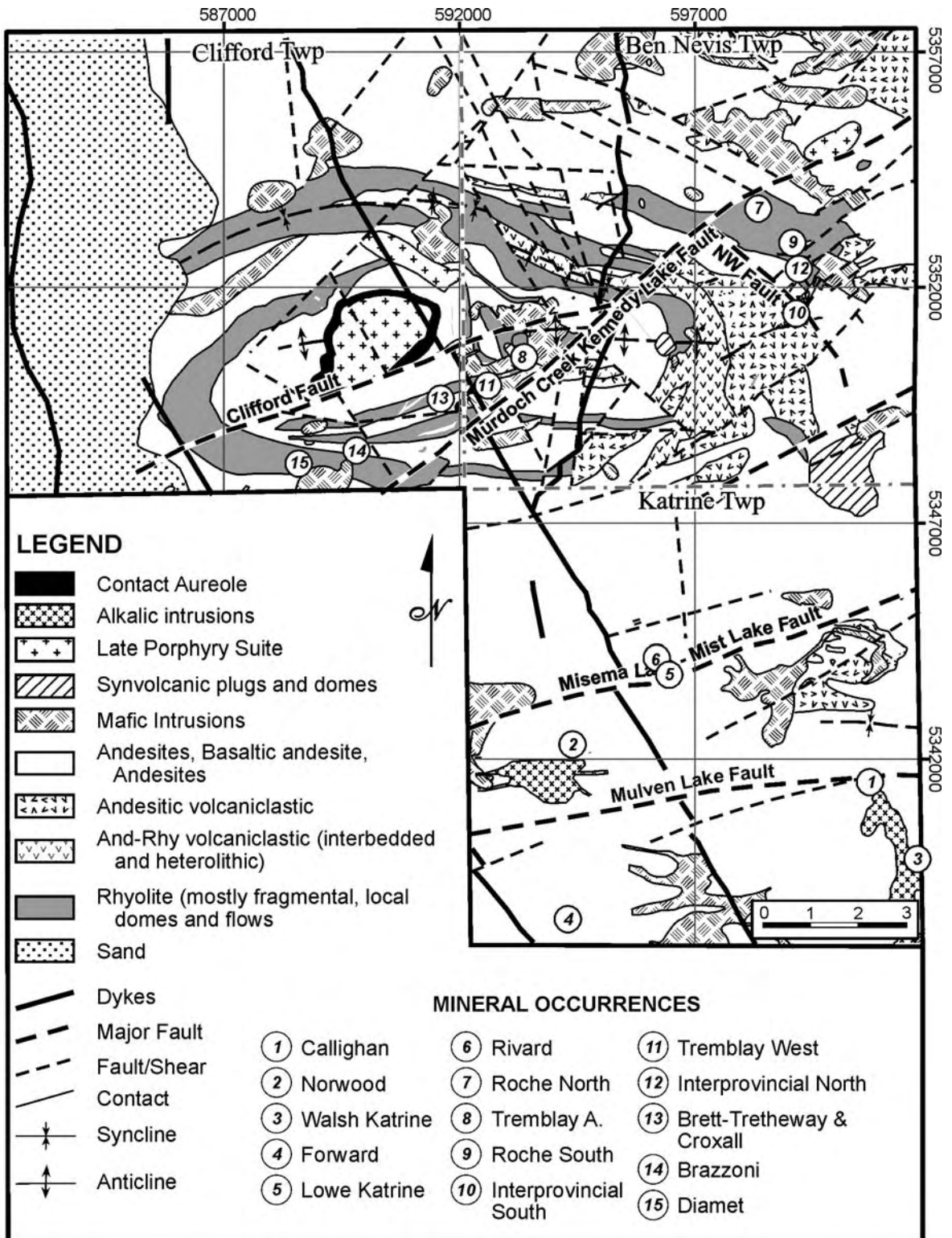


Figure 5. Geological map of the study area.

Geology of Katrine, Ben Nevis and Clifford Townships

KATRINE TOWNSHIP

Volcanic Rocks

Katrine Township is dominated by subaqueous andesite flows. The andesites throughout Katrine Township occur as pillowed and massive flows and flow breccias, with andesitic heterolithic pyroclastic deposits concentrated near the eastern limit of the township immediately south of the Misema Lake–Mist Lake fault. The andesite flows are both aphyric and plagioclase porphyritic, with 1-2 mm plagioclase phenocrysts ranging from 5 to 15% in abundance. Amygdules are commonly quartz and/or chlorite filled, are generally 5-7% in abundance, and are 1-3 mm in size, but 1.5 cm quartz amygdules are present in some localities. The pyroclastic rocks south of the Misema Lake–Mist Lake fault are of 2 types: tuff breccia (Photo 1a) and lapilli tuff. Both are heterolithic. The tuff breccia is characterized by 10-15% blocky fragments ranging from 0.5 to 15 cm with rare fragments over 50 cm in size. The fragments are non-vesicular plagioclase-phyric andesite, highly vesicular plagioclase-phyric andesite, highly vesicular aphyric (scoriaceous) andesite, quartz-phyric rhyolite, and jasper. The rhyolitic fragments are generally small (1-5 cm), and only 2 jasper fragments were observed (Photo 1b). The lapilli tuff fragments range from 1-3 cm in size and vary from clast supported (>70% fragments) to matrix supported (10-30% fragments) in a red-brown chloritized matrix.

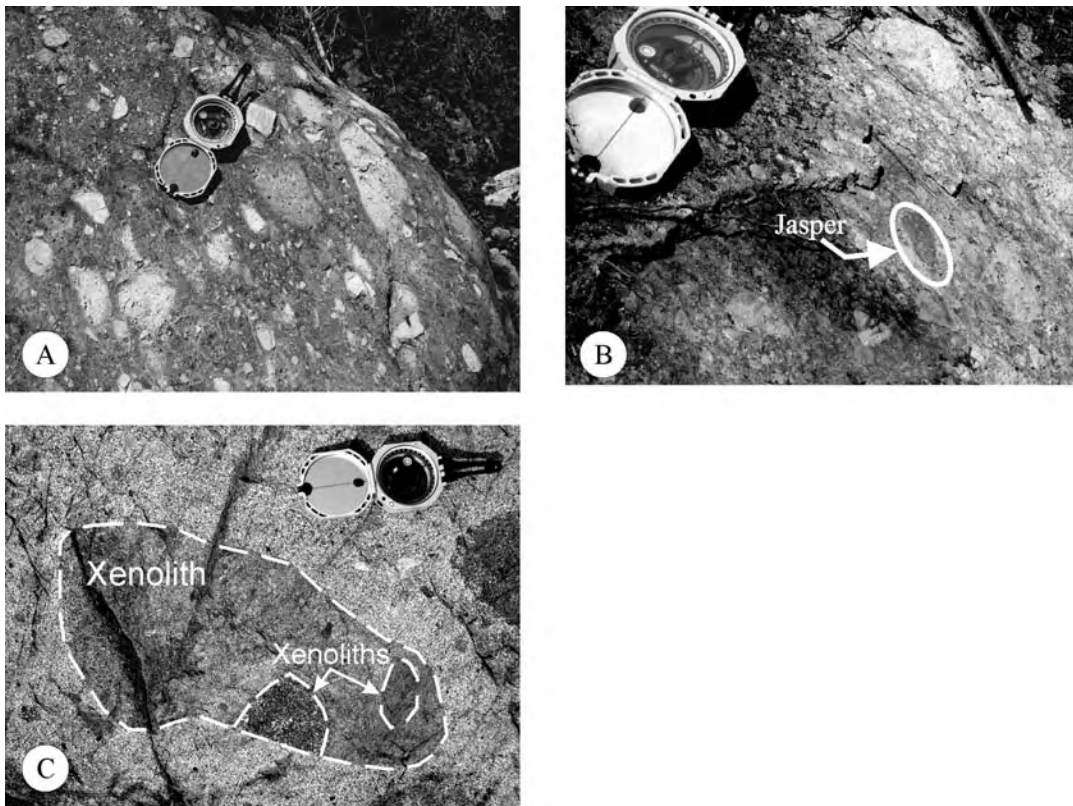


Photo 1. Katrine Township volcanic and intrusive rocks: a) heterolithic andesite tuff breccia; b) jasper fragment in the heterolithic andesite tuff breccia; c) xenoliths in the multi-phase alkalic stock.

Although no distinguishing features are present in outcrop to subdivide the andesites into domains, there is an apparent change in magnetic signature across the east-northeast-trending Misema Lake–Mist Lake fault (OGS 2003b; Figure 6; Map P.3543–Revised, back pocket), and the geochemical data in the next section (*see* “Geochemistry”) will be subdivided at this boundary to determine if any chemical differences occur across this fault. However, it should be noted that the available geophysical data was a collage of surveys, and different magnetic signatures may be due to survey differences. In the area of Kinabik Lake, south of the east- to east-northeast-trending Mulven Lake fault (Figure 5; Map P.3543–Revised), the Misema–Garrison subgroup contact, as interpreted by Goodwin (1979) and Ayer and Trowell (2000), has no magnetic expression (Figure 6), and in the area accessible to this study no evidence for the contact was observed. The geochemical analyses from either side of the proposed contact will be examined in the next section (*see* “Geochemistry”) to determine if the contact occurs in this area. Hogg (1964a) interpreted the Mulven Lake fault to be a faulted anticline. There is a change in facing direction of the pillowed andesites across the Mulven Lake fault: south of the fault, stratigraphy faces south and immediately north of the fault pillows face north (Map P.3543–Revised). Between the Mulven Lake and Misema Lake–Mist Lake faults (Figure 5; Map P.3543–Revised), an inversion in facing direction from north to south indicates the presence of an east-west-trending syncline interpreted by Hogg (1964a, 1964b) to be of limited westward extent. North of the Misema Lake–Mist Lake fault to the Katrine–Ben Nevis township boundary, the dominant facing direction of the andesites is south. The Katrine–Ben Nevis township boundary corresponds approximately to a change in gravity signature (OGS 1999), and the appearance of felsic volcanism to the north (Figure 5; Map P.3543–Revised).

Intrusive Rocks

Three types of Archean intrusions are observed in Katrine Township. Syenitic stocks occur in the southeast corner of the township, and in the area between Misema Lake and its North Arm. Small feldspar porphyry dykes of similar composition to these intrusions cut the volcanic rocks. The syenitic intrusion in the southeast corner of the township is polyphase, locally brecciated and contains xenolithic phases (Photo 1c). Xenoliths are heterolithic, ranging from ultramafic (pyroxenite) to felsic (syenitic, resembling other phases observed on the outcrop). The intrusions are part of the late intrusive suite in the Blake River Group that includes the Aldermac, Tarsac and Clericy syenites in Québec (Rive et al. 1990). Large diorite-gabbro intrusions, and associated dykes, occur in Katrine Township. These intrusions are considered to be part of the Blake River Group proper. The final type of intrusion in Katrine Township is high-level synvolcanic andesitic dykes. These dykes intruded andesite flows and flow breccias in the Lake Kinabik area and intrude the heterolithic lapilli crystal tuff south of the Misema Lake–Mist Lake fault. These intrusions are fine-grained and are distinguishable from flows in that they crosscut the stratigraphy, and have amoeboid margins, locally with magma apophyses that protrude into the unconsolidated host rock.

Proterozoic diabase dykes of the Matachewan swarm cross-cut the volcanic and intrusive suites in all three townships. These dykes typically are magnetic and can be mapped by geophysical signatures. In some cases, their localization appears to coincide with pre-existing structures.

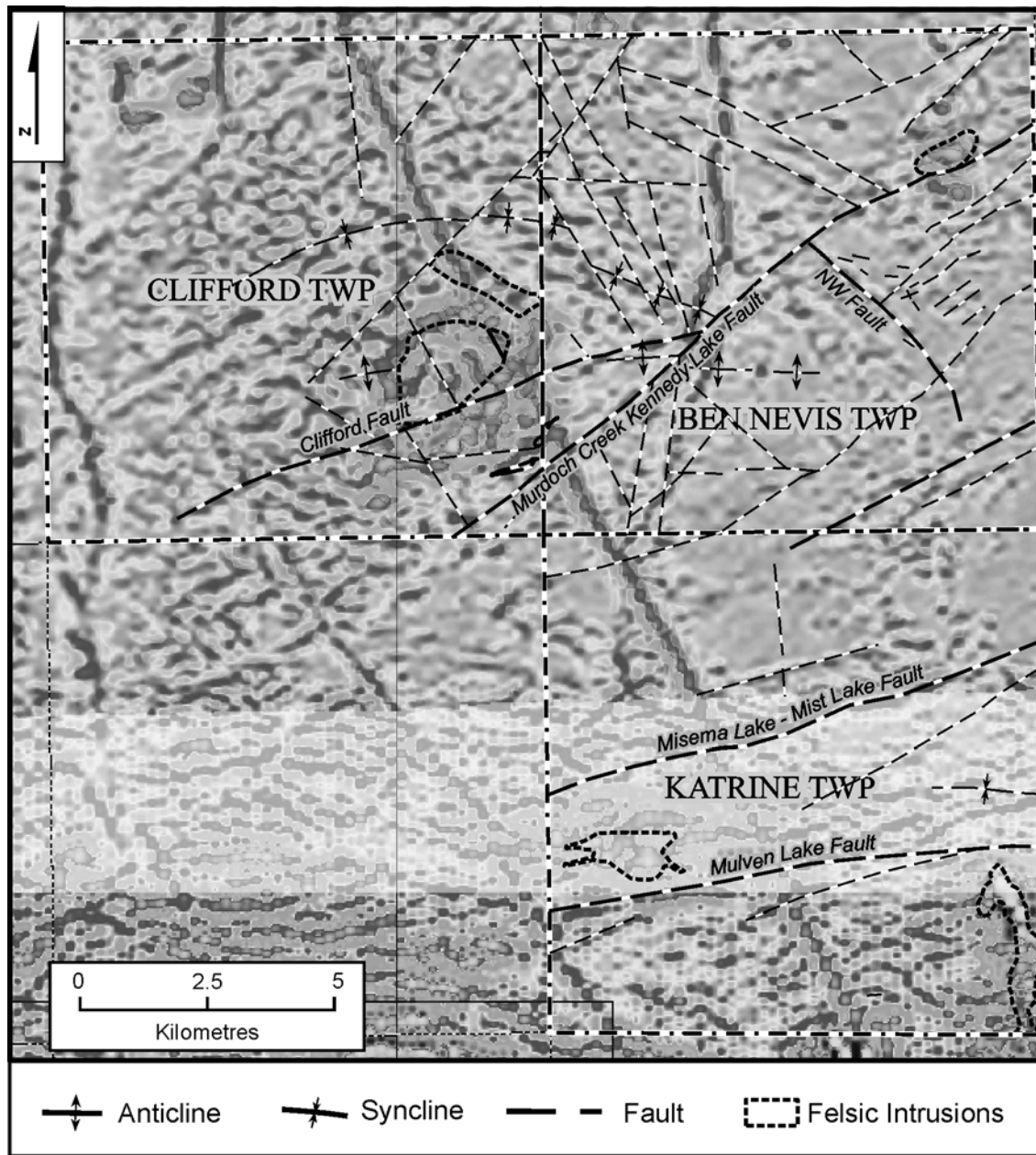


Figure 6. Grey-shaded second vertical derivative magnetics map for Clifford, Ben Nevis and Katrine townships, showing major structures. Darker shades of grey are magnetic highs.

BEN NEVIS TOWNSHIP

Volcanic Rocks

Ben Nevis Township contains a spectrum of volcanic rocks ranging from basaltic andesite through andesite to rhyolite. The township is divided into 2 main domains by the northeast-trending Murdoch Creek–Kennedy Lake fault (Figure 5). The area south of the fault includes the Interprovincial showings area (also known as the Canagau Mine area). The area north of the fault is designated the North Ben Nevis block. Within the area north of the fault is a fault slice lying between the Murdoch Creek–Kennedy Lake fault and the east-northeast-trending Clifford fault (Figure 5). The area between the faults extends from Ben Nevis into Clifford Township and will be described in the Clifford Township section. South of the Murdoch Creek–Kennedy Lake fault, the volcanic rocks are cross-cut by a northwest-trending fault (Riopel 1998), which will here be called the NW fault (Figure 5). This fault appears to represent a structural boundary within the Blake River Group stratigraphy in Ben Nevis Township, and the areas on either side of the fault will be discussed separately. The relationship between the blocks on either side of the NW fault could not be determined at the scale of this project and further detailed mapping is required to establish the relationship. The Clifford domal-anticline folds the volcanic and early intrusive rocks in Ben Nevis and Clifford townships around its east-west-trending axis. The anticline dies out in the west of the NW fault in Ben Nevis Township (Figure 5).

South of the Murdoch Creek–Kennedy Lake fault and west of the NW fault, the stratigraphy in Ben Nevis Township youngs outward from the Clifford domal anticline axis and nose. The oldest unit in the sequence consists of aphyric, pillowed, massive and brecciated andesite flows. Up stratigraphy, along the anticlinal axis, there is a small massive rhyolite dome. The dome is plagioclase-microphyric and has polygonally jointed breccia phases; it is interpreted to be extrusive. Immediately above the dome is a rhyolite breccia intruded by a quartz-feldspar porphyry dyke; along strike to the north, Jensen (1975a, 1975b) mapped a rhyolite tuff and tuff breccia unit (*see* P.3543–Revised). Along strike to the south, and overlying the rhyolite pyroclastic unit, is a unit of mixed pyroclastic rocks (P.3543–Revised). This unit consists of interlayered andesite tuffs, lapilli tuffs and tuff breccias, rhyolite tuffs and tuff breccias, and heterolithic pyroclastic breccias. Above the mixed pyroclastic unit is an andesitic unit dominated by tuffs and tuff breccias, but with interlayered pillowed flows and flow breccias. This unit is intruded by synvolcanic felsic dykes (P.3543–Revised). The Interprovincial South showing occurs in this package (Figure 5; P.3543–Revised). Outcrops visited in the showing area are characterized by local intense carbonatization, local silicification and felsic dykes intruding the andesitic flows (Photo 2a). The mixed pyroclastic unit is overlain by amygdaloidal andesitic flows exhibiting pillowed, massive and breccia facies. Synvolcanic intermediate to felsic dykes intrude this unit.

The NW fault cross-cuts the amygdaloidal andesite unit and the mixed pyroclastic unit (Riopel 1998; Figure 5; P.3543–Revised). West of the NW fault the facing directions vary from north-east on the north flank of the anticline to south-west on the south flank (P.3543–Revised). East of the NW fault few facing directions were observed; those present have southwest to west-southwest facings, except in the area of the Interprovincial showings, which have west-northwest facing directions. However, all the compiled facing directions east of the NW fault are south to southwest.

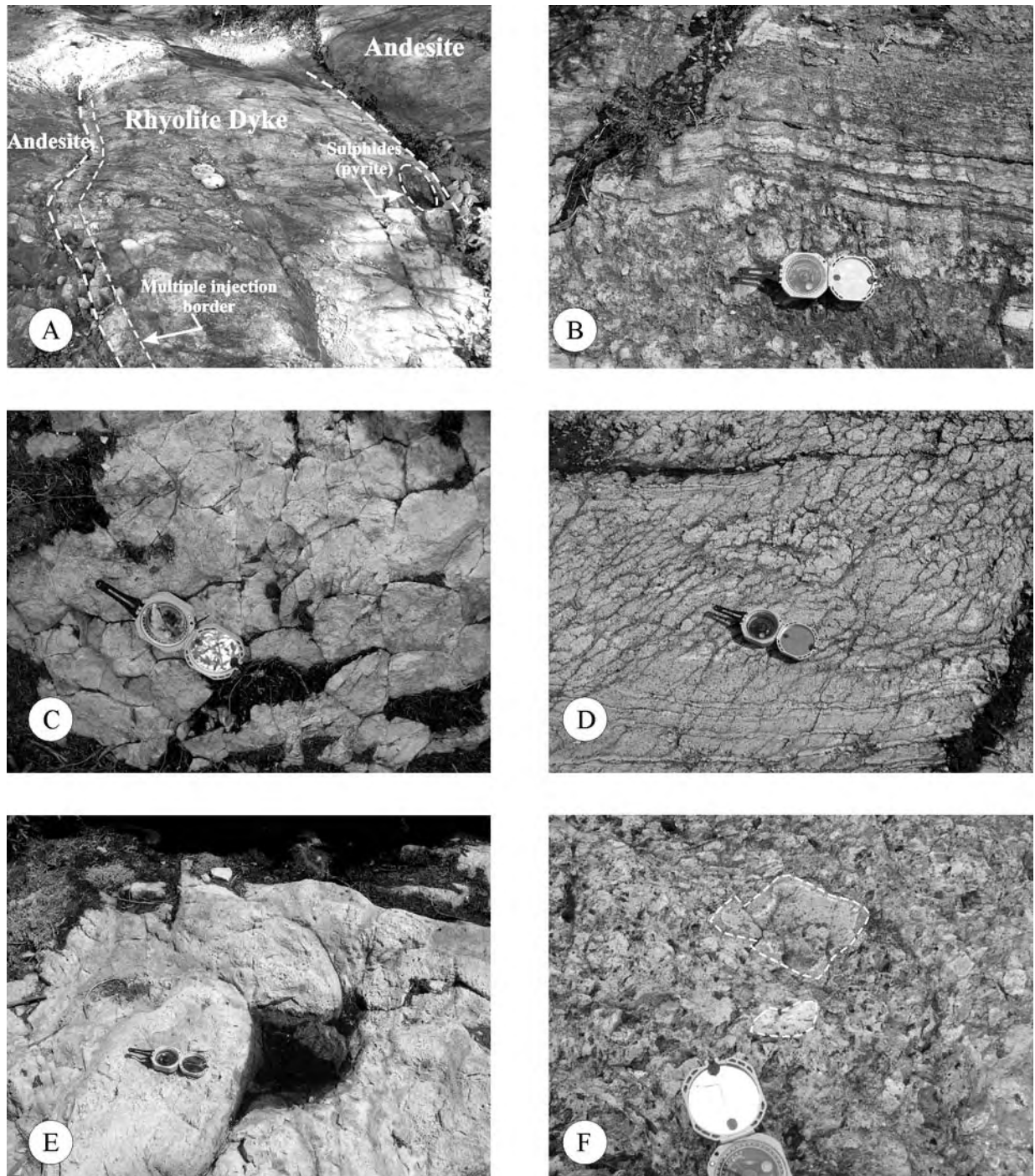


Photo 2. Ben Nevis Township volcanic rocks: a) rhyolite dyke intruded into andesite at the Interprovincial South showing; b) lapilli and bedded tuff, Canagau rhyolite; c) polygonally jointed rhyolite, Canagau rhyolite; d) tectonic overprinting of pyroclastic rhyolite producing pseudobreccia, Canagau rhyolite; e) epidotized and silicified (light grey) andesite pillows, north of the Murdoch Creek–Kennedy Lake fault; f) pyroclastic rhyolite showing reaction rim on a fragment, north of the Murdoch Creek–Kennedy Lake fault.

The rhyolite located immediately east of the fault is called the Canagau rhyolite (Pearson 1992; Riopel 1998; Figure 5; P.3543–Revised) and is host to the Roche North, Roche South and Interprovincial North showings (Canagau Mine). The Canagau rhyolite package consists predominantly of pyroclastic tuffs and tuff breccias (Photo 2b), with local massive polygonally jointed domes (Photo 2c), and lobe and breccia flows. The area is highly deformed; the deformation commonly masking the original textures and morphologies of the rhyolites (Photo 2d). The deformation is commonly associated with Fe-carbonate alteration and/or sericite alteration. Chlorite alteration also occurs, but does not appear to be deformation related. The rhyolites are commonly cut by andesitic synvolcanic dykes. The Canagau rhyolite terminates to the southeast (Figure 5; P.3543–Revised). A thick diorite dyke cross-cuts the andesite flows and pyroclastic rocks southeast of the Canagau rhyolite; in turn, a rhyolite dyke cross-cuts the diorite. A number of parallel northeast-trending faults, of unknown displacement, cross-cut the stratigraphy and the diorite intrusion southeast of the Canagau rhyolite. The andesite flows northeast of the Canagau rhyolite (Figure 5; P.3543–Revised) strike east-west to east-southeast and face to the south; thus, they are interpreted to underlie the Canagau rhyolite. These flows are locally interlayered with andesitic pyroclastic rocks.

The area north of the Murdock Creek–Kennedy Lake fault is dominated by southwesterly facing subaqueous andesite flows exhibiting pillowed, massive and breccia facies, with rare pyroclastic facies. The andesites are variably plagioclase porphyritic (porphyritic flows generally contain 3-5%, 1-2 mm plagioclase phenocrysts, with one highly porphyritic flow, 30% plagioclase phenocrysts, observed in the northeast corner of the township), and/or amygdaloidal (amygdaloidal flows contain 5-10% quartz, chlorite or rare carbonate amygdules, increasing to 20% near pillow rims). Some pillowed flows exhibit extreme epidote-quartz alteration of the pillow centres and rims (Photo 2e). Rhyolite pyroclastic rocks, tuffs and tuff breccias, occur above the andesites, and alternate with andesite flow units. The pyroclastic rhyolites (Photo 2f) are heterolithic lapilli and tuff breccias with accidental andesite fragments and variably textured (cherty, laminated, massive, fragmental) aphyric and porphyritic rhyolite fragments from 1-3 cm in size, and laminated tuffs with 3%, 1.5 mm quartz phenocrysts. Small, polygonally jointed massive rhyolites are present in very minor abundance in this area. Jensen (1975a, 1975b) interpreted the presence of a syncline north of the Murdock Creek–Kennedy Lake fault in Ben Nevis Township; this area was not accessible to the present study (Figure 5; P.3543–Revised).

Intrusive Rocks

Ben Nevis Township contains 3 types of Archean intrusions: late (post Blake River Group volcanism) intrusions; Blake River Group intermediate intrusions; and high-level synvolcanic dykes. The small granitoid stock in the northeast corner of the township, north of the Murdoch Creek–Kennedy Lake fault, is considered to be part of the same intrusive suite as the Clifford stock, described below and in more detail in MacDonald et al. (2005). The Ben Nevis intrusion corresponds to a magnetic high on the magnetic second vertical derivative maps, as does the Clifford stock (OGS 2003a; Figure 6). However, unlike the Clifford stock, it does not correspond to a gravity low (OGS 1999; Figure 7). The gravity low, instead, occurs south of the Murdoch Creek–Kennedy Lake fault in the area of the Canagau rhyolite, without, it should be noted, the magnetic high signature (OGS 2003a; Figure 6). It is, therefore, possible that an intrusion similar to the Clifford stock occurs at depth in the Canagau rhyolite area. Two porphyry dykes were observed south of the Murdoch Creek–Kennedy Lake fault and west of the NW fault. These appear to be late intrusions possibly related to the Clifford stock event (*see* MacDonald et al. 2005), rather than synvolcanic dykes, and are the only observed examples of that event in Ben Nevis Township south of the Murdoch Creek–Kennedy Lake fault.

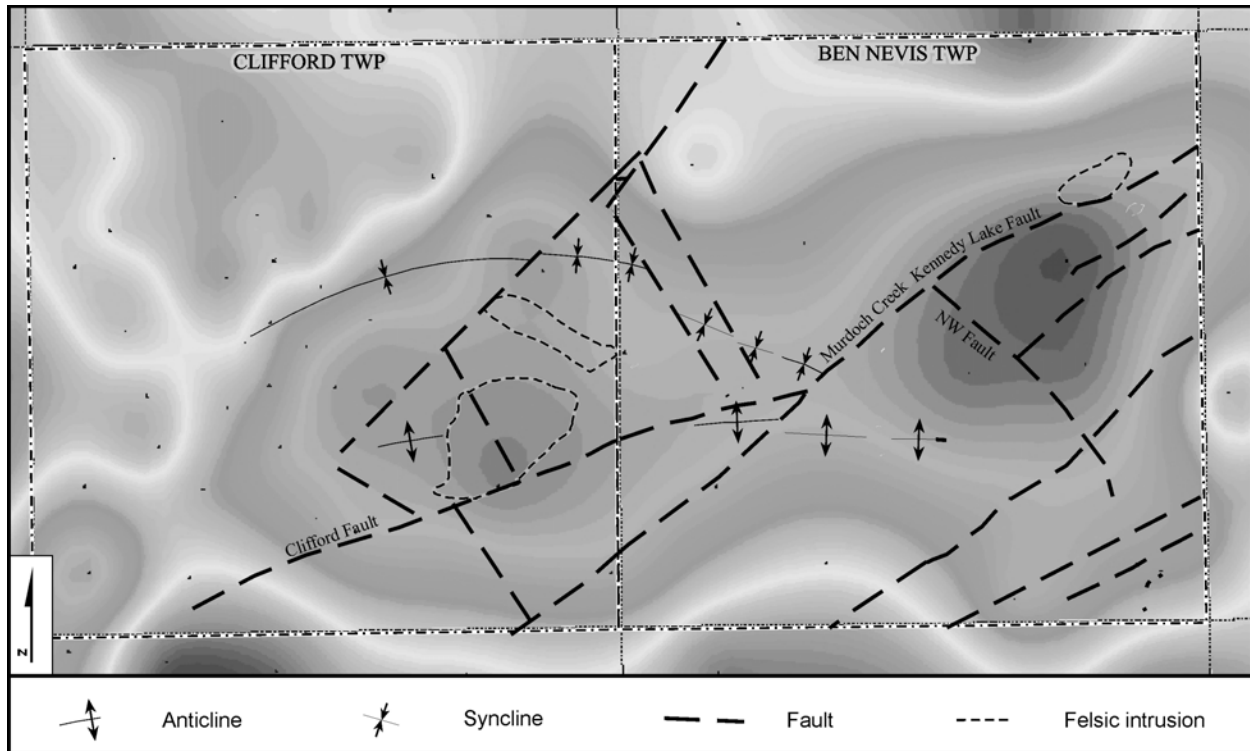


Figure 7. Grey-shaded gravity map of Clifford and Ben Nevis townships, showing the major structures and intrusions. Darker shades of grey are gravity lows.

Medium- to coarse-grained diorite-gabbro bodies and dykes, similar to those in Katrine Township, intrude the Ben Nevis volcanic pile, north and south of the Murdoch Creek–Kennedy Lake fault, and are considered to be part of the Blake River magmatic event. In one outcrop, southeast of the Canagau rhyolite, a high-level rhyolite dyke intrudes the diorite, indicating the synvolcanic origin for the diorites.

The high-level synvolcanic intrusions comprise andesite and rhyolite dykes, rhyolite cryptodomes, and a composite quartz-feldspar porphyry (QFP) plug. The andesite dykes are most easily recognized where they intrude rhyolitic volcanic rocks. They commonly have amoeboid contacts, indicating that the host rock was unconsolidated, and locally exhibit multiple injection borders (Photo 3a). Conversely, the rhyolite dykes intrude andesite flows, which often exhibit varying degrees of silicification near the dykes (Photo 3b). These rhyolite dykes commonly have sharp contacts, and locally exhibit multiple injection borders (Photo 2a). Sulphide mineralization is commonly concentrated in the multiple injection borders in both dyke lithologies. Two rhyolite domes are present in the study area; both occur along the axis of the Clifford domal anticline. The first, described above with the felsic volcanic rocks is interpreted to be extrusive. The second dome, in Ben Nevis Township south of the Clifford fault, is interpreted to be a cryptodome and is described with Clifford Township, below. A high-level composite QFP plug occurs in the southeast corner of Ben Nevis Township, and extends into Katrine Township. This plug was mapped in Ben Nevis Township (Jensen 1975b) as a rhyolite, and in Katrine Township (Hogg 1964b) as a diorite. Both felsic and intermediate lithologies are present in the intrusion, as is a breccia facies consisting of andesitic fragments in a deformed QFP matrix (Photo 3c). The QFP outcrops are massive with no evident volcanic features; the diorite is also massive but the outcrop is of very poor quality.

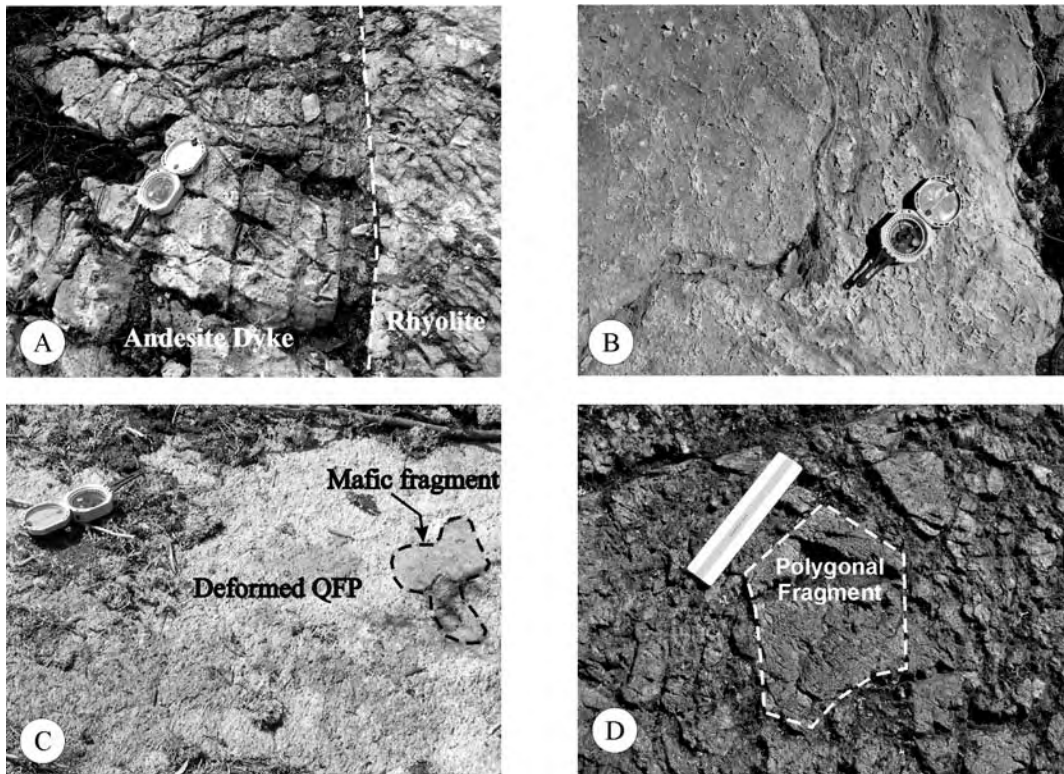


Photo 3. Ben Nevis Township intrusive and volcanic rocks: a) multiple injection borders in andesite dyke intruded into rhyolite; b) network silicification of andesite near synvolcanic rhyolite dykes; c) mafic fragment in deformed phase of QFP plug at the Ben Nevis–Katrine township boundary; d) monolithic carapace breccia of rhyolite with polygonally jointed, flow-banded rhyolite clasts, from cryptodome in western Ben Nevis Township.

CLIFFORD TOWNSHIP

Volcanic Rocks

The southeastern corner of Clifford Township was systematically mapped by S. Piercey (*see* MacDonald et al. 2005) at a scale of 1:5000. The Clifford Township map area extended into Ben Nevis Township as a natural extension of the fault block between the Clifford and Murdoch Creek–Kennedy Lake faults, and data from the volcanic rocks examined in Piercey’s study are incorporated here.

There appears to be little displacement along the Clifford fault, and the stratigraphy is considered continuous across it. In the area, the stratigraphy consists of a southward-younging succession of basaltic andesite, andesite, and felsic volcanoclastic rocks, that are interpreted to record 2 cycles of volcanism and comprise 5 volcanic to volcanoclastic units, and associated synvolcanic diabase/gabbro intrusions (Figure 8). The lowermost packages consist of pillowed to massive, basaltic andesite to andesite that is amygdaloidal and variably plagioclase porphyritic; where porphyritic plagioclase crystals are 2-3 mm long and relatively euhedral. Conformably overlying the amygdaloidal basaltic andesite is a package of andesitic volcanoclastic rocks. Péloquin and Piercey (2003) interpreted this package as consisting of andesitic flows, but recent investigations of drill core from Wallbridge Mining Company Ltd. illustrate that these rocks are actually andesitic tuffs, lapilli tuffs, and tuff breccias. These volcanoclastic rocks are matrix supported and consist mainly of fine-grained, grey to grey-black andesitic tuff with varying

amounts of feldspar lapilli and black andesitic fragments. Feldspar grains range from <1 mm to 5 mm in size and are euhedral to subhedral; in places they comprise 30-40% of the rock. Black andesitic fragments are not easily discernable on surface but in drill core they are typically subrounded to subangular, range from <1 cm up to 10 cm in size, and in places comprise 20-30% of the rock. Overlying this andesitic tuff unit is the first of two felsic volcanoclastic units consisting of a matrix-supported felsic tuff breccia (nomenclature from Fisher 1966). On surface these tuff breccias appear monomictic to weakly polymictic; however, in drill core these samples are clearly polyolithic and contain clasts of andesite, basaltic andesite, dacite and rhyolite, which are angular to subrounded and range in size from 1-30 cm. All the clasts are within a matrix of fine siliceous ash material. Overlying the latter felsic tuff breccia is a second unit of amygdaloidal and variably plagioclase-porphyrific basaltic andesite to andesitic tuff with small plagioclase feldspar crystals: less than 1 mm and up to 2-3 mm. The uppermost stratigraphic unit is a second felsic tuff breccia to lapilli tuff, very similar to the underlying felsic tuff breccia, consisting of a matrix-supported breccia with angular clasts of predominantly dacite to rhyolite. There appears to be a southward younging of the tuff breccia into a lapilli tuff on a regional scale, suggesting normal grading outward from the Clifford stock (Jensen 1975a, 1975b).

Minor felsic flows and cryptodomes occur within the study area. In southern Clifford Township, there are felsic flows associated with a primarily felsic volcanoclastic package. These flows are white, aphyric rhyolitic rocks that are relatively massive in nature. In the extension of Piercey's Clifford Township study area into western Ben Nevis Township, there are flow-banded rhyolitic volcanoclastic rocks spatially associated with synvolcanic rhyolitic to dioritic dykes, which are interpreted to be part of a cryptodome. The rhyolitic volcanoclastic rocks are different than most felsic volcanoclastic rocks in the area in that they are clast-supported, monolithic, and consist of polygonally jointed rhyolite fragments that have flow banding (Photo 3d). Rhyolitic intrusive rocks that intrude these felsic volcanoclastic rocks are fine-grained, quartz-plagioclase porphyritic and have irregular margins; they are synvolcanic in nature as shown by the U-Pb age date of 2695.6 ± 2.1 Ma (Hamilton in Ayer et al. 2005). The diorites are also porphyritic; plagioclase is the ubiquitous phenocryst phase, but chlorite pseudomorphs of a mafic phenocryst phase were observed locally.

Intrusive Rocks

In Clifford Township the main intrusive phases are the Clifford stock and related dykes, and diorite-gabbro dykes and sills. The Clifford stock is located in the core of the Clifford domal anticline and consists of a relatively equigranular tonalite to granodiorite, commonly hornblende-bearing and locally hornblende-biotite-bearing. The intrusion does not appear to be polyphase and contains xenoliths of the surrounding wall rock in only a few localities. Southeast of the Clifford stock, numerous east- to northeast-striking dyke- to sill-like intrusions cut the volcanic sequence; they are interpreted to be related to the Clifford stock. The dykes are fine- to medium-grained, variably feldspar porphyritic, locally pyrite-bearing, siliceous, and dacitic to rhyolitic in composition. The dykes crosscut stratigraphy; they have very straight walls in most places, suggesting emplacement into solidified host rock material, but are irregular in some localities due to being potentially emplaced into dilation zones or when they are associated with hydrothermal brecciation. Locally, the dykes are associated with xenoliths of very angular fragments of wall rock and the breccias are interpreted to be due to forceful emplacement of the dykes into solid wall rock. They are also spatially associated with breccia-pipes (e.g., Croxall occurrence) and stockworks of pyrite-quartz-gold-molybdenite veins. The mafic intrusive units in Clifford Township are similar to those observed in Katrine and Ben Nevis townships; they are metamorphosed and hard to distinguish from massive mafic-intermediate volcanic rocks. These rocks intrude all stratigraphic units in the area, and are mostly dioritic, locally gabbroic, forming sheet-like and dyke-like intrusions. Some of the dykes have amygdules suggesting emplacement at high levels, and supporting a synvolcanic origin (Gibson et al. 1999).

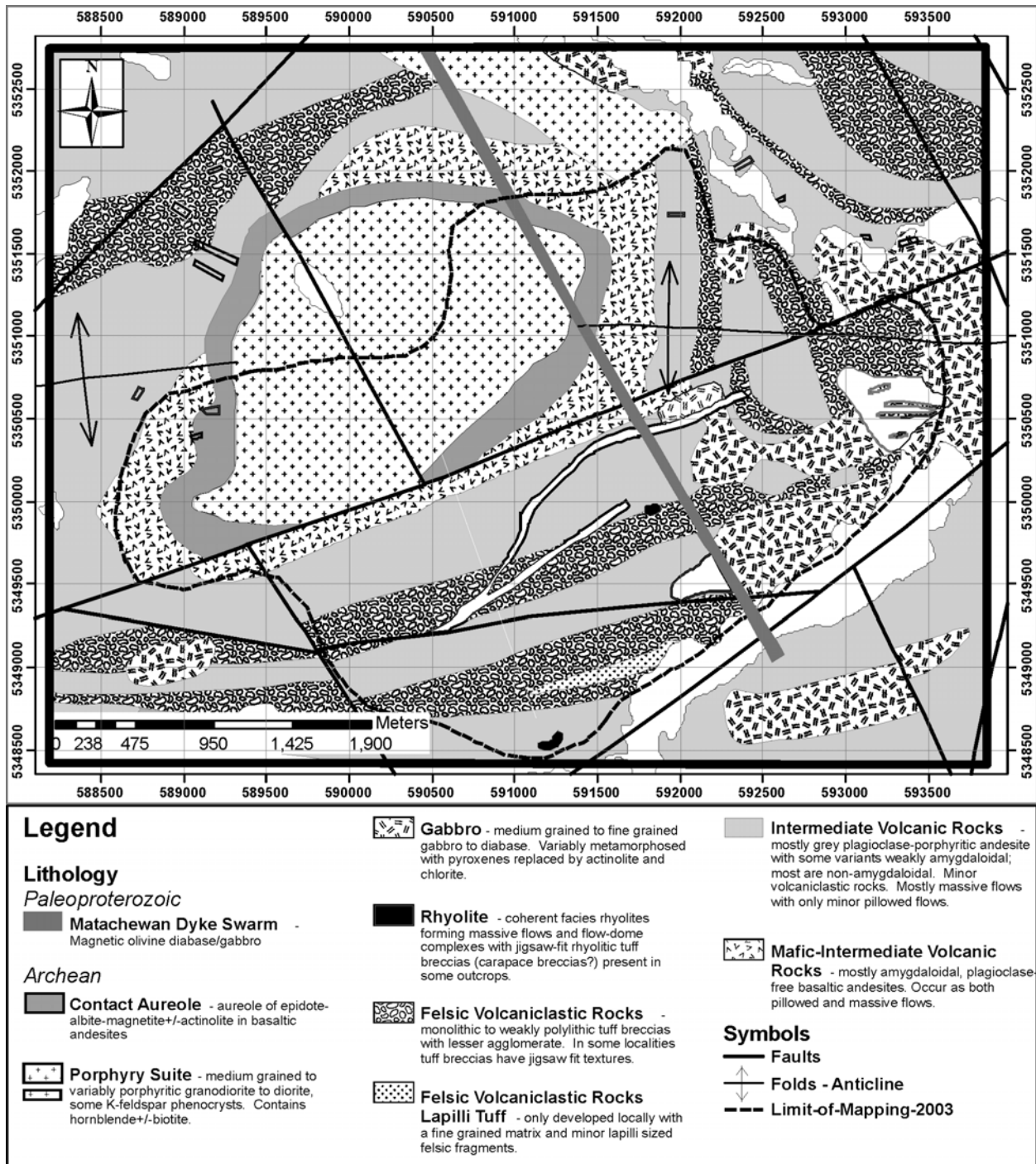


Figure 8. Geological map of Clifford Township (from MacDonald et al. 2005). Geology based on the mapping of Piercey et al. (2004), Pélouin and Piercey (2003), and Jensen (1975).

Geochemistry

Samples for geochemical analysis were taken of the volcanic and intrusive rocks in Katrine, Ben Nevis and Clifford townships. The geochemistry of the Clifford Township area rocks, particularly the Clifford stock and its associated dykes, and including the volcanic sequence in the southwestern corner of Ben Nevis Township, is discussed in detail in the Discover Abitibi Intrusion Subproject (MacDonald et al. 2005). Here, the volcanic rocks of that study will be placed in the context of the larger area covered by this study.

The Clifford stock and its associated felsic dykes will not be treated in this study. The intrusive rocks studied will include the high-level synvolcanic dykes, the high-level felsic plug and cryptodome, and the Blake River diorite dykes and intrusions. A late alkalic intrusive suite occurs in the study area, but was not studied. Samples of the intrusive rock types are fewer and more widely dispersed than the volcanic samples; consequently the treatment of these rocks will be less detailed.

VOLCANIC ROCKS

In general, the Blake River Group volcanic rocks sampled in this study range from basalt to rhyolite, with andesites being the dominant rock type. A SiO_2 wt % histogram of the rock types shows this (Figure 9a). This histogram, along with the SiO_2 line-diagram (Figure 9b), shows that the Blake River Group in this area is not bimodal, as no significant silica gap occurs.

The progression of volcanic rock types from basalt to rhyolite is also seen on the LeBas et al. (1986) classification diagram (Figure 10a). Here, the domination of basaltic andesites and andesites in the area is clear. Four samples fall in the alkalic rock fields on this diagram, and two of the rhyolites exhibit low $\text{Na}_2\text{O}+\text{K}_2\text{O}$ values. These phenomena are considered to be due to alteration and/or the sulphide or oxide content of the rocks. On a standard Irvine and Baragar (1971) AFM diagram (Figure 11a), the vast majority of volcanic rocks fall in the calc-alkalic field, with few samples falling in the tholeiitic field.

Plotting the samples on a Large et al. (2001) alteration box diagram (Figure 12a) shows them to be concentrated along the divide line between diagenetic and hydrothermal alteration. The “tholeiitic” mafic rocks from the AFM diagram fall outside the least altered basalt/andesite box along the division line toward the epidote-calcite corner of the diagram. The majority of the samples of mafic “calc-alkalic” rocks fall within the least altered box, clustered along the diagenetic–hydrothermal alteration divide. Epidotization is common in the mafic rocks as a product of metamorphism, and is also visible on outcrop as a more intense alteration: as epidotized pillow rims and/or centres, and as epidote pods in massive flows. The felsic rocks of this study, dacites and rhyolites, also cluster along the divide line between diagenetic and hydrothermal alteration, with samples falling outside the least altered dacite and rhyolite boxes, indicating carbonatization on the one hand, and sericitization on the other. Both alteration types were observed in outcrop. Carbonatization is particularly evident in the area of the Roche and Interprovincial showings, and sericitization is common in the rhyolites throughout the area, in particular in the matrices of volcanoclastic rocks.

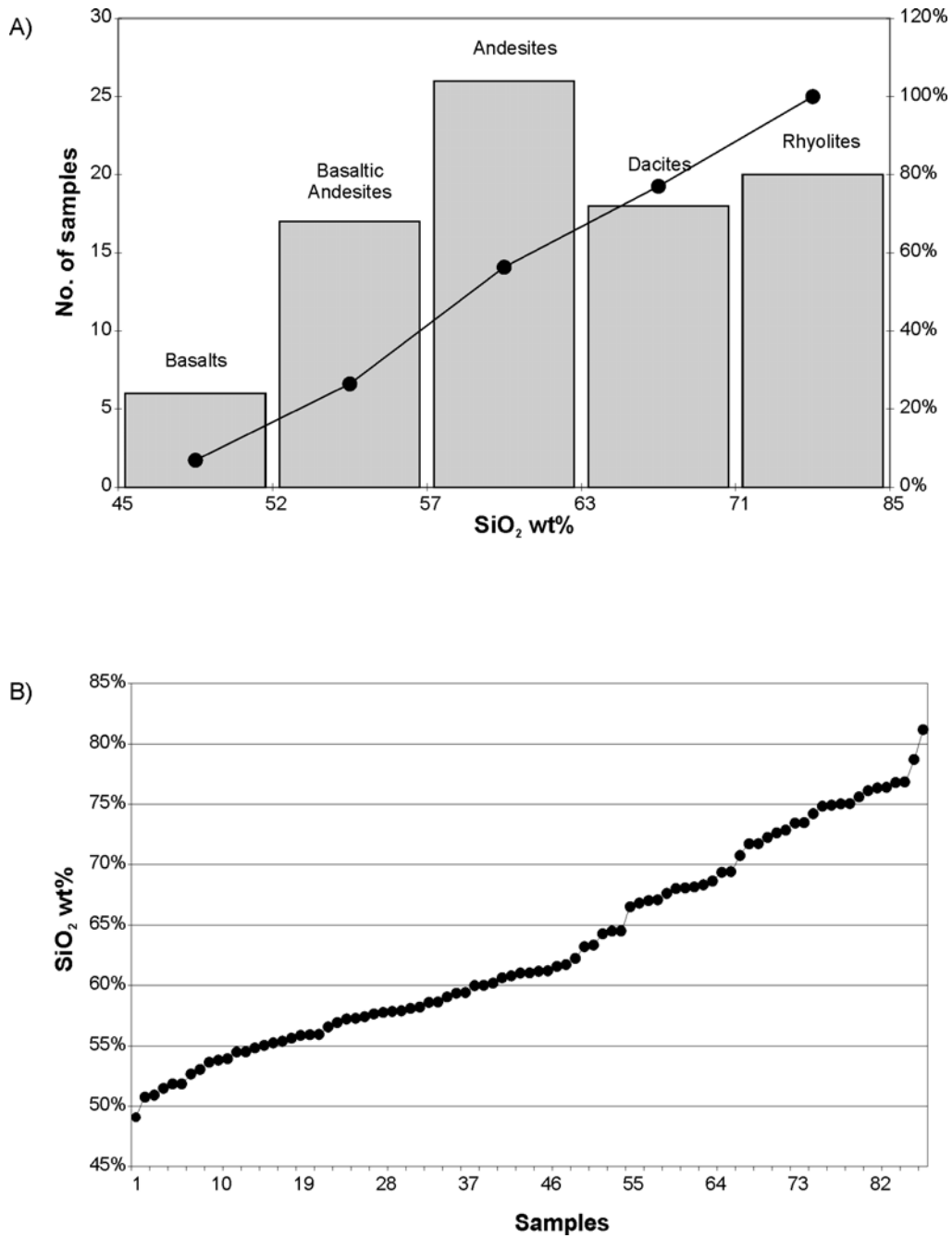


Figure 9. SiO₂ content of the volcanic rocks in the study area: a) SiO₂ wt % histogram. Class intervals are SiO₂ wt % contents of rock types; b) linear plot of SiO₂ wt %.

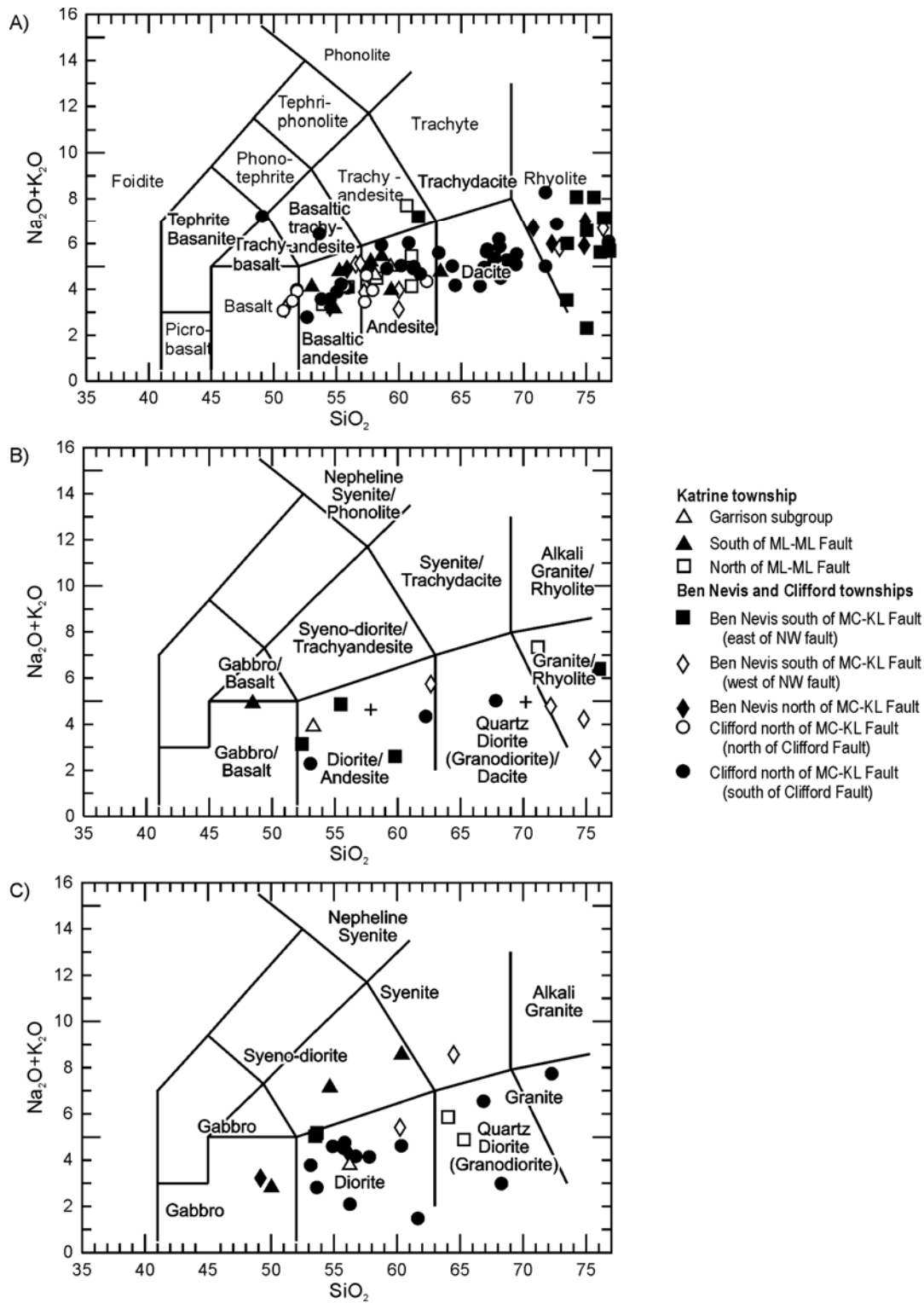


Figure 10. Rock classification diagram (Na_2O wt % + K_2O wt % versus SiO_2 wt %; LeBas et al. 1986; plotted using IgPet2001) for: a) the volcanic rocks; b) the high-level synvolcanic intrusions; c) the intrusive rocks. (ML-ML Fault = Mist Lake–Misema Lake fault; MC-KL Fault = Murdoch Creek–Kennedy Lake fault)

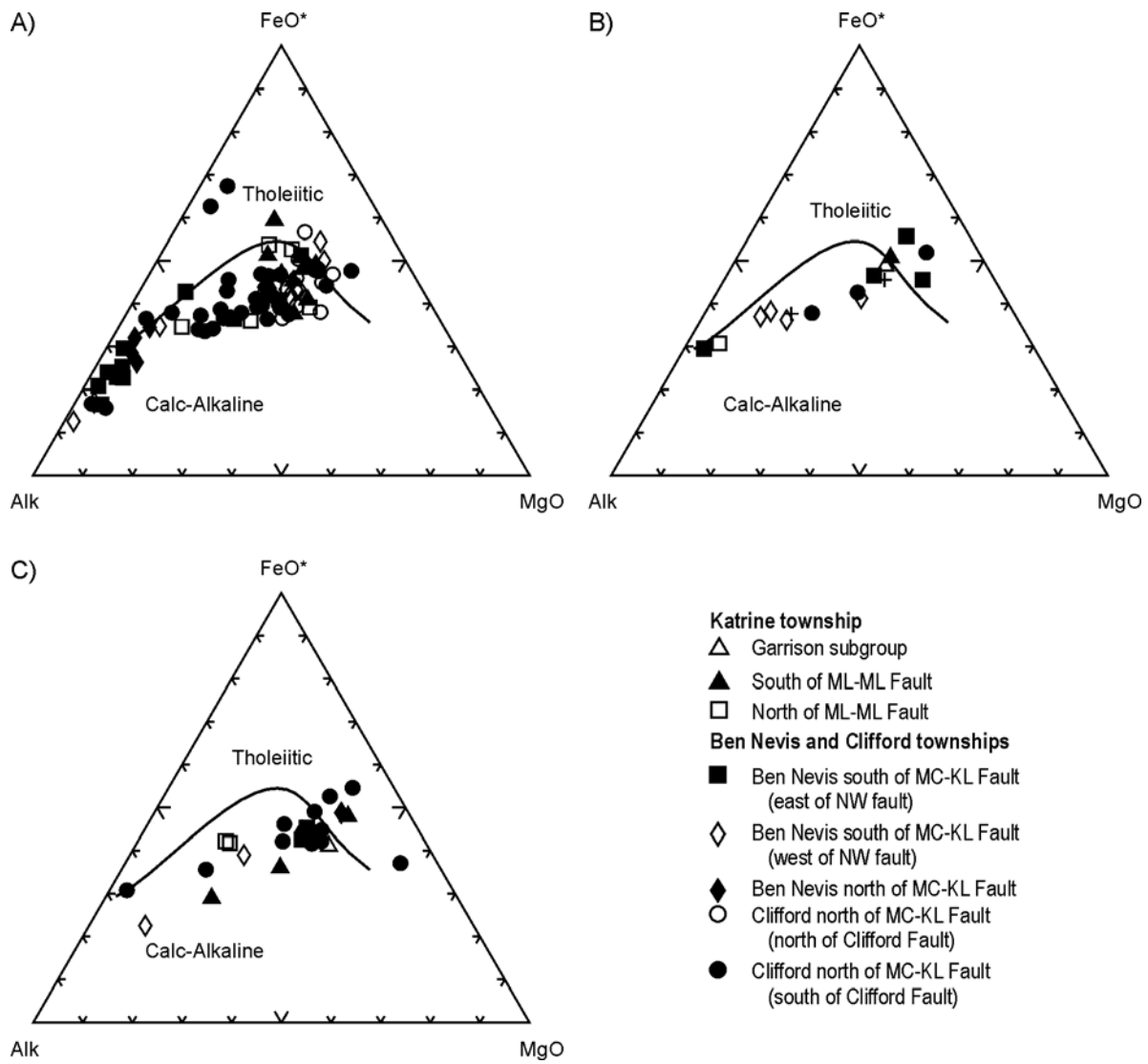


Figure 11. AFM diagram (Irvine and Baragar 1971; plotted using IgPet2001) for a) the volcanic rocks; b) the high-level synvolcanic intrusions; c) the intrusive rocks.
 (ML-ML Fault = Mist Lake–Misema Lake fault; MC-KL Fault = Murdoch Creek–Kennedy Lake fault)

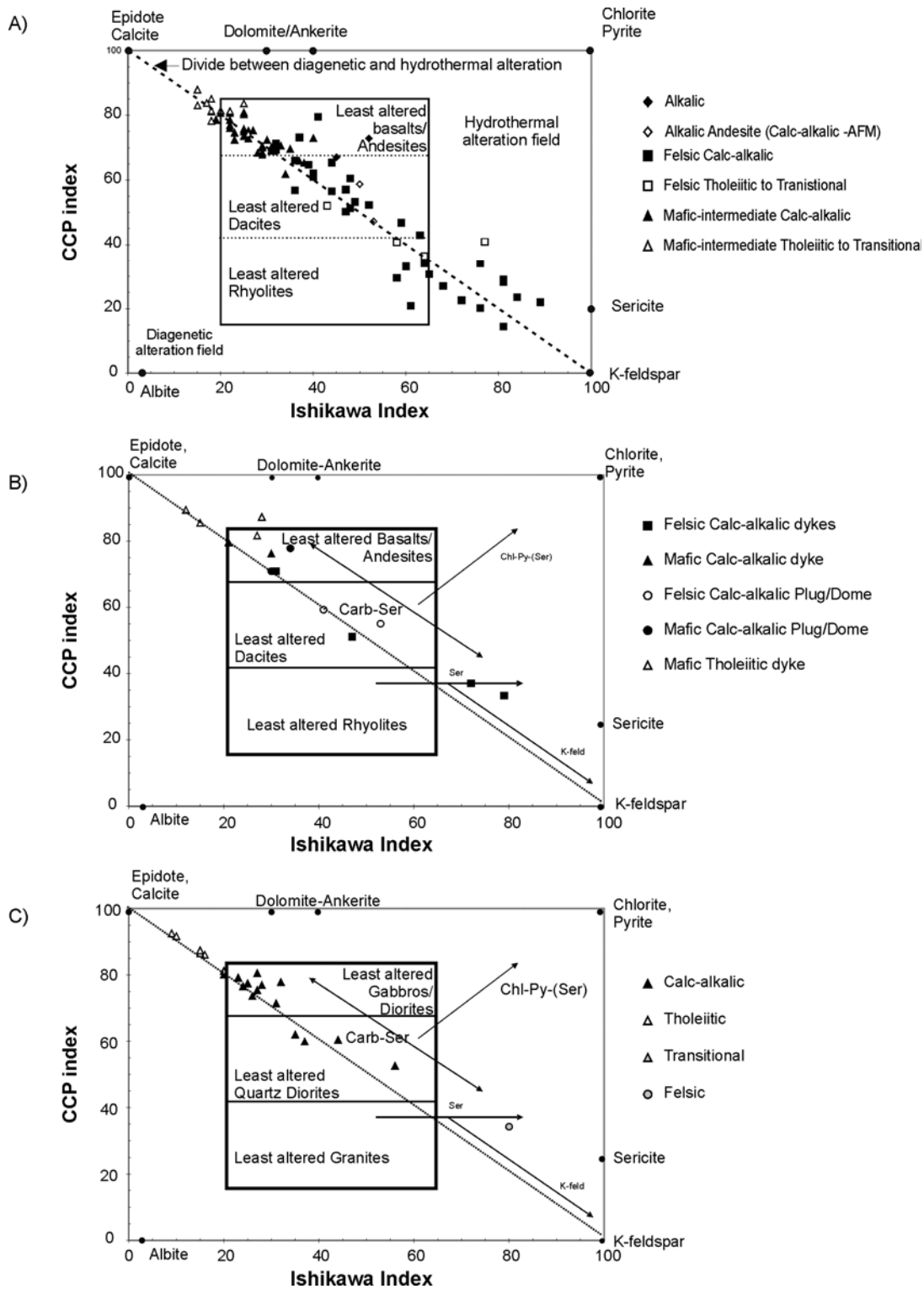


Figure 12. Alteration box plot (Large et al. 2001) for a) the volcanic rocks; b) the high-level synvolcanic intrusions; c) the intrusive rocks. Figure a) indicates the hydrothermal and diagenetic alteration fields; figures b) and c) show the alteration mineral assemblage progressions.

$$\text{Ishikawa index} = 100 \times (\text{K}_2\text{O} + \text{MgO}) / (\text{K}_2\text{O} + \text{MgO} + \text{Na}_2\text{O} + \text{CaO}).$$

$$\text{CCP index} = 100 \times (\text{MgO} + \text{FeO}) / (\text{MgO} + \text{FeO} + \text{Na}_2\text{O} + \text{K}_2\text{O})$$

Mafic to Intermediate Volcanic Rocks

On an MgO versus FeO_{total} diagram (Figure 13a), the mafic-intermediate samples (with the notable exception of the 2 samples that fell in the trachybasalt field of the total alkali–silica diagram (LeBas et al. 1986; Figure 10a)) show no iron enrichment. The “tholeiitic” samples have only slightly higher iron contents than the “calc-alkalic” samples, and not the high iron expected of tholeiitic rocks. On TiO₂ and Al₂O₃ versus SiO₂ diagrams (Figures 14a and 15a), the “tholeiitic” and “calc-alkalic” rocks fall in the same fields, again with the exception of the “trachybasalts”, which show low TiO₂ on the TiO₂ versus SiO₂ diagram. This would indicate that there is only one “chemical affinity” in the area, and that the “trachybasalts” most likely contain a sulphide mineral phase, or a high Fe–low Ti oxide phase. The alteration indicated by the alteration box plot (Figure 12a) does not affect the behaviour of the major elements in Figures 13a, 14a and 15a, as most of the samples designated “altered” fall along the trends defined by the “unaltered” samples.

Trace element data supports the hypothesis of a single chemical affinity. On Zr/Y versus Y ppm and (La/Yb)_{cn}¹ versus Yb_{cn} (Figures 16a and 17a), the “tholeiitic” mafic-intermediate samples are not distinguishable from the “calc-alkalic” samples. On the (La/Yb)_{cn} versus Yb_{cn} diagram there appear to be 2 populations of mafic rocks that do not correspond to the “tholeiitic” versus “calc-alkalic” classifications on the AFM diagram (Figure 11a). The populations are divided at Yb approximately 12 x chondrite. The population Yb_{cn} <12 is characterized by chondrite-normalized La/Yb ratios dominantly >4, whereas the population with Yb_{cn} >12 generally has (La/Yb)_{cn} <4. Although the two populations overlap on Yb_{cn} versus SiO₂ wt % and Yb_{cn} versus MgO wt % diagrams (Figures 18a and b), the lower Yb_{cn} value mafic volcanic rocks are not the most mafic, and cannot therefore be the precursors to the higher Yb_{cn} rocks.

On a chondrite-normalized spider diagram (Figure 19), andesites with Yb_{cn} >12 exhibit negative Nb anomalies, small to large positive Zr and Hf anomalies, and both negative and positive Sr anomalies (Figures 19a and b). Samples with negative Sr anomalies have no to small negative Eu anomalies, and negative Ti anomalies; whereas samples with positive Sr anomalies have no Eu anomalies and very small negative Ti anomalies. The Yb_{cn} >12 andesites also exhibit negative Nb anomalies, and positive Zr and Hf anomalies; however, they exhibit negative and positive anomalies for both Sr and Ti (Figures 19a and c). In these samples the Ti anomalies correspond in amplitude and direction to the Sr anomalies. Titanite was observed as an accessory mineral (Thompson 2005) in thin sections of the rocks with positive Sr and Ti anomalies, and the relationship between these elements may be explained by the retention or fractionation of this mineral.

Both andesite types occur in Katrine Township, north and south of the Misema Lake–Mist Lake fault (Figure 19a). Both samples taken in the area previously designated as the Garrison subgroup of the Lower Blake River Group have Yb_{cn} <12. However, Yb_{cn} <12 andesites also occur in the Misema subgroup in Katrine Township; the geochemistry thus supports the geophysical evidence that no lithological boundary occurs in this area.

North of the Murdoch Creek–Kennedy Lake fault in Ben Nevis and Clifford townships, the mafic volcanic rocks sampled had, with two exceptions, Yb_{cn} <12 (Figures 19b and c). There appears to be no relationship between the two anomalous samples: one taken from the northeast corner of Ben Nevis Township; the other from Clifford Township south of the Clifford fault. South of the Murdoch Creek–Kennedy Lake fault, all but one of the mafic volcanic samples had Yb_{cn} >12. The one anomalous sample came from the south limb of the Clifford anticline and is associated with rhyolites that also have low Yb_{cn} values.

¹cn = chondrite normalized

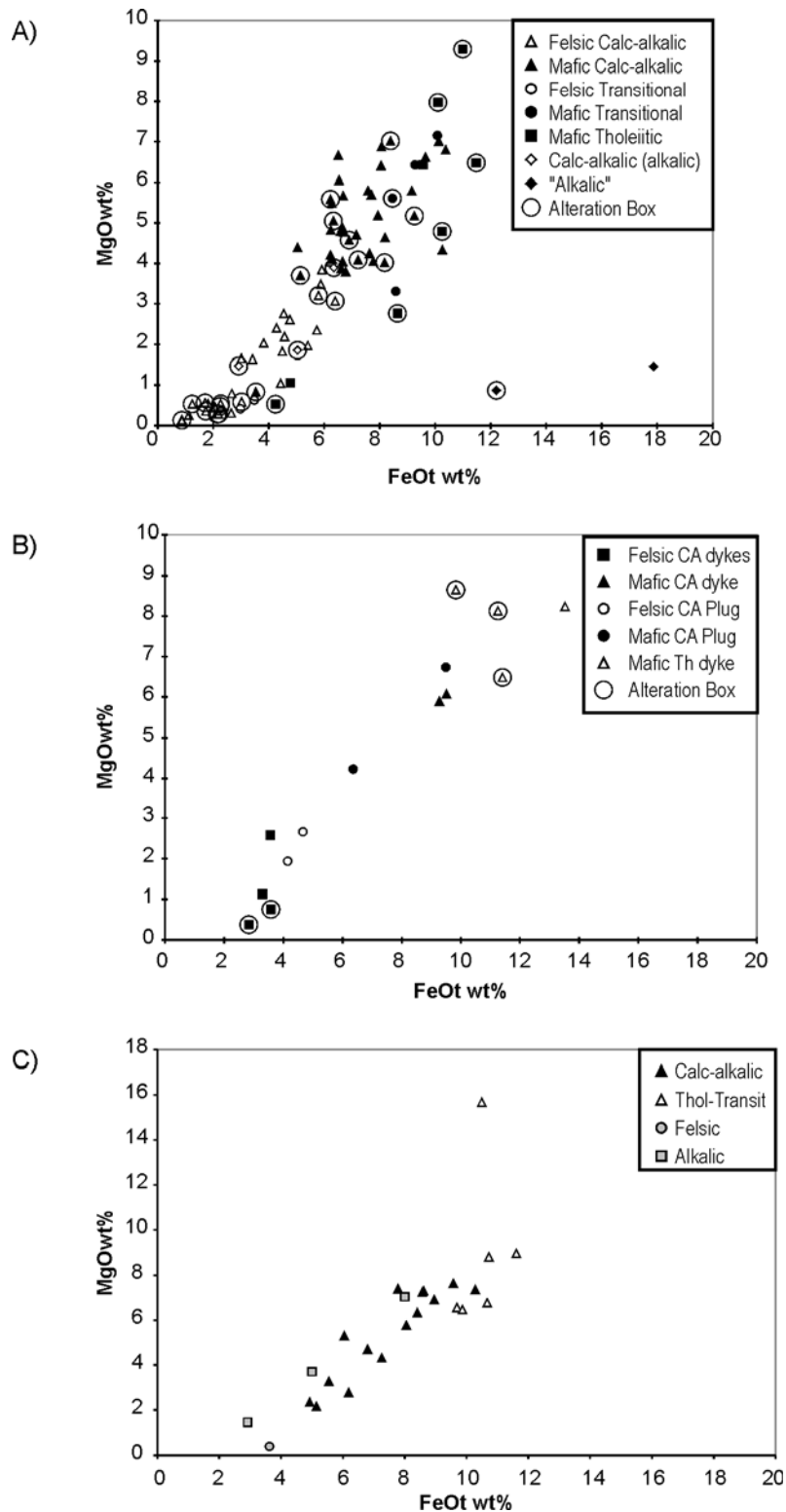


Figure 13. MgO wt % versus FeO_{total} wt % for a) the volcanic rocks; b) the high-level synvolcanic intrusions; c) the intrusive rocks. (CA = Calc-alkalic; Th = Tholeiitic; Thol-Transit = Transitional between Calc-alkalic and Tholeiitic; Alteration Box = samples that fell outside the unaltered boxes on the Large et al. 2001 alteration box plot, Figure 12.)

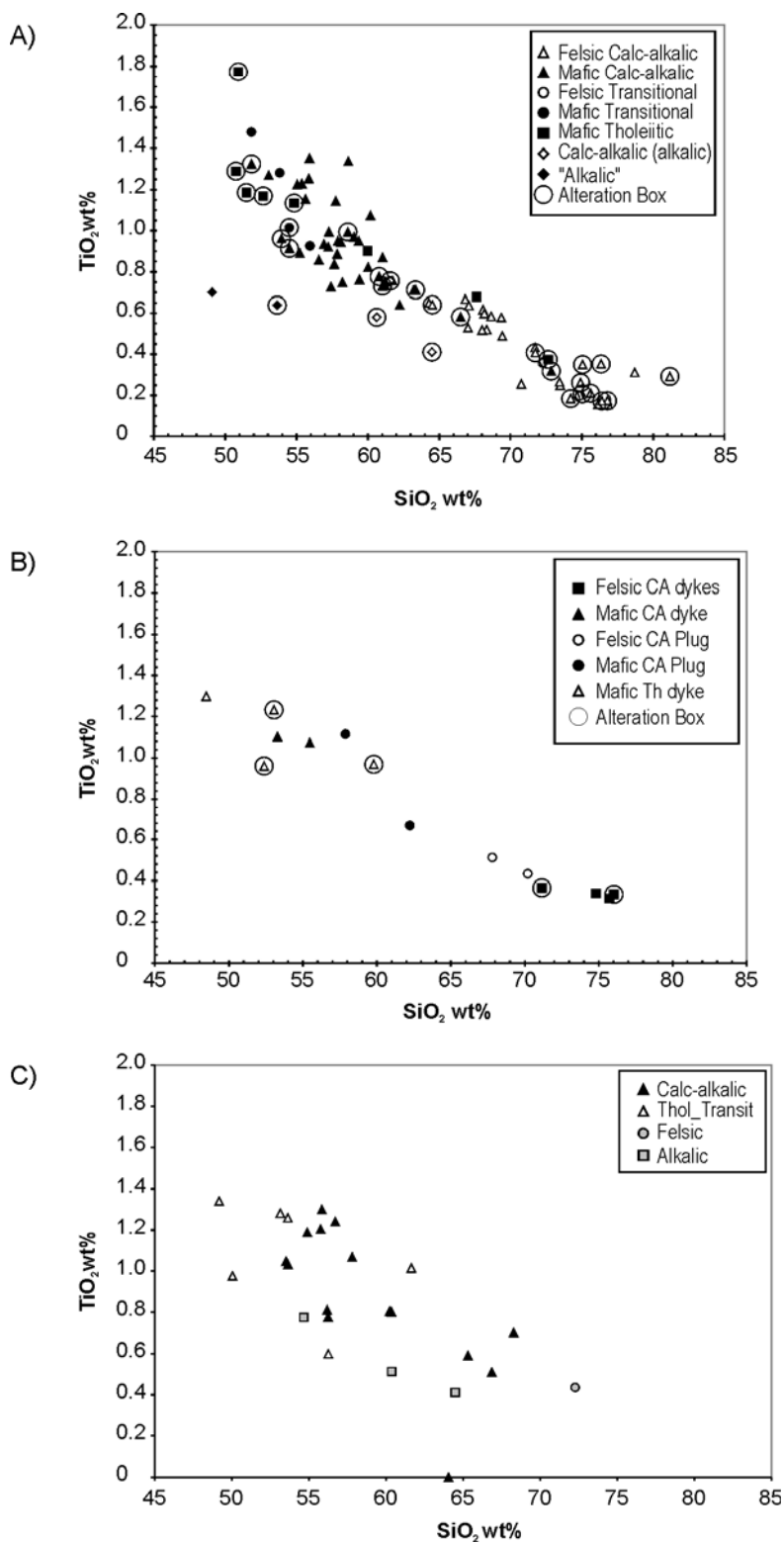


Figure 14. TiO_2 wt % versus SiO_2 wt % for a) the volcanic rocks; b) the high-level synvolcanic intrusions; c) the intrusive rocks. (CA = Calc-alkalic; Th = Tholeiitic; Thol-Transit = Transitional between Calc-alkalic and Tholeiitic; Alteration Box = samples that fell outside the unaltered boxes on the Large et al. 2001 alteration box plot, Figure 12.)

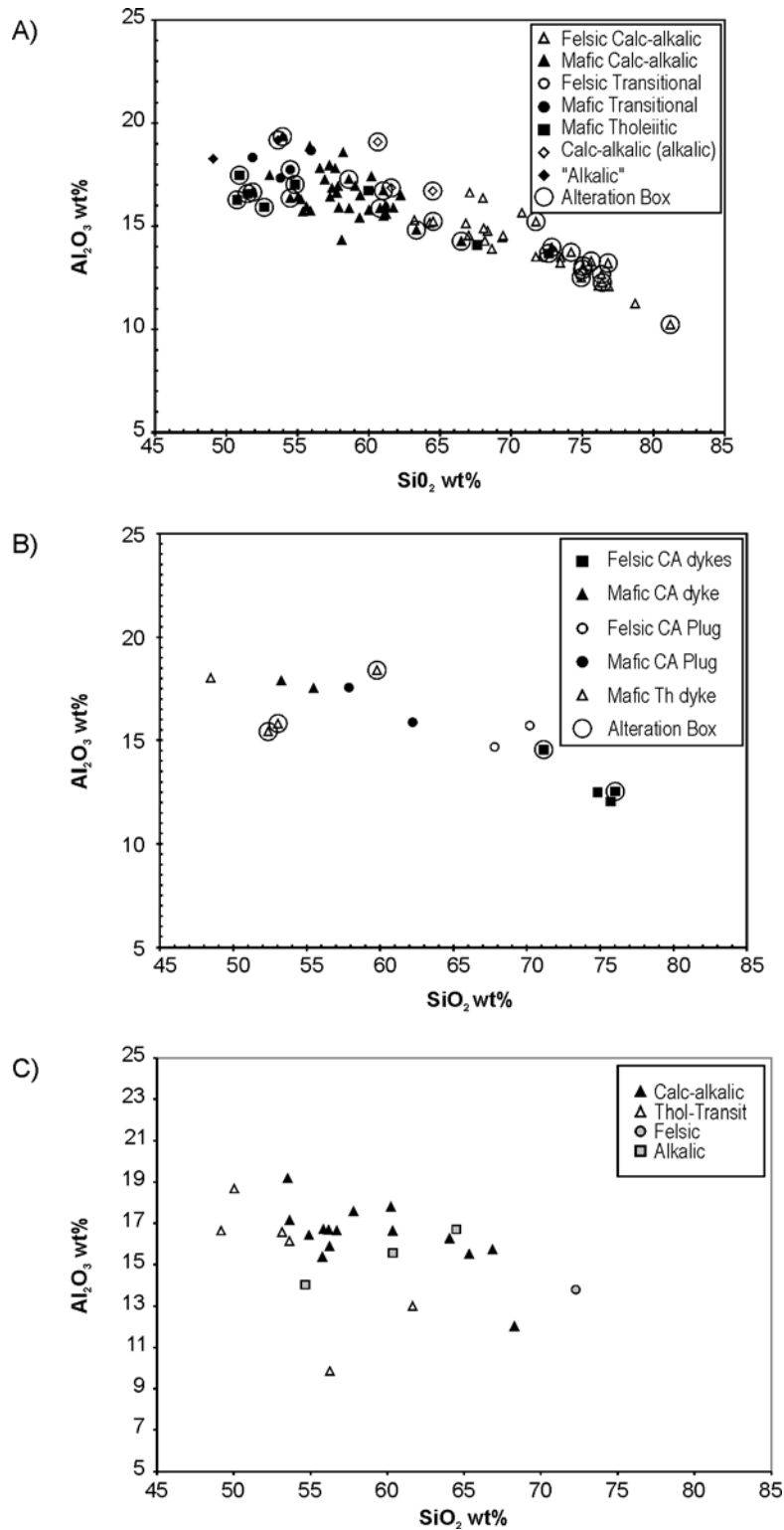


Figure 15. Al_2O_3 wt % versus SiO_2 wt % for a) the volcanic rocks; b) the high-level synvolcanic intrusions; c) the intrusive rocks. (CA = Calc-alkalic; Th = Tholeiitic; Thol-Transit = Transitional between Calc-alkalic and Tholeiitic; Alteration Box = samples that fell outside the unaltered boxes on the Large et al. 2001 alteration box plot, Figure 12.)

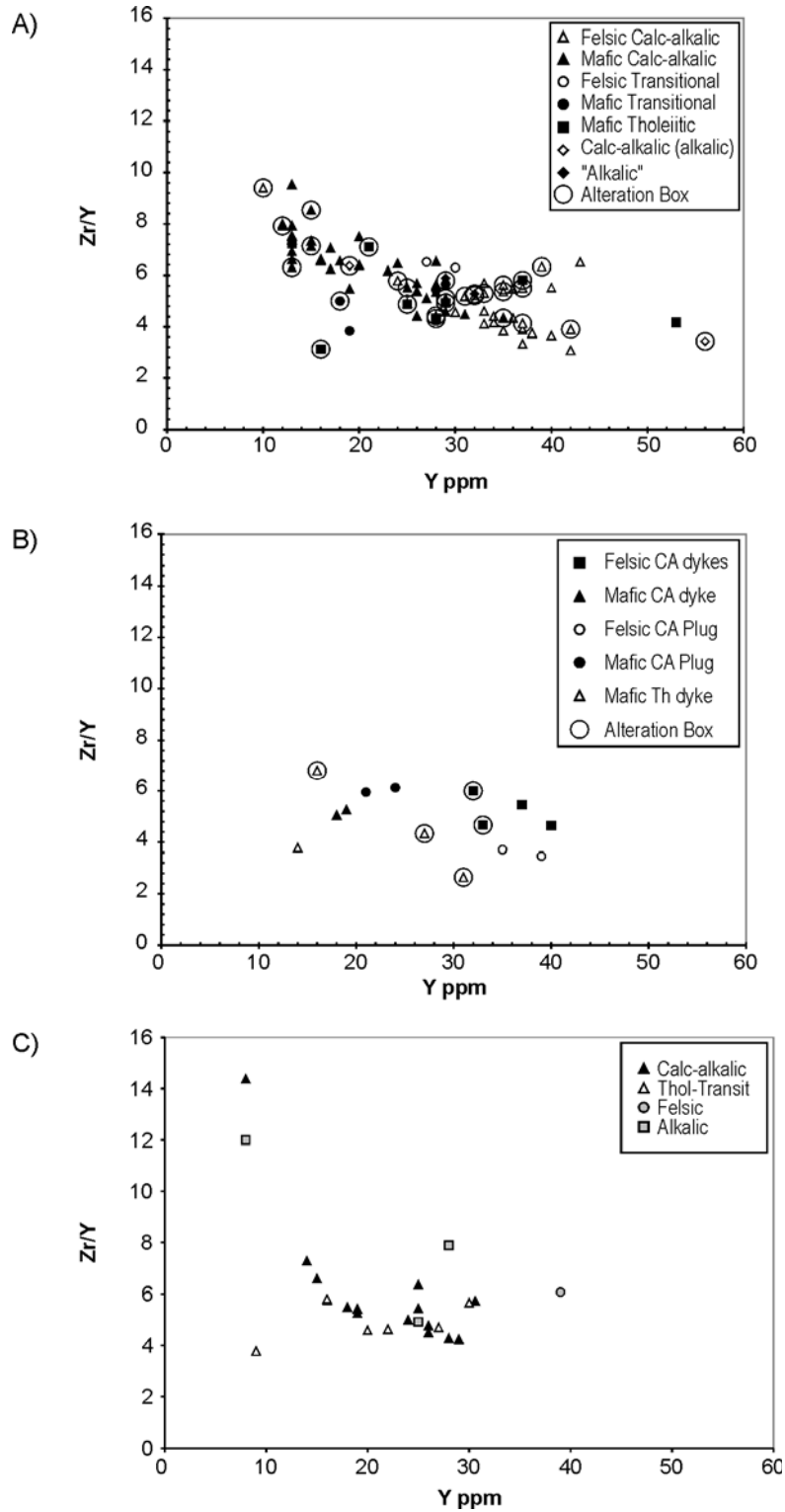


Figure 16. Zr/Y versus Y ppm for a) the volcanic rocks; b) the high-level synvolcanic intrusions; c) the intrusive rocks. (CA = Calc-alkalic; Th = Tholeiitic; Thol-Transit = Transitional between Calc-alkalic and Tholeiitic; Alteration Box = samples that fell outside the unaltered boxes on the Large et al. 2001 alteration box plot, Figure 12.)

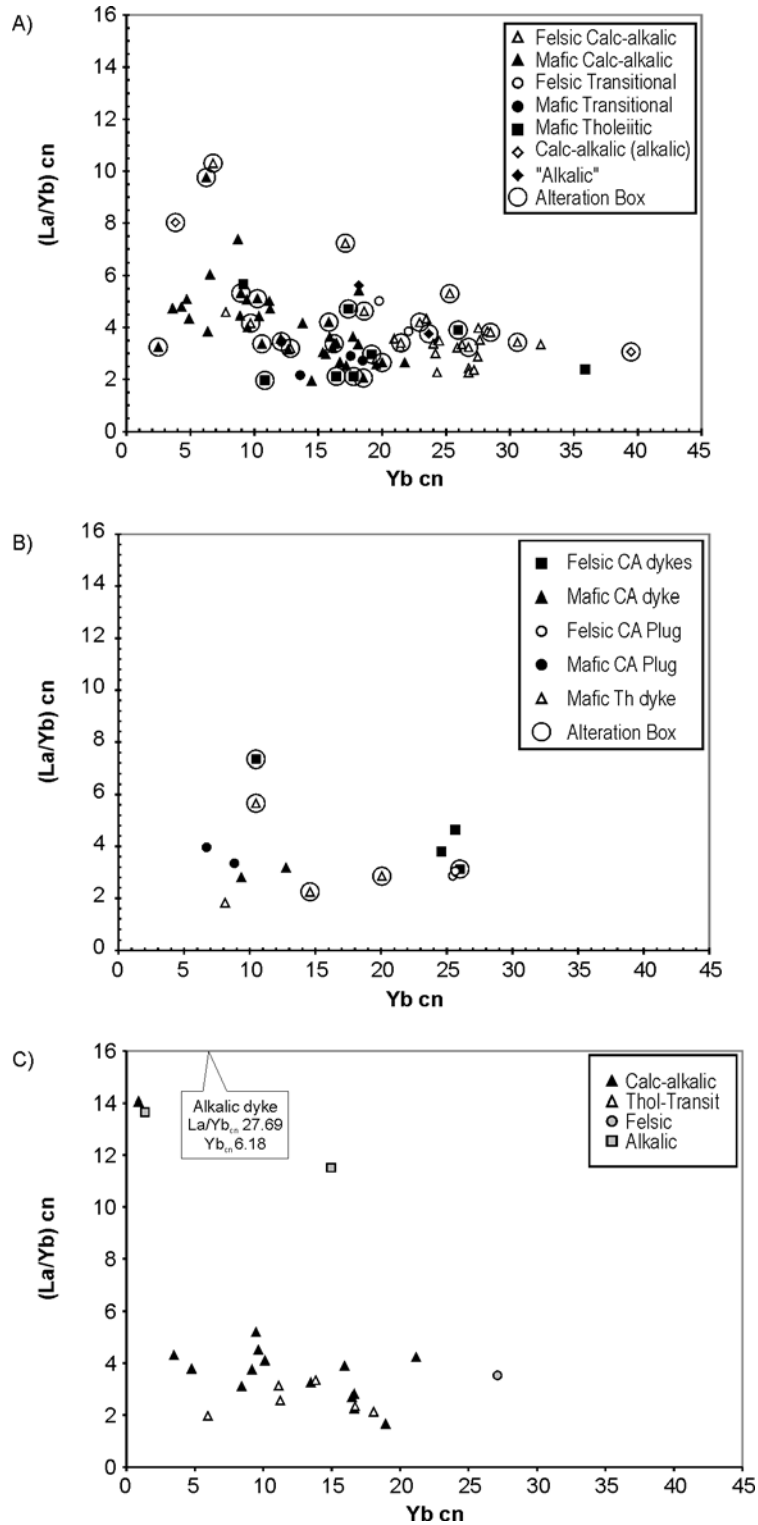


Figure 17. $(La/Yb)_{cn}$ versus Yb_{cn} for a) the volcanic rocks; b) the high-level synvolcanic intrusions; c) the intrusive rocks. (CA = Calc-alkalic; Th = Tholeiitic; Thol-Transit = Transitional between Calc-alkalic and Tholeiitic; Alteration Box = samples that fell outside the unaltered boxes on the Large et al. 2001 alteration box plot, Figure 12.)

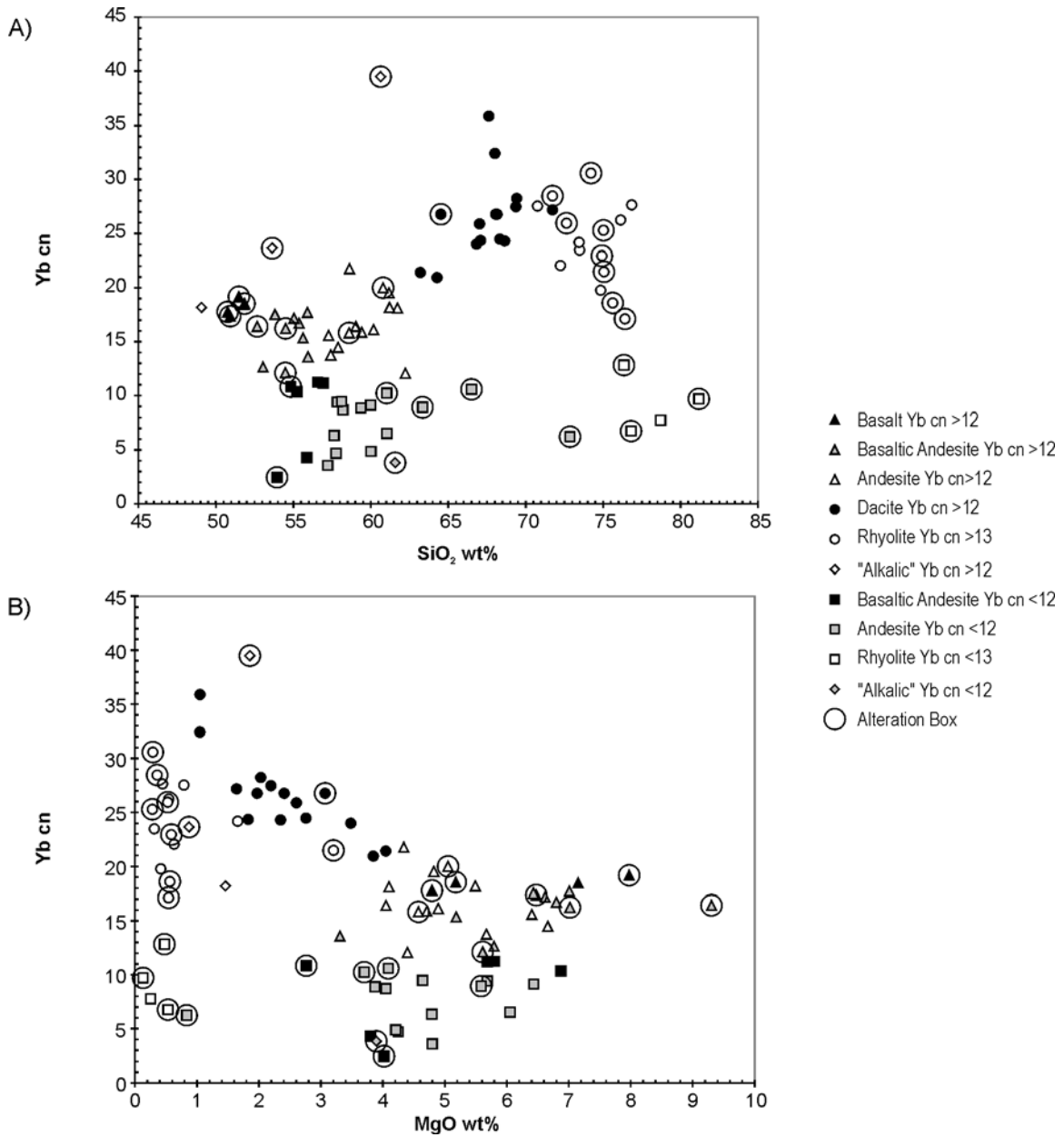


Figure 18. Yb_{cn} versus a) SiO₂ wt % and b) MgO wt % for the volcanic rocks. (Alteration Box = samples that fell outside the unaltered boxes on the Large et al. 2001 alteration box plot, Figure 12.)

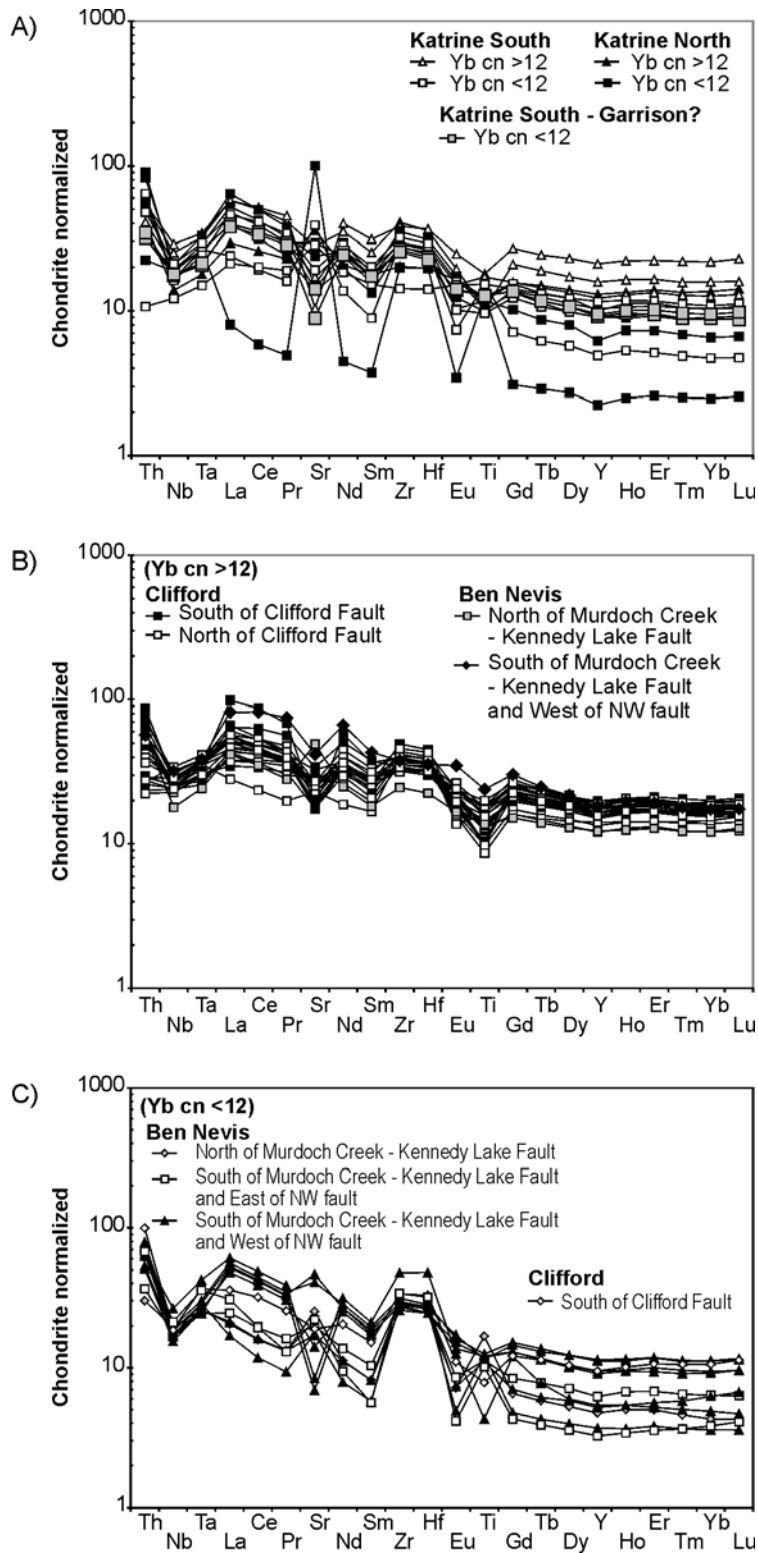


Figure 19. Chondrite-normalized spider plots for the mafic-intermediate volcanic rocks: a) Katrine Township mafic-intermediate volcanic rocks, both $Yb_{cn} < 12$ and > 12 ; b) Clifford and Ben Nevis township mafic-intermediate volcanic rocks with $Yb_{cn} > 12$; c) Clifford and Ben Nevis township mafic-intermediate volcanic rocks with $Yb_{cn} < 12$. (Chondrite normalizing values are C1 chondrite from Sun and McDonough 1989.)

Felsic Volcanic Rocks

The felsic rocks in Ben Nevis and Clifford townships are nearly equal proportions of dacites to rhyolites. On the AFM diagram (Figure 11a), the samples fall within the calc-alkalic field. Only 2 samples fall in the tholeiitic field: one is an isolated dacite near the western Ben Nevis Township boundary, south of the Murdoch Creek–Kennedy Lake fault, and the second is a rhyolite flow adjacent to the cryptodome in Ben Nevis Township south of the Clifford fault. No difference between the “calc-alkalic” and “tholeiitic” felsic rocks is seen on major element plots (Figures 13a, 14a and 15a).

On the Zr/Y versus Y ppm diagram, there are two populations of felsic rocks (Figure 16a). One has Zr/Y ratios over 5; the ratios remain the same with increasing Y ppm. The other has Zr/Y ratios below 5 and exhibits decreasing Zr/Y ratios with increasing Y. This trend is due to Zr contents remaining stable in the second population as Y contents increase. On a $(La/Yb)_{cn}$ versus Yb_{cn} diagram (Figure 17a), the samples with Zr/Y over 5 are not easily distinguishable from those with Zr/Y less than 5. However, on the $(La/Yb)_{cn}$ versus Yb_{cn} diagram of Lesher et al. (1986; Figure 20a), the felsic rocks with Zr/Y <5 have slightly lower La/Yb_{cn} . This is also seen on a Zr/Y versus $(La/Yb)_{cn}$ diagram (Figure 20b). The samples with Zr/Y over 5 exhibit higher La/Yb_{cn} ratios, with an overlap in La/Yb_{cn} ratios between 3.2 and 3.9. On a La_{cn} versus Yb_{cn} diagram (Figure 20c), both populations exhibit grossly increasing La_{cn} with increasing Yb_{cn} , but the Zr/Y >5 samples have higher La_{cn} values for the same Yb_{cn} values as the Zr/Y <5 samples.

Lesher et al. (1986) classified the Misema rhyolites as FII, and the felsic volcanic samples in this study fall within their criteria (Table 1). It should be noted, however, that there is considerable overlap between FII and FIIIa rhyolites (Lesher et al. 1986; Hart et al. 2004; Table 1).

Table 1. Geochemical criteria for the classification of rhyolites into F-types (Lesher et al. 1986; Hart et al. 2004).

Rhyolite Type	Y (ppm)	Yb (ppm)	Sc (ppm)	$(La/Yb)_{cn}$ ³	$(La/Yb)_{cn}$ ⁴	$(La/Yb)_{cn}$ ⁵	Zr/Y
FII (Magusi) ¹	38-48	3.9-5.8	7.8-12	2.3-2.7	--	4.37-5.13	6.2-7.0
FII ²	11-73	1.3-7.9	--	--	1.3-8.8	1.39-9.42	3.2-12.12
FIIIa (Noranda) ¹	25-70	3.4-9.3	7.0-20	1.5-2.8	--	2.85-5.32	3.9-6.8
FIIIa ²	25-96	3.4-9.3	--	--	1.5-3.5	1.61-3.75	3.9-7.7
This study (Zr/Y <5)	29-56	3.56-6.7	3-11.9	2.07-3.54	2.10-3.32	2.26-3.86	3.07-4.61
This study (Zr/Y >5)	10-43	1.15-5.51	2-10.1	2.94-9.47	2.98-9.62	3.2-10.32	5.19-9.4

¹ Lesher et al. 1986

² Hart et al. 2004

³ (Leedy chondrite from Masuda et al. (1973))/1.20

⁴ Average of 10 chondrites, from Nakamura (1974)

⁵ C1 chondrite from Sun and McDonough (1989)

On spider diagrams (Figure 21a and b), the Zr/Y <5 felsic rocks exhibit similar HREE, and similar to slightly lower LREE compared to the Zr/Y >5 felsic rocks. A distinct subpopulation of 4 samples occurs within the Zr/Y >5 population. This subpopulation has Yb_{cn} <13. Two of these samples were from the same area in the southwestern part of Ben Nevis Township where the andesite with Yb_{cn} <12 occurred, indicating a possible relationship between the low Yb_{cn} populations. The third sample was from the small felsic plug (possibly a cryptodome) in the southwestern part of Ben Nevis Township along the axis of the Clifford anticline. The fourth sample was from the southernmost part of the area south of the Clifford fault in Clifford Township. All but one of the felsic samples, in both Zr/Y >5 and <5 populations, show negative Nb, Sr, Eu and Ti anomalies, and positive Zr and Hf anomalies. The anomalous sample has Yb_{cn} <12 and is from the south limb of the Clifford anticline in Ben Nevis Township; it exhibits a positive Sr anomaly with a negative Eu anomaly. This is believed to be an alteration effect.

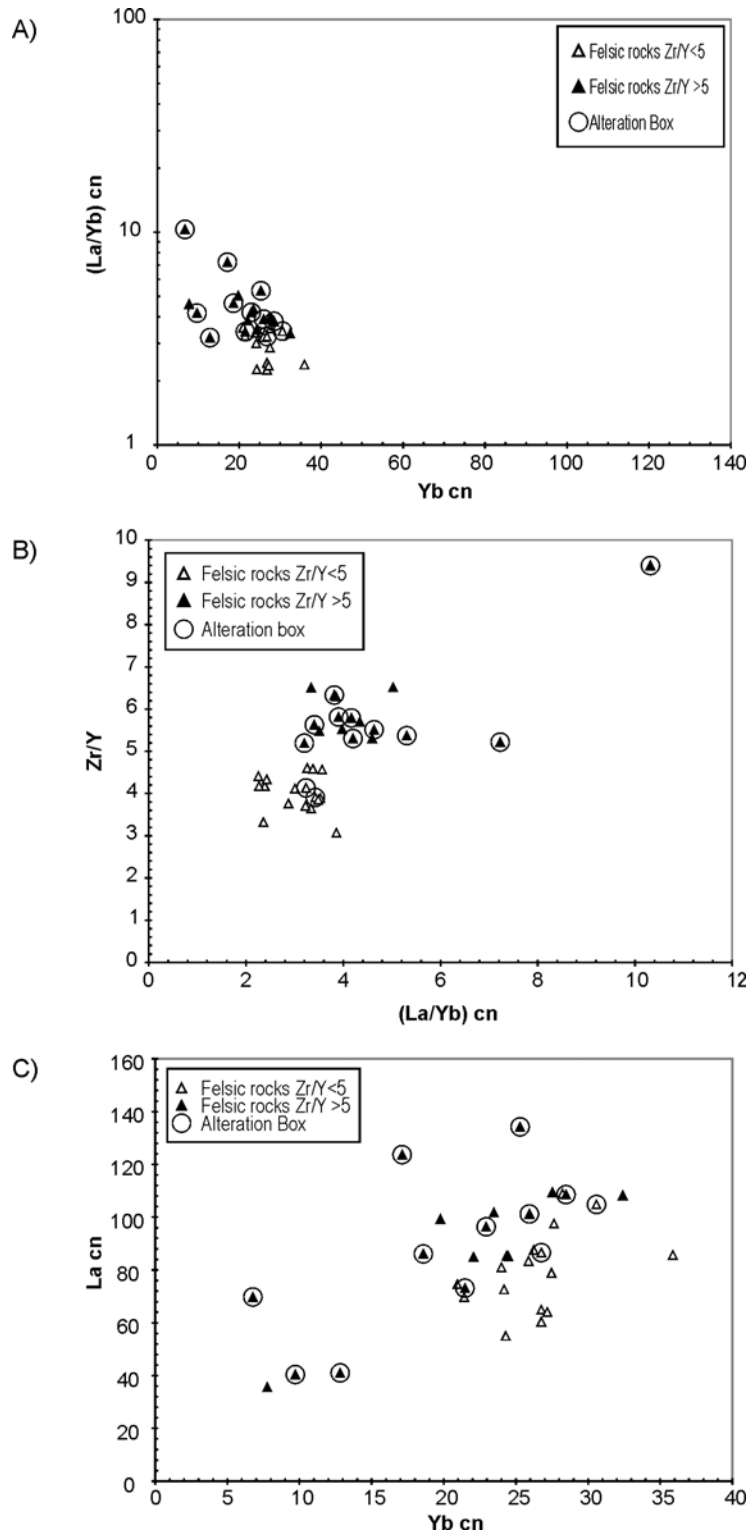


Figure 20. a) $(La/Yb)_{cn}$ versus Yb_{cn} diagram from Leshner et al. (1986) for the felsic volcanic rocks; b) Zr/Y versus $(La/Yb)_{cn}$ diagram for the felsic volcanic rocks; c) La_{cn} versus Yb_{cn} diagram for the felsic volcanic rocks. (Alteration Box = samples that fell outside the unaltered boxes on the Large et al. 2001 alteration box plot, Figure 12.)

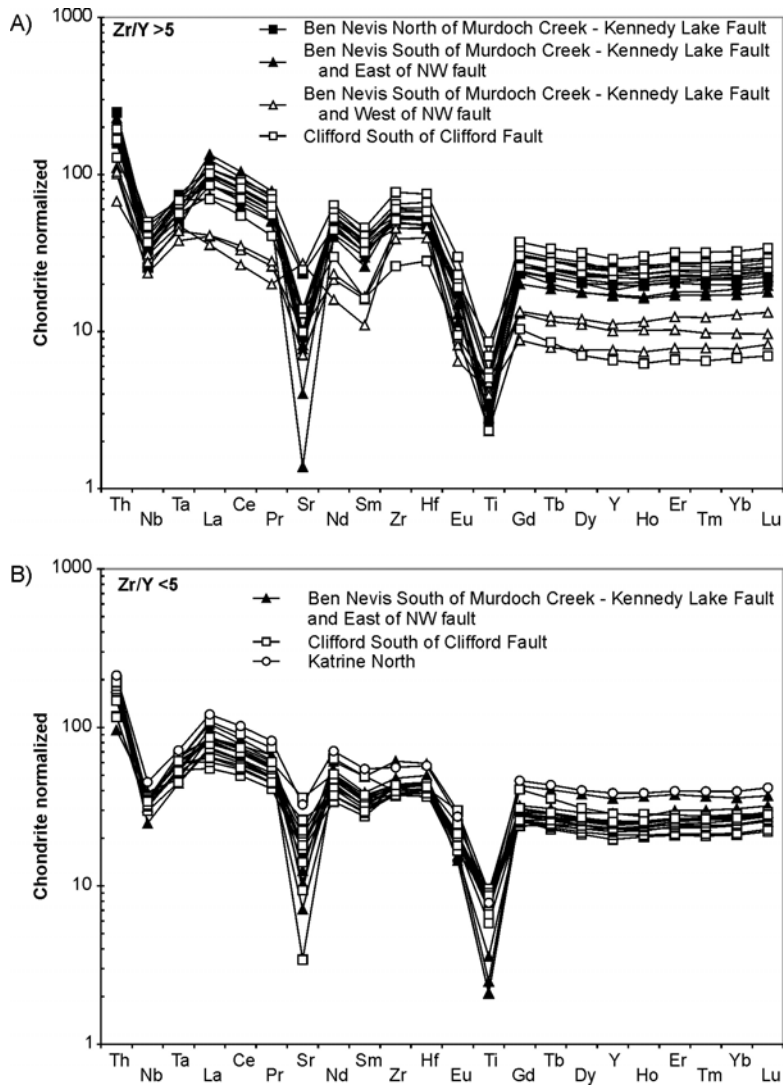


Figure 21. Chondrite normalized spider plots for the felsic volcanic rocks: a) felsic volcanic rocks with $Zr/Y > 5$; b) felsic volcanic rocks with $Zr/Y < 5$. (Chondrite normalizing values are C1 chondrite from Sun and McDonough 1989.)

The $Zr/Y < 5$ rhyolites occur throughout Ben Nevis and Clifford townships, whereas the $Zr/Y > 5$ rhyolites occur only in the Canagau rhyolite area and immediately south of the Clifford fault. Notably, 8 of the $Zr/Y < 5$ samples come from 2 drill holes in the South Clifford block. The sole felsic volcanic rock observed in Katrine Township occurs north of the Misema Lake–Mist Lake fault near the Ben Nevis–Katrine township boundary. This dacite has $Zr/Y < 5$ and is the most evolved of the samples on the spider diagram (Figure 21b), but is otherwise not distinguishable from the other felsic volcanic rocks.

Using the method of Watson and Harrison (1983), zircon saturation temperatures were calculated for the rhyolites in Ben Nevis and Clifford townships (Table 2). Zircon saturation temperatures are the temperatures at which zircon saturates in a melt and begins to crystallize (Watson and Harrison 1983); this is argued to be close to the temperature of emplacement. The rhyolites having Zr/Y ratio > 5 generally have Zr saturation temperatures $> 775^{\circ}\text{C}$, whereas the rhyolites with $Zr/Y < 5$ have lower temperatures (Figure 22a). Seven rhyolite samples gave Zr saturation temperatures $> 800^{\circ}\text{C}$. They occur in the South

Clifford Block rhyolites (including the rhyolite adjacent to the cryptodome), in the rhyolites in the Canagau Mine area, and in a pyroclastic rhyolite north of the Murdoch Creek–Kennedy Lake fault in Ben Nevis Township. The rhyolite sample giving a Zr saturation temperature of 897°C is microcrystalline, equigranular, aphyric to sparsely quartz microphyric, compared to the other rhyolites sampled that were clearly plagioclase or quartz-plagioclase phyric. The rhyolite sample was taken from a mechanically stripped outcrop in the Interprovincial North showing area, which exhibited intense chlorite alteration and associated sulphide mineralization.

Table 2. Calculated Zr saturation temperature for the rhyolites (using method of Watson and Harrison 1983). (MC-KL = Murdoch Creek–Kennedy Lake)

Sample number	Zr/Y	T (°C)	Classification	Structural Block
03ASP0068.1.1	<5	760	Dacite	Ben Nevis south of MC-KL fault and east of NW fault
03ASP0146.1.1	<5	774	Rhyolite	Ben Nevis south of MC-KL fault and east of NW fault
03ASP0179.1.1	<5	759	Rhyolite	Ben Nevis south of MC-KL fault and east of NW fault
03ASP0170.1.1	<5	767	Rhyolite	Ben Nevis south of MC-KL fault and east of NW fault
03ASP0176.1.1	<5	774	Rhyolite	Ben Nevis south of MC-KL fault and east of NW fault
WC04-03, 62.65-62.79	<5	743	Dacite Tuff	Clifford south of Clifford fault
P03-001	<5	746	Dacite	Clifford south of Clifford fault
03SJP088-1	<5	774	Dacite	Clifford south of Clifford fault
WC04-03, 68.12-68.25	<5	763	Dacite Tuff	Clifford south of Clifford fault
03SJP031-1-1	<5	772	Dacite	Clifford south of Clifford fault
P03-003	<5	741	Dacite	Clifford south of Clifford fault
WC04-03, 131.59-131.7	<5	762	Dacite Tuff	Clifford south of Clifford fault
WC04-08, 123.7-123.9	<5	755	Dacite Tuff	Clifford south of Clifford fault
WC04-03, 154.75-154.90	<5	745	Dacite Tuff	Clifford south of Clifford fault
WC04-03, 146.0-146.16	<5	766	Dacite Tuff	Clifford south of Clifford fault
WC04-08, 132.4-132.55	<5	750	Dacite Tuff	Clifford south of Clifford fault
WC04-03, 76.27-76.41	<5	750	Dacite Tuff	Clifford south of Clifford fault
03ASP0144.1.2	>5	819	Rhyolite Lapilli Tuff	Ben Nevis north of MC-KL fault
03ASP0143.1.1	>5	788	Rhyolite Lapilli Tuff	Ben Nevis north of MC-KL fault
03ASP0135.1.2	>5	775	Rhyolite Massive	Ben Nevis north of MC-KL fault
03ASP0141.1.3	>5	777	Rhyolite Massive	Ben Nevis north of MC-KL fault
03ASP0175.1.1	>5	780	Rhyolite Massive	Ben Nevis south of MC-KL fault and east of NW fault
03ASP0087.1.1	>5	790	Rhyolite Lobe & Breccia	Ben Nevis south of MC-KL fault and east of NW fault
03ASP0121.1.1	>5	806	Rhyolite Lobe & Breccia	Ben Nevis south of MC-KL fault and east of NW fault
03ASP0147.1.1	>5	897	Rhyolite Lobe & Breccia	Ben Nevis south of MC-KL fault and east of NW fault
03ASP0075.1.1	>5	784	Rhyolite Massive	Ben Nevis south of MC-KL fault and east of NW fault
03ASP0028.1.1	>5	776	Rhyolite Breccia	Ben Nevis south of MC-KL fault and west of NW fault
03ASP0027.1.1	>5	772	Rhyolite Breccia	Ben Nevis south of MC-KL fault and west of NW fault
03ASP0059.2.1	>5	788	Rhyolite Massive	Ben Nevis south of MC-KL fault and west of NW fault
03SJP053-1	>5	808	Dacite	Clifford south of Clifford fault
WC04-08, 158.61-158.94	>5	829	Dacite	Clifford south of Clifford fault
03SJP068-1-1	>5	748	Rhyolite	Clifford south of Clifford fault
03SJP068-36	>5	805	Rhyolite	Clifford south of Clifford fault
03ASP0133.1.1	>5	807	Rhyolite Massive	Clifford south of Clifford fault

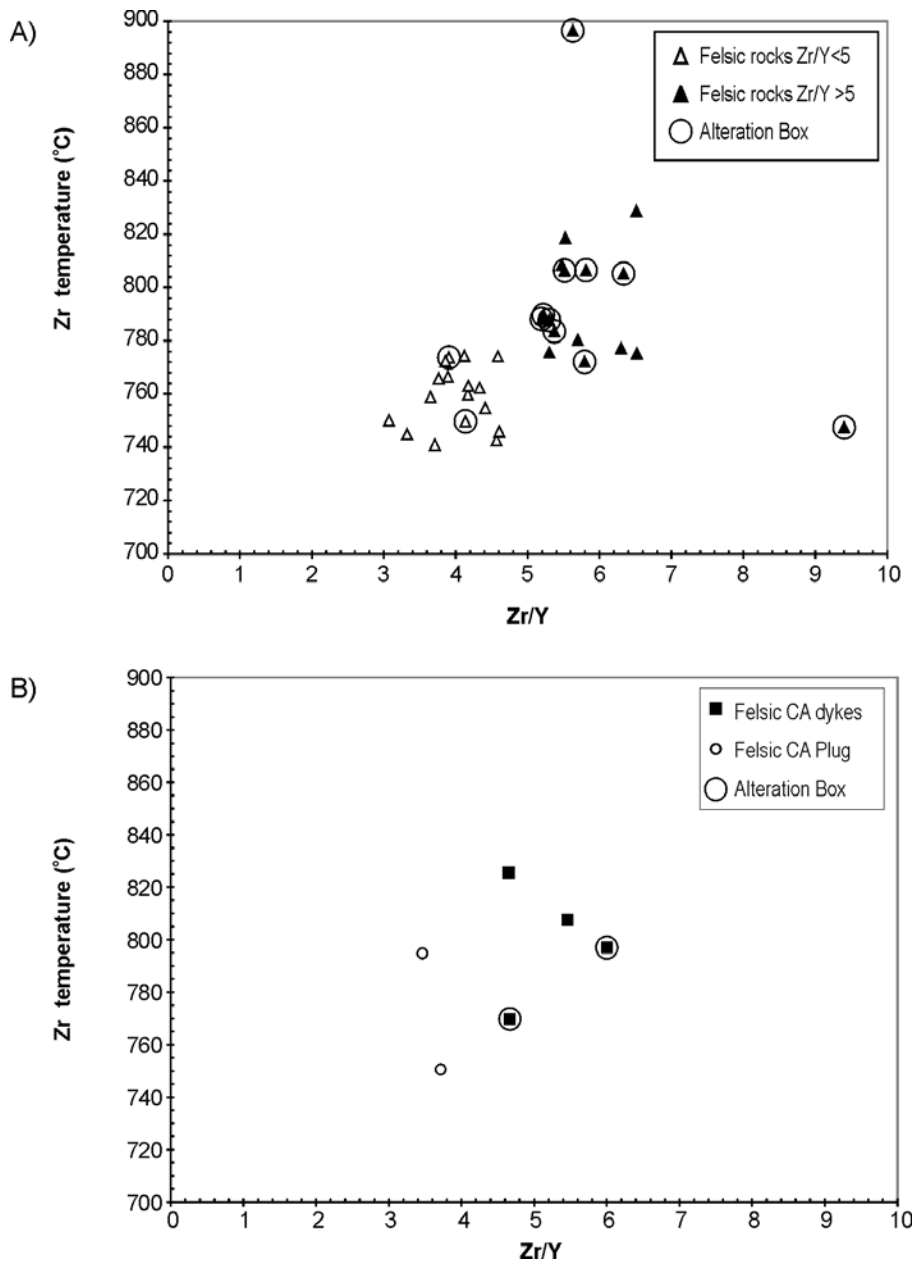


Figure 22. Calculated Zr saturation temperature (°C) versus Zr/Y for a) the felsic volcanic rocks, and b) the felsic high-level synvolcanic intrusions. (Alteration Box = samples that fell outside the unaltered boxes on the Large et al. 2001 alteration box plot, Figure 12.)

INTRUSIVE ROCKS

Three types of intrusive rocks will be presented in this section: high-level synvolcanic intrusions including dykes and cryptodomes or plugs, Blake River diorite dykes and intrusions, and a late alkalic stock with associated dykes.

High-Level Synvolcanic Intrusions

The high-level synvolcanic intrusions take two forms: dykes that, without contact relationships, would be mapped as volcanic; and intrusive masses that include breccia phases and are interpreted as cryptodomes or plugs.

On the LeBas et al. (1986) classification diagram (Figure 10b), the high-level synvolcanic intrusions all fall within the sub-alkalic field and exhibit the same rock types as the extrusive rocks: basalts through andesites to rhyolites. These synvolcanic intrusion samples also fall along the same trend as the volcanic samples on the Irvine and Baragar (1971) AFM plot (Figure 11b), with most of the samples being calc-alkalic in nature. On the Large et al. (2001) alteration box plot (Figure 12b), the syn-volcanic intrusions resemble the volcanic rocks in that they fall along the diagenetic–hydrothermal alteration divide line, most of the “tholeiitic” rocks fall outside the least altered box toward the Epidote-Carbonate corner, and the “altered” felsic rocks indicate carbonatization or sericitization. On major element and trace element plots (Figures 13b, 14b, 15b, 16b and 17b), the similarity between the synvolcanic intrusions and the volcanic rocks is also evident. There is not, however, enough data for the synvolcanic intrusions to define the populations seen in the volcanic rocks. On chondrite-normalized spider diagrams (Figure 23a), the mafic-intermediate synvolcanic intrusions appear similar to the mafic volcanic rocks with $Yb_{cn} > 12$ (Figure 19b), with the exception of an andesite dyke intruding the heterolithic andesite lapilli tuff in Katrine Township south of the Misema Lake–Mist Lake fault. The felsic synvolcanic dykes have spider diagram patterns (Figure 23b) resembling the felsic volcanic rocks (Figure 21); the felsic dyke with low chondrite-normalized heavy rare earth values ($Yb_{cn} = 10.47$) was intruded into the diorite lying south of the Canagau rhyolite. Its pattern is similar to that of the rhyolite from the southernmost part of Clifford Township (Figure 21a). The two subvolcanic intrusions—the cryptodome between the Murdoch Creek–Kennedy Lake and the Clifford faults in Ben Nevis Township, and the composite quartz-feldspar porphyry plug at the Ben Nevis–Katrine township boundary—exhibit similar spider diagram patterns for both their felsic and mafic phases (Figure 23c). The felsic (QFP) phases resemble the felsic synvolcanic dykes, and therefore, the rhyolites of the area. The spider diagram patterns of the mafic-intermediate phases do not, however, resemble the mafic-intermediate synvolcanic dykes (Figure 23a), instead resembling the patterns of the mafic-intermediate volcanics with $Yb_{cn} < 12$ (Figure 19c). Zircon saturation temperature calculations (Table 3; Figure 22b) show that the felsic phase of the cryptodome has a temperature $< 775^{\circ}\text{C}$, as does the felsic dyke from Katrine Township north of the Misema Lake–Mist Lake fault. The composite plug from the Ben Nevis–Katrine township boundary and the felsic dykes have zircon saturation temperatures $> 775^{\circ}\text{C}$, as do the rhyolites with $Zr/Y > 5$ (Figure 22a).

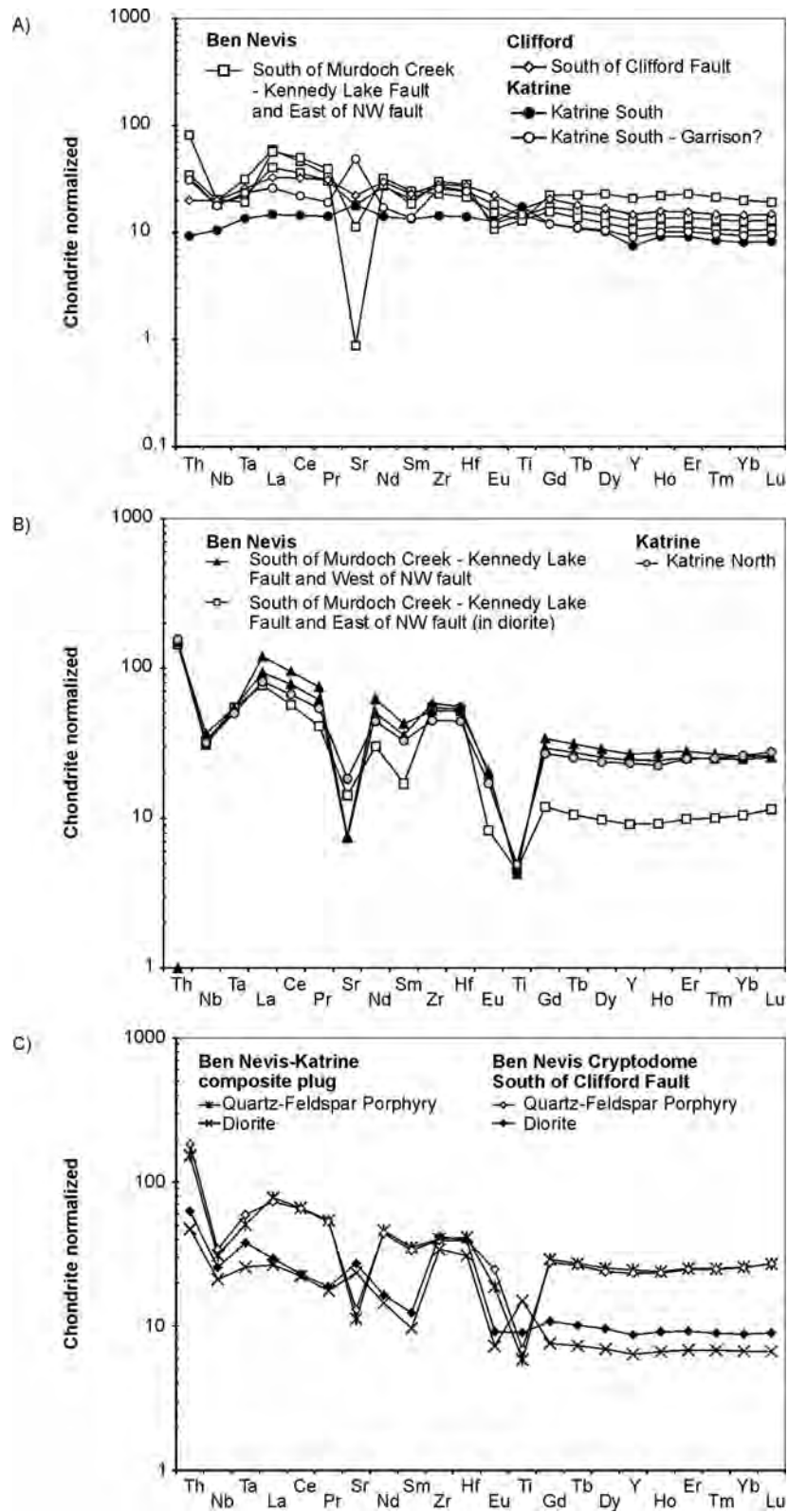


Figure 23. Chondrite-normalized spider plots for the high-level synvolcanic intrusions: a) mafic-intermediate dykes; b) felsic dykes; c) the cryptodome in Ben Nevis Township and the composite plug at the Ben Nevis–Katrine township boundary. (Chondrite normalizing values are C1 chondrite from Sun and McDonough 1989.)

Table 3. Calculated Zr saturation temperature for the high-level synvolcanic intrusions (using method of Watson and Harrison 1983).

Sample number	Zr/Y	T (°C)	Classification	Structural Block
03ASP0126.2.1	6.00	796.98	Rhyolite Dyke	Ben Nevis south of Murdoch Creek–Kennedy Lake fault and east of NW fault
03ASP0198.2.1	4.67	769.78	Rhyolite Dyke	Katrine north of Misema Lake–Mist Lake fault
03ASP0207.2.1	4.65	825.47	Rhyolite Dyke	Ben Nevis south of Murdoch Creek–Kennedy Lake fault and west of NW fault
03ASP0162.2.1	5.46	807.52	Rhyolite Dyke	Ben Nevis south of Murdoch Creek–Kennedy Lake fault and west of NW fault
03ASP0130.1.2	3.71	750.57	Quartz Feldspar Porphyry	Clifford south of Clifford fault
04ASP512-1.1	3.46	794.83	Quartz Feldspar Porphyry	At Ben Nevis–Katrine boundary

Intrusions

The majority of intrusions in the Blake River Group in the study area are mafic to intermediate dykes and irregular masses. A felsic dyke occurs at the western edge of Ben Nevis Township immediately south of the Clifford fault, and an alkalic stock with associated dykes is located in the southeastern corner of Katrine Township.

The nature, alkalic versus subalkalic, and the dominance of mafic and intermediate intrusions are seen on the modified total alkali–silica classification diagram (Figure 10c; LeBas et al. 1986). The alkalic intrusions will not be discussed here. The majority of the sub-alkalic intrusions, like the volcanic rocks and the high-level synvolcanic intrusions, fall in the calc-alkalic field of the Irvine and Baragar (1971) AFM diagram (Figure 11c). The samples falling in the tholeiitic field come from south of the Clifford fault in Clifford Township, the northeast corner of Ben Nevis Township, and immediately south of the Misema Lake–Mist Lake fault in the eastern part of Katrine Township. In the case of the diorite-gabbro intrusion in Ben Nevis Township, a second sample of the intermediate phase falls in the calc-alkalic field. This indicates that, like the volcanic rocks, there is likely only one chemical affinity in this intrusion. On the Large et al. (2001) alteration box plot (Figure 12c), the intrusive rocks behave in the same fashion as the volcanic rocks and the high-level synvolcanic intrusions. On major element diagrams (Figures 13c, 14c and 15c), one sample shows anomalously high MgO content, and lower Al₂O₃ content for the same SiO₂ value as the volcanic rocks. This sample is from a mafic intrusion in Ben Nevis Township south of the Clifford fault. On trace element ratio diagrams (Figures 16c and 17c), the intrusions plot in the same areas as the volcanic rocks with one exception: the gabbro intruding the heterolithic lapilli tuff in Katrine Township has a low Zr/Y ratio with low Y content (Figure 16c) and a low La/Yb_{cn} ratio with a low Yb_{cn} value (Figure 17c). A feldspar-porphyrityc dyke and a quartz-feldspar-porphyrityc dyke from the vicinity of the small rhyolite dome in the nose of the anticline, in the southwest part of Ben Nevis Township, have very high Zr/Y and La/Yb_{cn} ratios (Figures 16c and 17c). These units are likely related to the Clifford intrusive event (*see* MacDonald et al. 2005) and are the only confirmed examples of that event south of the Murdoch Creek–Kennedy Lake fault in Ben Nevis Township. As with the high-level synvolcanic intrusions, there are not enough intrusion samples to delineate the populations observed in the volcanic rocks. In Ben Nevis and Clifford townships, the spider diagram patterns of the intrusive rocks (Figure 24a) resembles those of the mafic to intermediate volcanic rocks with Yb_{cn} > 12 (Figure 17b), although the Yb_{cn} contents of the intrusion samples are as low as 9. The only felsic sample from Clifford Township has a spider pattern similar to, but slightly more evolved than the mafic to intermediate intrusions (Figure 24a). The samples of the porphyry dykes mentioned above (Clifford event; *see* MacDonald et al. 2005) have very low Yb_{cn} values (0.88 and 1.35) and their spider patterns exhibit HREE depletion (Figure 22a). In Katrine Township (Figure 24b), the 2 samples from the mafic-intermediate intrusion sampled north of

the Misema Lake–Mist Lake fault have trace element patterns similar to the adjacent volcanic unit, and to the mafic to intermediate volcanic rocks with $Yb_{cn} < 12$ sampled in Ben Nevis and Clifford townships (Figures 19a and c). The mafic to intermediate intrusion in the heterolithic lapilli tuff south of the Misema Lake–Mist Lake fault has a trace element pattern similar to nearby volcanic units. The sample from the mafic to intermediate stock south of the Mulven Lake fault (Figure 24a, Katrine South-Garrison sample) has as trace element pattern similar to the mafic to intermediate volcanic rocks sampled in that area, and to the majority of samples between the Mulven Lake and Misema Lake–Mist Lake faults, and north of the Misema Lake–Mist Lake fault (Figure 19a). The geochemical similarities between the intrusive rocks and the volcanic rocks suggest that they are part of the synvolcanic intrusive phase of the magmatism forming the Blake River Group.

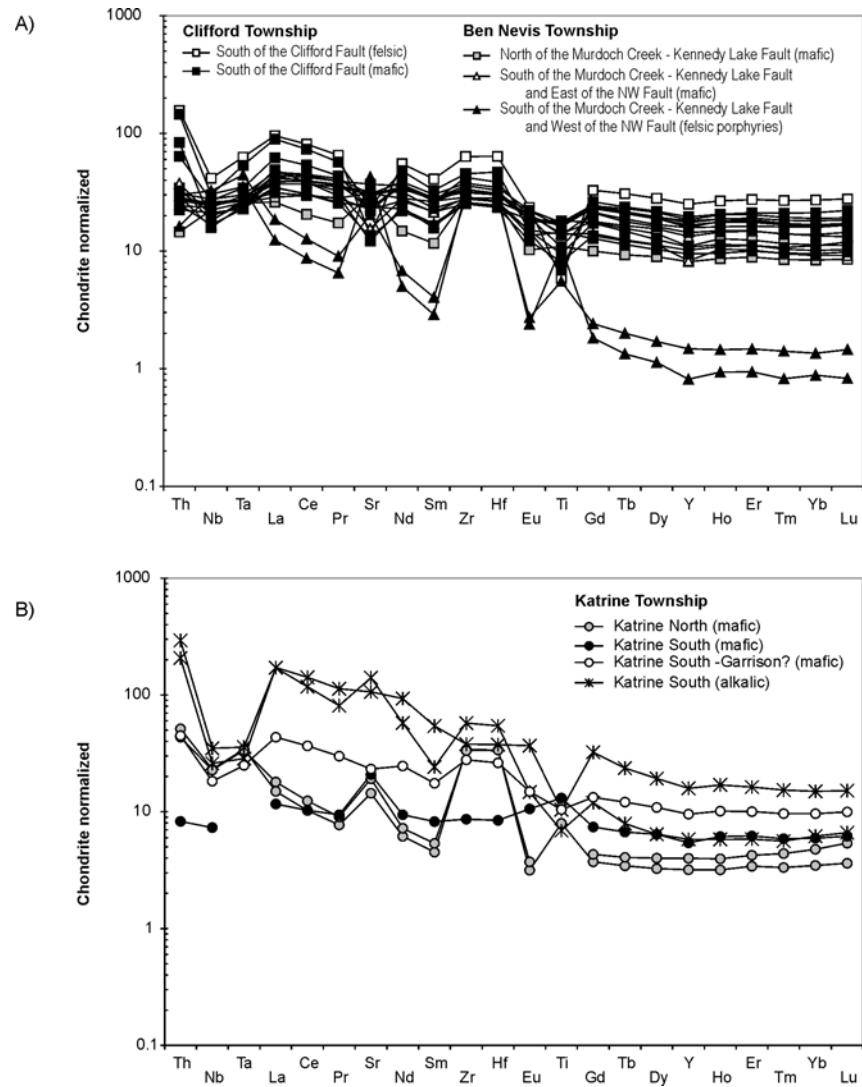


Figure 24. Chondrite-normalized spider plots for the intrusive rocks: a) Clifford and Ben Nevis townships, including the Clifford-phase porphyry dykes; b) Katrine Township, including the alkalic stock and dykes. (Chondrite normalizing values are C1 chondrite from Sun and McDonough 1989.)

SUMMARY

On major element diagrams there is a progression from mafic to felsic rocks in the Blake River Group of the study area. On the chondrite-normalized spider diagrams, the mafic and felsic patterns overlap. However, the patterns are not a simple progression from mafic to felsic. In particular, mafic rocks with the low Yb_{cn} values are known to be more evolved in regards to major elements (higher SiO_2 and lower MgO) and have higher La/Yb_{cn} ratios. These rocks also have more pronounced negative Nb anomalies. As the rocks do not greatly deviate from the hydrothermal–diagenetic alteration divide on the Large et al. (2001) alteration box plot, the differences in rock chemistry are not considered to be due to alteration, but to be a primary effect. The felsic rocks in the study area exhibit 2 trends in Zr/Y ratios. As for the mafic rocks, the felsic rocks do not deviate from the hydrothermal–diagenetic alteration divide on the alteration box plot, and thus the populations are also considered primary rather than alteration induced.

The geochemical similarity between the high-level synvolcanic intrusions and the volcanic rocks supports the field evidence for their synvolcanic nature. The interpretation that the composite QFP-diorite intrusion at the Ben Nevis–Katrine township boundary is a synvolcanic plug is supported by its chemical similarity to the cryptodome in Ben Nevis Township south of the Clifford fault. The cryptodome has been radiometrically dated at 2699.8 ± 3.6 Ma (Hamilton in Ayer et al. 2005), showing it to be synvolcanic. The volcanism in the Canagau Mine area of Ben Nevis Township has been radiometrically dated at 2696.6 ± 1.3 Ma (Hamilton in Ayer et al. 2005), and a rhyolite in Pontiac Township, to the east, has a radiometric age of 2701 ± 2 Ma (Corfu et al. 1989).

The mafic to intermediate intrusive bodies in the study area also have the same chemical characteristics as the hosting volcanic rocks, and are considered to be part of the Blake River Group magmatic event. Two porphyry dykes from Ben Nevis Township have chemical signatures similar to the Clifford phase intrusions (*see* MacDonald et al. 2005) and are interpreted as being related to that event. The alkalic stock and its associated dykes in the southeast corner of Katrine Township are interpreted as being part of the late-phase plutonism described as Suite K in Rive et al. (1990).

Alteration and Mineralization Styles

In Clifford Township, MacDonald et al. (2005) recognized 3 alteration and mineralization styles: 1) contact metamorphic alteration around the Clifford stock with minor pyrite mineralization; 2) VMS-style alteration and mineralization; and 3) intrusion-related or porphyry-style alteration and Cu-Mo-Au mineralization. In Ben Nevis Township, the second (VMS) style alteration is present, as well as Fe-carbonate alteration apparently related to north-northwest-trending faults and shear zones. In Katrine Township, VMS-style alteration also occurs but there is not enough data to properly classify alteration types.

Regional metamorphism in the area is low-grade prehnite-pumpellyite facies (Hannington et al. 2003; Jensen 1975a, 1975b). The Clifford stock exhibits a well-defined contact aureole surrounding it for 200-300 m (MacDonald et al. 2005). In the aureole, the andesites to basaltic andesites exhibit a distinctive dark colouration and contain ubiquitous magnetite, lath-like needles of plagioclase (albite?), epidote patches, and, in some cases, amphibole (actinolite?) (Photo 4a). Minor pyrite is present in the metamorphic aureole.

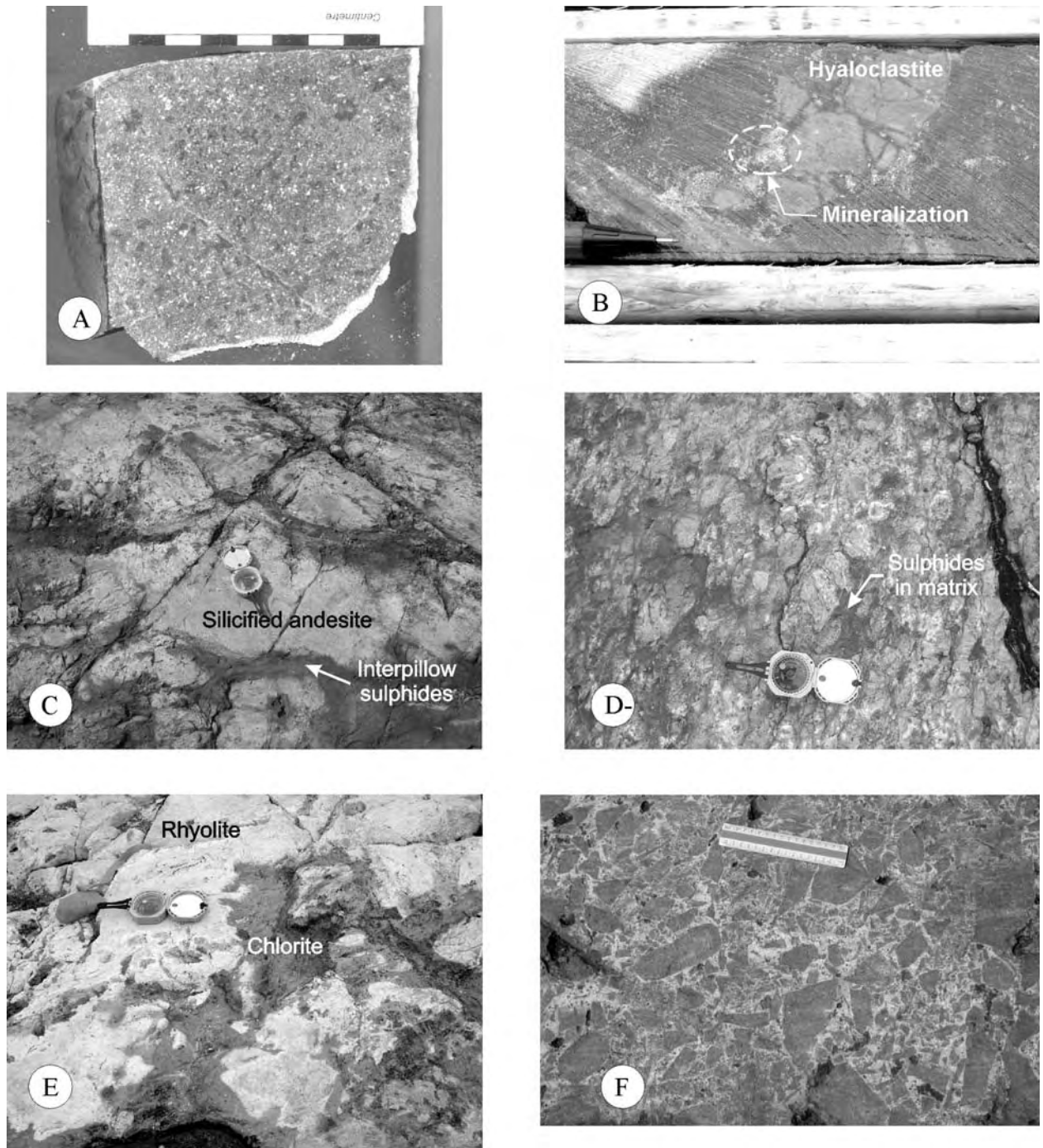


Photo 4. a) Typical recrystallized basaltic andesite of the Blake River Group with albite (white laths) and magnetite (black clots) from the contact aureole of the Clifford stock; b) pillow lava with chlorite alteration at the edge of the pillow, silicification of the hyaloclastite (white fragments), and a sulphide assemblage of pyrite-chalcopyrite, from Clifford Township; c) highly silicified pillows with pyrite in the interpillow hyaloclastite, Interprovincial South showing; d) rhyolite breccia with pyrite in the breccia matrix, Interprovincial North showing; e) highly chloritized rhyolite, Interprovincial North showing; f) breccia pipe occurrence from the Brett-Tretheway (Croxall) prospect with angular andesite fragments within a sea of quartz and sulphide minerals.

In Clifford Township, volcanogenic massive sulphide (VMS)-style alteration is present on surface and in drill core. Chlorite-quartz-epidote-pyrite assemblages commonly fill amygdules in varying proportions and are interpreted to represent semi-conformable-style alteration (e.g., Galley 1993). Most common are quartz-pyrite fillings but there are also epidote-quartz-pyrite, chlorite-quartz, and chlorite-pyrite infillings. These mineral assemblages are also present in some rocks, commonly the more mafic members of the Blake River Group, as patches, typically near permeable zones in the rocks (i.e., near hyaloclastite or in volcanic breccias). Silicification and chlorite alteration are present in some drill holes, and are associated with sulphide mineralization and interpreted to be more indicative of proximal, high temperature alteration (e.g., Franklin 1993). This style of alteration and mineralization is present only in drill core and occurs associated with the lowermost basaltic andesite pillow lava sequence. The mineralization is generally restricted to hyaloclastite along pillow margins (Photo 4b). Along these margins, chalcopyrite, pyrite and quartz are found interstitial to angular hyaloclastite; sulphides comprise a maximum of ~10% of the rock (Photo 4b). Hyaloclastite fragments are either bleached to a white-pink colour and silicified or are completely chlorite altered with or without epidote (Photo 4b). Finer grained ash-sized material in between the hyaloclastite is typically completely replaced by chlorite.

Quartz-pyrite-filled amygdules are also present locally in Ben Nevis and Katrine townships, but are more common in Ben Nevis than in Katrine, where it is rare. In Ben Nevis Township, pyrite also occurs along fractures and in the multiple injection borders of both rhyolitic (Photo 2a) and andesitic high-level synvolcanic dykes, in the rims of silicified pillows (Photo 4c), and in the matrix of brecciated rhyolite (Photo 4d). Network silicification is common in the andesites that have been intruded by rhyolitic synvolcanic dykes in the Interprovincial South showing area (Photo 3b). Sericite alteration is common in the felsic volcanic rocks; however, it should be noted that most of the felsic volcanic rocks are fragmental, and that the matrix would be expected to alter to sericite under metamorphic conditions. Intense chlorite alteration with associated sulphide mineralization is present on one mechanically stripped outcrop (Photo 4e). This same outcrop is cut by a Fe-carbonate-altered deformation zone. Epidote-quartz and quartz alteration occur in the pillowed facies of the andesites in Ben Nevis Township (Photo 2e) and is concentrated in pillow rims or in pillow centres. The flow breccias associated with these pillowed facies also exhibit epidote-quartz or quartz alteration.

In Clifford Township, MacDonald et al. (2005) recognized porphyry Cu-Au-Mo-style alteration overprinting, and younger than, the VMS-style alteration. The porphyry-style alteration is present both on surface and in drill core, and is associated with numerous breccia-pipe-style occurrences on surface (e.g., Brett-Tretheway / Croxall prospect). On surface, the mineralization is not easily visible and occurs within breccia pipes, like the Croxall prospect. These pipes are broadly radial in nature and spatially associated with rhyolite porphyry and brecciated porphyry; in between the brecciated porphyry there is abundant quartz±sulphide mineralization forming the interstices between porphyry clasts (Photo 4f; E. Chaloux, unpublished data). Alteration associated with this style of mineralization is commonly silicification and pyrite alteration near the breccia pipes, whereas outside of the breccia pipes the regional wall rocks have a randomly oriented network of millimetre- to centimetre-scale quartz, epidote, K-feldspar, hematite and calcite (±sericite) veins. In drill core, mineralization and alteration are associated primarily with a randomly oriented vein network that exhibits a complex paragenesis. The veinlets form a stockwork a few millimetres up to a few centimetres in width. The paragenesis seems to be, from oldest to youngest: 1) epidote, chlorite and sericite; 2) quartz-pyrite; 3) dark grey quartz-pyrite-chalcopyrite-molybdenum (and gold?); and 4) hematite-calcite-±K-feldspar. This paragenesis is not always present and some events appear to be synchronous and overlap in some drill holes. Nonetheless, there seems to be an intermediate Cu-Mo-Au event associated with dark grey quartz veins, and all alteration styles are cut by late hematite-calcite±K-feldspar veins. The veins that host mineralization are widespread across all rock types but most Mo-(and Au?)-rich zones are also hosted by dykes of rhyolitic feldspar porphyry similar to the Clifford stock; this suggests that this porphyry-style mineralization is a distinctly younger hydrothermal event in Clifford Township and likely related to the emplacement of the Clifford stock.

Although the porphyry-style alteration and mineralization described in Clifford Township was not recognized in Ben Nevis Township during the course of this study, Pearson (1992) describes an alloclastic breccia within a dacite dyke in Ben Nevis Township, which may be a porphyry-style breccia pipe:

“The mechanically stripped area of the Erhart showing [Interprovincial South showing in this report] consists of a sequence of andesites (massive, brecciated and pillowed) with facing directions to the southwest, which are crosscut by dacite dykes. The dykes are generally oriented N010° to N045° exhibiting rectilinear to irregular contacts, with locally brecciated chill margins. The border has flow laminations, followed by a massive section with columnar joints. The dyke and the wallrocks are crosscut by many small faults, whose distribution suggests movement synchronous with the intrusions. The centre of the dacite dyke is cut by a monolithic alloclastic breccia with fragments of the same composition as the dyke. This alloclastic breccia is the principal host to the mineralization (pyrite, galena, sphalerite, gold, chalcopyrite) and is a major feature cutting the entire zone of outcrops. Locally, the periphery of the dyke exhibits patches of chlorite alteration and is cut by two orientations of chlorite stringers forming an orthogonal pattern” [translated by Pélouquin from Pearson 1992].

The synvolcanic interpretation of the mineralization cannot be overruled as the age of the dyke hosting the breccia and mineralization is unknown, and no chemical analyses are available for the dyke. However, the description by Pearson (1992) is very similar to the breccias in drill core and at the Croxall showing in Clifford Township described above (MacDonald et al. 2005; E. Chaloux, unpublished data). The presence of “Clifford-like” dykes south of the Murdoch Creek–Kennedy Lake fault, and the presence of a gravity low in the Interprovincial showing area similar to that centred on the Clifford stock (OGS 1999; Figure 7), suggests that a Clifford-type intrusion may occur at depth in Ben Nevis Township south of the Murdoch Creek–Kennedy Lake fault. Further investigation is necessary to test this hypothesis.

The 3 types of mineral showing for the study area are listed in the Ontario Geological Survey (OGS) Mineral Deposit Inventory (OGS 2002): precious metals, base metals and diamonds (Table 4). In Katrine Township, the showings are generally polymetallic with gold being the dominant commodity (Table 4; locations on Map P.3543–Revised, back pocket). All of the showings in Katrine Township are classified as vein-replacement deposits. In Ben Nevis Township, the showings are also listed as polymetallic, but with Zn as the dominant commodity (Table 4; locations on Map P.3543–Revised). The showings are classified as volcanic associated with two exceptions. The first exception is the Tremblay, A., a gold-zinc showing, which is described as an “unknown hard rock deposit type”. In MacDonald et al. (2005) and this study, the host rock to the Tremblay A. showing is interpreted to be a cryptodome (location 8 on Map P.3543–Revised). The second exception to the volcanic-associated deposit classification is the Interprovincial North showing, which is described as a vein-replacement deposit (Table 4; location 12 on Map P.3543–Revised). Wolfe (1977) interpreted the Interprovincial North mineralization to be consistent with stringer mineralization in alteration pipes below exhalative massive sulphide deposits. However, Jensen (1975a) describes the mineralization as being, at least in part, hosted in “fractures and shear zones”. As mentioned above, the interpretation of the Interprovincial South showing may need to be revised. It is described by Pearson (1992) as hosted within a breccia and stringers in a dyke; the age of the dyke must be determined before the mineralization can be classified as volcanic. Mineralization was observed in Ben Nevis Township (by the authors and D. Hunter, personal communication) in veins and along the multiple injection borders of high-level synvolcanic dykes. In Clifford Township, the two types of showings are polymetallic and diamond. The diamond showing (Table 4) was not examined in this study. The polymetallic Brett-Tretheway showing is classified as intrusion related in the Mineral Deposit Inventory (OGS 2002). Based on the work by Piercey (in MacDonald et al. 2005) and E. Chaloux (unpublished data), the Croxall showing (not listed in OGS 2002) is also intrusion-related, porphyry-style mineralization. The Brazzoni showing is classified as a vein-replacement deposit in the Mineral Deposit Inventory (OGS 2002). The description of this showing in Jensen (1975a) includes the presence of porphyry dykes in all the old workings; this association suggests that the veins may be intrusion-related.

SUMMARY

VMS-style alteration and mineralization is present in Clifford, Ben Nevis and Katrine townships, and porphyry-style alteration and mineralization is present in Clifford Township. However, there are indications that a porphyry system may have existed in Ben Nevis Township. The gravity low in Ben Nevis Township south of the Murdoch Creek–Kennedy Lake fault resembles that centred on the Clifford stock in Clifford Township, and suggests the presence of a similar intrusion at depth in Ben Nevis Township. Two small Clifford-event porphyry dykes occur in Ben Nevis Township south of the Murdoch Creek–Kennedy Lake fault indicating that the Clifford intrusive event extends south of the fault. Finally, the description of the mineralized brecciated dyke at the Interprovincial South showing resembles the breccia recognized at the Croxall porphyry breccia pipe showing, and the age of the Interprovincial South dyke should be determined to test if the mineralization is indeed related to the Clifford porphyry event.

On one mechanically stripped outcrop in the Interprovincial North showing area, intense chloritization of a rhyolite with associated sulphide mineralization occurs. Most of the mineralization observed in Ben Nevis Township was in the form of quartz-pyrite-filled amygdules, and in the area of the Interprovincial and Roche showings, in the form of sulphide veins in high-level synvolcanic dykes or sulphides concentrated in the multiple injection borders of those dykes. However, intensely Fe-carbonatized deformation zones cross-cut the area of the Interprovincial and Roche showings, and the literature describes mineralization occurring in veins within these deformation zones. It is, therefore, likely that remobilization of the synvolcanic mineralization occurred during a deformation event.

In Katrine Township, the mineral showings are all polymetallic vein-replacement deposits. Although VMS-style alteration and mineralization, e.g., quartz-pyrite-filled amygdules, occur in Katrine Township, it is rare, and no showings occurred in those areas.

Table 4. Mineral prospects and occurrences in the study area, from the Ontario Geological Survey Mineral Deposit Inventory (OGS 2002).

Number on Map P.3543-Revised	Name	Alternative Name	Township	UTM E (Nad27)	UTM N (Nad27)	Classification	Commodity	Deposit Type	Comments	MDI Number
1	Callighan	Mulven Lake	Katrine	600800	5341312	Occurrence	Au, Cu	Vein/Replacement deposits		MDI32D04NE00022
2	Norwood		Katrine	594397	5342091	Occurrence	Au, Pb, Zn	Vein/Replacement deposits		MDI32D04NE00023
3	Walsh-Katrine	Wadge; Walsh-Tucker	Katrine	601720	5339660	Occurrence	Au, Cu, Pb	Vein/Replacement deposits		MDI32D04NE00024
4	Forward	Anderson, T.; Misema Lake	Katrine	594293	5338390	Occurrence	Cu	Vein/Replacement deposits		MDI32D04NE00029
5	Low-Katrine		Katrine	596451	5343576	Occurrence	Au, Cu	Vein/Replacement deposits		MDI32D04NE00030
6	Rivard	Lowe; Raitanen	Katrine	596210	5343850	Occurrence	Cu	Vein/Replacement deposits		MDI32D04NE00018
7	Roche-North		Ben Nevis	598338	5353455	Occurrence	Zn, Pb, Ag, Au	Volcanic Associated		MDI32D05SE00040
8	Tremblay, A.		Ben Nevis	593370	5350302	Occurrence	Au, Zn	Unknown Hard Rock Deposit Type		MDI32D05SE00042
9	Roche-South		Ben Nevis	599062	5352733	Occurrence	Zn	Volcanic Associated		MDI32D05SE00045
10	Interprovincial-South	Ehrhart	Ben Nevis	599148	5351229	Occurrence	Zn, Pb, Cu	Volcanic Associated		MDI32D05SE00046
11	Tremblay-West		Ben Nevis	592402	5349645	Occurrence	Cu, Au	Volcanic Associated		MDI32D05SE00047
12	Interprovincial-North	Canagau	Ben Nevis	599199	5352179	Prospect	Zn, Pb, Au, Cu, Ag	Vein / Replacement Deposits	Shaft; Underground Workings, Replacement Veins; Was Previously Classed as a Developed Prospect	MDI32D05SE00041
*	Brazzoni		Clifford	589841	5348355	Occurrence	Cu, Au	Vein / Replacement Deposits	Kirkland Lake Paper Coordinates DO NOT Match MDI digital Coordinates	MDI32D05SW00034
*	Brett-Tretheway		Clifford	591529	5349493	Occurrence	Au, Cu, Mo	Felsic to Intermediate Intrusion Associated		MDI32D05SW00035
*	Croxall		Clifford				Au, Mo, Cu	Felsic to Intermediate Intrusion Associated	Breccia Pipe	
*	Diamet		Clifford	588825	5348100	Occurrence	Diamond Kimberlite	Alkaline Intrusion Associated		MDI32D05SW00006

* Locations of Clifford Township occurrences are shown on Figure 5.

Discussion and Conclusion

The volcanic rocks of Katrine, Ben Nevis and Clifford townships belong to the Misema subgroup of the Blake River Group. No evidence was seen in this study for the presence of the Garrison–Misema subgroup boundary in Katrine Township; further studies in the southern part of Katrine Township and in McVittie Township, to the south, should be undertaken to determine the position and nature of that stratigraphic boundary.

The Misema subgroup of the Blake River Group in Ben Nevis Township has a U-Pb age of 2696.6 ± 1.3 Ma (Hamilton in Ayer et al. 2005). This is younger than the pre-cauldrone phase of the Noranda subgroup (2701 ± 1 Ma; Mortensen 1993), younger than the Misema subgroup in Pontiac Township, to the east (2701 ± 2 Ma; Corfu et al. 1989), and of the same age as the post-cauldrone phase of the Noranda subgroup (the Renault-Dufresnoy formation: $2697.9 +1.3/-0.7$ (Mortensen 1993) and 2696 ± 1.1 Ma (Lafrance et al. 2003), and the Bousquet formation: 2698.6 ± 1.5 Ma, 2698.0 ± 1.5 Ma and 2694 ± 2 Ma (Lafrance et al. 2003)). Thus, the Ben Nevis–Clifford volcanic complex formed late in the Blake River Group volcanic event.

Subaqueous andesite flows are the dominant rock type in the study area. In Katrine Township, pyroclastic rocks are rare, and felsic volcanic rocks even rarer. In Ben Nevis and Clifford townships there is a spectrum of subaqueous volcanic rocks from basalt to rhyolite. Both flow and pyroclastic facies occur in all rock types, but the felsic volcanic rocks are dominantly pyroclastic with rare flow or dome facies. High-level synvolcanic dykes, which can only be distinguished from extrusive rocks by their cross-cutting relationships, occur in all rock types throughout the study area. Mafic-intermediate dykes and irregular masses, which are comagmatic with the Blake River Group volcanism, also occur throughout the study area.

The Noranda cauldron sequence of the Noranda subgroup hosts the majority of VMS deposits in the Blake River Group (Gibson 1989; Gibson and Watkinson 1990). The volcanism in the Noranda cauldron is flow dominated (de Rosen-Spence 1976; Gibson 1989; Paradis 1990), as is the pre-cauldron volcanism (Péloquin et al. 1989a, 1989b; Péloquin 2000). However, pyroclastic rocks form an important part of the post-cauldron volcanism (Trudel 1978, 1979; Goutier 1997; Lafrance et al. 2003). The Ben Nevis–Clifford volcanic centre has a large pyroclastic component. This volcano may be a subaqueous composite stratovolcano (Williams and McBirney 1979) constructed on a mafic to intermediate volcanic “floor” represented by the Misema subgroup in Katrine Township. The increase in pyroclastic rocks, and the pumiceous and scoriaceous nature of some of the fragments, indicates shallow depth of emplacement.

The geochemistry of the Ben Nevis–Clifford volcanic centre also differs from the Noranda volcanism. Noranda has long been known to be bimodal (andesite–rhyolite) and have 2 end-member andesite affinities: tholeiitic and calc-alkalic (or LREE-enriched) (e.g., Goodwin 1977; Gélinas et al. 1977; Laflèche et al. 1992; Péloquin 2000; Péloquin et al. 2001). In contrast, the Misema subgroup in the study area is unimodal (andesite dominant) with no silica gap, and there are no true tholeiites in the area.

The differences between the Ben Nevis–Clifford volcanic centre and the Noranda cauldron indicate that mineral exploration in Ben Nevis and Clifford townships should not be limited strictly to Noranda-type Cu-Zn VMS deposits. The presence of VMS-style alteration and mineralization in the area indicates that a synvolcanic hydrothermal system existed. However, the apparent concentration of the mineralization in the synvolcanic dykes, as veins or in the multiple injection margins, suggests that fluids were channelized within the dykes. Thus, the present exposure may represent the feeder zone of the hydrothermal system (Figure 25). The structural complexity of the area must first be unravelled. The

influence of the NW fault and the Fe-carbonatized deformation zones on the stratigraphy of the area should be determined, and the possibility that the area is affected by complex folding examined.

The recognition of a porphyry system related to the Clifford stock in Clifford Township by Piercey (Piercey et al. 2004; MacDonald et al. 2005) opens up a new avenue for exploration. The gravity low in Ben Nevis Township is similar to that corresponding to the Clifford stock in Clifford Township and suggests a “Clifford-type” intrusion at depth. The occurrence of Clifford-event porphyry dykes in Ben Nevis Township confirms that the Clifford intrusive event extends south of the Murdoch Creek–Kennedy Lake fault.

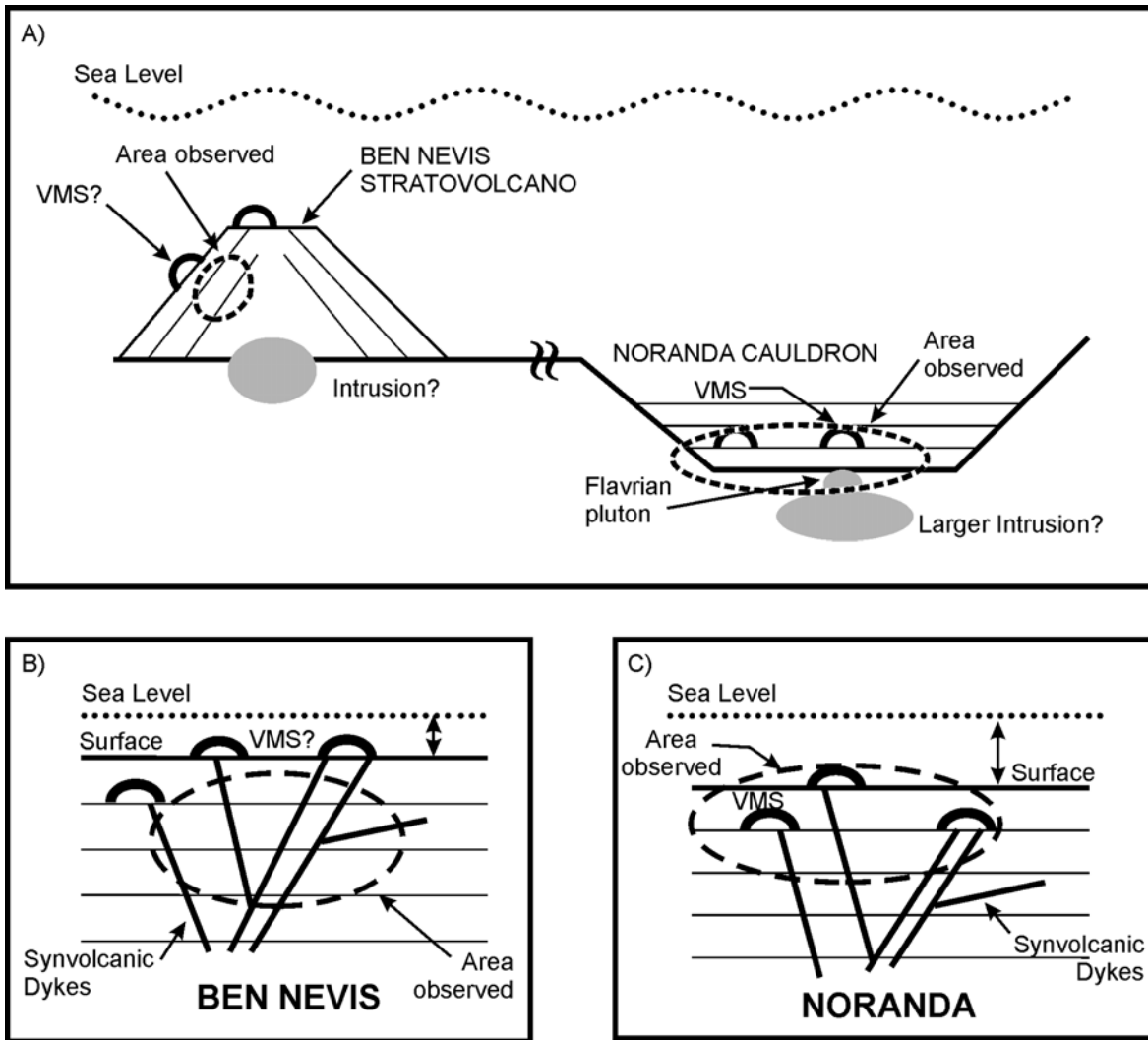


Figure 25. Schematic diagrams (not to scale) of a) the Ben Nevis–Clifford stratovolcano in relationship to the Misema mafic lava plain (Katrine Township and western Québec) and the Noranda cauldron, indicating possible areas of present exposure, b) the Ben Nevis–Clifford stratovolcano indicating the possible area of present exposure, and c) the Noranda cauldron indicating the possible area of present exposure.

References

- Ayer, J.A., Berger, B.R. and Trowell, N.F. 1999. Geological compilation of the Lake Abitibi area, Abitibi greenstone belt; Ontario Geological Survey, Preliminary Map P.3398, scale 1:100 000.
- Ayer, J.A. and Trowell, N.F. 2000. Geological compilation of the Kirkland Lake area, Abitibi greenstone belt; Ontario Geological Survey, Preliminary Map P.3425, scale 1:100 000.
- Ayer, J., Thurston, P.C., Bateman, R., Dubé, B., Gibson, H.L., Hamilton, M.A., Hathway, B., Hocker, S., Houlié, M., Hudak, G., Lafrance, B., Leshner, C.M., Ispolatov, V., MacDonald, P.J., Péloquin, A.S., Piercey, S.J., Reed, L.E. and Thompson, P.H. 2005. Overview of results from the Greenstone Architecture Project: Discover Abitibi Initiative; Ontario Geological Survey, Open File Report 6154.
- Bailes, A., Galley, A.G., Hannington, M.D., Holk, G., Katsube, J., Paquette, F., Paradis, S., Santaguida, F. and Taylor, B.E. 1998. The use of regional-scale alteration zones and subvolcanic intrusions in the exploration for volcanic-associated massive sulphide deposits; *in* Canadian Mining Industry Research Organization (CAMIRO) - Exploration Division, Third Annual Report, 94E07, p.1-40.
- Baragar, W.R.A. 1968. Major-element geochemistry of the Noranda volcanic belt, Québec – Ontario; *Canadian Journal of Earth Sciences*, v.5, p.773-790.
- Burnham, O.M. and Schweyer, J. 2004. Trace element analysis of geological samples by inductively coupled plasma mass spectrometry at the Geoscience Laboratories: revised capabilities due to improvements to instrumentation; *in* Summary of Field Work and Other Activities 2004, Ontario Geological Survey, Open File Report 6145, p.54-1 to 54-20.
- Corfu, F. 1993. The evolution of the southern Abitibi greenstone belt in light of precise U-Pb geochronology; *Economic Geology*, v.88, p.1323-1340.
- Corfu, F., Krogh, T.E., Kwok, Y.Y. and Jensen, L.S. 1989. U-Pb zircon geochronology in the southwestern Abitibi greenstone belt, Superior Province; *Canadian Journal of Earth Sciences*, v.26, p.1747-1763.
- Corfu, F. and Noble, S. 1992. Genesis of the southern Abitibi greenstone belt, Superior Province, Canada: evidence from zircon Hf isotope analyses using single filament technique; *Geochimica Cosmochimica Acta*, v.56, p.2081-2097.
- de Rosen-Spence, A.F. 1976. Stratigraphy, development and petrogenesis of the central Noranda volcanic pile, Noranda, Quebec; unpublished PhD thesis, University of Toronto, Toronto, Ontario, 166p.
- Fisher, R.V. 1966. Rocks composed of volcanic fragments and their classification; *Earth Science Reviews*, v.1, p.287-298.
- Franklin, J.M. 1993. Volcanic-associated massive sulphides; *in* Mineral deposit modelling, Geological Association of Canada, Special Paper 40, p.315-334.
- Franklin, J.M., Sangster, D.F. and Lydon, J.W. 1981. Volcanic-associated massive sulphide deposits; *Economic Geology*, Anniversary Volume, p.485-627.
- Galley, A. 1998. Characteristics of composite subvolcanic intrusive complexes associated with Precambrian VMS districts; *in* The use of regional-scale alteration zones and subvolcanic intrusions in the exploration for volcanic-associated massive sulphide deposits, Canadian Mining Industry Research Organization (CAMIRO) - Exploration Division, Third Annual Report, 94E07, p.1-40.

- Galley, A.G. 1993. Characteristics of semi-conformable alteration zones associated with volcanogenic massive sulphide districts; *Journal of Geochemical Exploration*, v.48, p.175-200.
- Gélinas, L., Brooks, C., Perrault, G., Carignan, J., Trudel, P. and Grasso, F. 1977. Chemostratigraphic divisions within the Abitibi volcanic belt, Rouyn-Noranda, Québec; *in* *Volcanic regimes in Canada*, Geological Association of Canada, Special Paper 16, p.265-295.
- Gibson, H.L. 1989. The geology and reconstruction of the Mine sequence and the Noranda cauldron of the Noranda complex, northwestern Québec; unpublished PhD thesis, Carleton University, Ottawa, Ontario, 715p.
- Gibson, H.L. and Watkinson, D.H. 1990. Volcanogenic massive sulphide deposits of the Noranda cauldron and shield volcano, Québec; *in* *The northwestern Québec polymetallic belt: a summary of 60 years of mining exploration*, Canadian Institute of Mining and Metallurgy, Special Volume 43, p.119-132.
- Gibson, H.L., Morton, R.L. and Hudak, G.J. 1999. Submarine volcanic processes, deposits, and environments favorable for the location of volcanic-associated massive sulfide deposits; *in* *Volcanic-associated massive sulfide deposits: processes and examples in modern and ancient environments*, *Reviews in Economic Geology*, v.8, p.13-51.
- Gledhill, T.L. 1928a. Ben Nevis, Kamiskotia, and other base metal areas, Districts of Cochrane and Timiskaming; Ontario Department of Mines, Annual Report, v.37, pt.3, 52p.
- 1928b. Ben Nevis, Kamiskotia, and other base metal areas, Districts of Cochrane and Timiskaming; Ontario Department of Mines, Map 37g, scale 1 inch to 1 mile.
- Goodwin, A. M. 1977. Archean volcanism in Superior Province, Canadian Shield; *in* *Volcanic regimes in Canada*, Geological Association of Canada, Special Paper 16, p.205-241.
- 1979. Archean volcanic studies in the Timmins - Kirkland Lake - Noranda region of Ontario and Québec; Geological Survey of Canada, Bulletin 278, 51p.
- Goutier, J. 1997. Géologie de la région de Destor; Québec, Ministère des ressources naturelles du Québec, Rapport Géologique RG 96-13, 37p.
- Grunsky, E.C. 1986. Recognition of alteration in volcanic rocks using statistical analysis of lithochemical data; *in* *Volcanology and Mineral Deposits*, Ontario Geological Survey, Miscellaneous Paper 129, p.124-173.
- 1988. Multivariate and spatial analysis of lithochemical data from metavolcanics with zones of alteration and mineralization in Ben Nevis township, Ontario; unpublished PhD thesis, University of Ottawa, Ottawa, Ontario, 710p.
- Hannington, M.D., Barrie, C.T. and Bleeker, W. 1999. The giant Kidd Creek volcanogenic massive sulphide deposit, western Abitibi Subprovince, Canada: Preface and Introduction; *in* *The Giant Kidd Creek volcanogenic massive sulphide deposit, western Abitibi Subprovince, Canada*, *Economic Geology*, Monograph, v.10, p.1-30.
- Hannington, M.D. and Kjarsgaard, I.M. 1998. Mineral-chemical studies of regional-scale hydrothermal alteration in the Central Blake River Group, western Abitibi Subprovince: Part II. Ben Nevis Volcanic Complex; *in* *The use of regional-scale alteration zones and subvolcanic intrusions in the exploration for volcanic-associated massive sulphide deposits*; Canadian Mining Industry Research Organization (CAMIRO) - Exploration Division, Third Annual Report, 94E07, p.77-122.
- Hannington, M.D., Santaguida, F., Kjarsgaard, I.M. and Cathles, L.M. 2003. Regional-scale hydrothermal alteration in the Central Blake River Group, western Abitibi subprovince, Canada: implications for VMS prospectivity; *Mineralium Deposita*, v.38, p.393-422.

- Hart, T.R., Gibson, H.L. and Leshner, C.M. 2004. Trace element geochemistry and petrogenesis of felsic volcanic rocks associated with volcanogenic massive Cu-Zn-Pb sulfide deposits; *Economic Geology*, v.99, p.1003-1013.
- Hogg, W.A. 1964a. Arnold and Katrine townships; Ontario Department of Mines, Geological Report 29, 13p.
- 1964b. Arnold and Katrine townships; Ontario Department of Mines, Map 2061, scale 1 inch to ½ mile.
- Hutchinson, R.W. 1973. Volcanogenic sulfide deposits and their metallogenic significance; *Economic Geology*, v.68, p.1223-1246.
- Irvine, T.N. and Baragar, W.R.A. 1971. A guide to the classification of the common volcanic rocks; *Canadian Journal of Earth Sciences*, v.8, p.523-549.
- Jensen, L.S. 1975a. Geology of Clifford and Ben Nevis townships, District of Cochrane; Ontario Geological Survey, Geoscience Report 132, 55p.
- 1975b. Clifford and Ben Nevis townships; Ontario Geological Survey, Map 2283, scale 1 inch to ½ mile.
- Jensen, L.S. and Langford, F.F. 1985. Geology and petrogenesis of the Archean Abitibi belt in the Kirkland Lake area, Ontario; Ontario Geological Survey, Miscellaneous Paper 123, 130p.
- Jolly, W.T. 1977. Relations between Archean lavas and intrusive bodies of the Abitibi greenstone belt, Ontario - Québec; *in* Volcanic regimes in Canada; Geological Association of Canada, Special Paper 16, p.311-330.
- Knight, C.W. 1920a. Ben Nevis gold area; Ontario Department of Mines, Annual Report 29, pt.3, 27p.
- 1920b. Ben Nevis gold area; Ontario Department of Mines, Map 29e, scale 1 inch to 1½ miles.
- Lafleche, M.R., Dupuy, C. and Bougault, H. 1992. Geochemistry and petrogenesis of Archean mafic volcanic rocks of the southern Abitibi Belt, Québec; *Precambrian Research*, v.57, p.207-241.
- Lafrance, B., Moorhead, J. and Davis, D. W. 2003. Cadre géologique du camp minier de Doyon-Bousquet-LaRonde; *Géologie Québec, Ressources Naturelles du Québec, Étude ET2002-07*, 43p.
- Lafrance, B., Dion, C., Rhéaume, P. and Legault, M. 2004. Levés géologiques et métallogénie au sein du Groupe de Blake River et des unités adjacentes; Québec Exploration 2004, Québec, Ressources Naturelles du Québec : <http://www.quebecexploration.qc.ca/2004/photopresentation-141-142.asp>.
- Large, R.R., Gemmell, J.B., Paulick, H. and Huston, D.L. 2001. The alteration box plot: a simple approach to understanding the relationships between alteration mineralogy and lithochemistry associated with VHMS deposits; *Economic Geology*, v.96, p.957-971.
- LeBas, M.J., LeMaître, R.W., Streckeisen, A. and Zanettin, B. 1986. A chemical classification of volcanic rocks based on the total alkali silica diagram; *Journal of Petrology*, v.27, p.745-750.
- Leshner, C.M., Goodwin, A.M., Campbell, I.H. and Gorton, M.P. 1986. The geochemistry of ore-associated and barren, felsic metavolcanic rocks in the Superior Province, Canada; *Canadian Journal of Earth Sciences*, v.23, p.222-237.
- MacDonald, P.J., Piercey, S.J. and Hamilton, M.A. 2005. An integrated study of intrusive rocks spatially associated with gold and base metal mineralization in Abitibi greenstone belt, Timmins area and Clifford Township: Discover Abitibi Initiative; Ontario Geological Survey, Open File Report 6160, 210p.

- Masuda, A., Nakamura, N. and Tanaka, T. 1973. Fine structures of mutually normalized rare-earth patterns of chondrites; *Geochimica Cosmochimica Acta*, v.37, p.239-248.
- MERQ-OGS 1983. Lithostratigraphic map of the Abitibi Subprovince; Ontario Geological Survey / Ministère de l'Énergie et des Ressources du Québec, Map 2484, scale 1:500 000 (also catalogued as MERQ, DV 83-16 in Québec).
- Mortensen, J.K. 1993. U-Pb geochronology of the eastern Abitibi Subprovince. Part 2: Noranda - Kirkland Lake area; *Canadian Journal of Earth Sciences*, v.30, p.29-41.
- Nakamura, N. 1974. Determination of REE, Ba, Fe, Mg, Na and K in carbonaceous and ordinary chondrites; *Geochimica Cosmochimica Acta*, v.38, p.757-775.
- Ontario Geological Survey 1999. Single master gravity and aeromagnetic data for Ontario, ASCII format; Ontario Geological Survey, ERLIS Data Set 1035.
- Ontario Geological Survey 2002. Mineral Deposit Inventory Version 2 (MDI2) - October 2002 Release; Ontario Geological Survey, Digital Data.
- 2003a. Ontario airborne geophysical surveys, magnetic and electromagnetic data, Kidd-Munro, Blake River area MEGATEM® II survey; Ontario Geological Survey, Geophysical Data Set 1044a to d.
- 2003b. Ontario airborne geophysical surveys, magnetic and electromagnetic data, grid and profile data, ASCII and Geosoft® formats, Kirkland Lake area; Ontario Geological Survey, Geophysical Data Set 1022.
- Paradis, S. 1990. Stratigraphy, volcanology and geochemistry of the New Vauze - Norbec area, Central Noranda Volcanic Complex, Québec, Canada; unpublished PhD thesis, Carleton University, Ottawa, Ontario, 695p.
- Pearson, V. 1992. Géologie de la partie centrale de la propriété Ben Nevis. Minnova Inc.; Assesment File 2.14827, 39p.
- Péloquin, A.S. 2000. Reappraisal of the Blake River Group stratigraphy and its place in the Archean volcanic record; unpublished Thèse de doctorat, Université de Montréal, Montréal, Québec, 189p.
- 2004. Precambrian geology of Ben Nevis and Katrine townships; Ontario Geological Survey, Preliminary Map P.3543-Revised, scale 1:20 000.
- Péloquin, A.S. and Piercey, S.J. 2003. Discover Abitibi. Base Metal Subproject 3: Geology and base metal mineralization in Ben Nevis, Katrine, and Clifford townships; *in* Summary of Field Work and Other Activities 2003, Ontario Geological Survey, Open File Report 6120, p.41-1 to 41-8.
- Péloquin, A.S., Verpaelst, P., Paradis, S., Gaulin, R. and Cousineau, P. 1989a. Projet Blake River Ouest Cantons de Duprat et de Dufresnoy, SNRC 32D/06; Ministère de l'Énergie et des Ressources du Québec, Rapport Interimaire, MB 89-02, 176p.
- Péloquin, A.S., Verpaelst, P., and Gaulin, R. 1989b. Le Blake River dans les cantons de Duprat, de Montbray, de Beauchastel et de Dasserat; Ministère de l'Énergie et des Ressources du Québec, Rapport Interimaire MB 89-64, 89p.
- Péloquin, A.S., Ludden, J.N. and Verpaelst, P. 1995. The Blake River Group in Québec: a 2.7 Ga in situ propagating volcanic basin hosting volcanogenic massive sulphide deposits; *Precambrian '95*, Montréal, Canada, 1995, p.271.

- Péloquin, A.S., Verpaelst, P., Ludden, J.N., Dejou, B. and Gaulin, R. 2001. La Stratigraphie du Groupe du Blake River Ouest, Ceinture de l'Abitibi, Québec; Ministère des Ressources Naturelles du Québec, Service Géologique du Nord-Ouest, Étude ET98-03, 37p.
- Piercey, S.J., Hamilton, M.A., Pelouquin, A.S. and Chaloux, E. 2004. Discover Abitibi Project, Intrusion Subproject: Updates on studies of the Clifford stock and Blake River Group, Clifford Township; *in* Summary of Field Work and Other Activities 2004, Ontario Geological Survey, Open File Report 6145, p.44-1 to 44-14.
- Ridler, R.H. 1970. Relationship of mineralization to volcanic stratigraphy in the Kirkland - Larder Lakes area, Ontario; Geological Association of Canada, Proceedings v.21, p.22-42.
- Riopel, J. 1998. Rapport de forage 1998, option Canagau (004), canton Ben Nevis, District de Larder Lake, NTS 32D/05; Mines et Exploration Noranda Inc., Kirkland Lake Resident Geologist Office, Assessment File 2.19082, 25p.
- Rive, M., Pintson, H. and Ludden, J.N. 1990. Characteristics of late Archean plutonic rocks from the Abitibi and Pontiac Subprovinces, Superior Province, Canada; *in* The northwestern Québec polymetallic belt: a summary of 60 years of mining exploration, Canadian Institute of Mining and Metallurgy, Special Volume 43, p.65-76.
- Sangster, D.F. 1972. Precambrian volcanogenic massive sulphide deposits in Canada: a review; Geological Survey of Canada, Paper 72-22, 44p.
- Sun, S.-s. and McDonough, W.F. 1989. Chemical and isotopic systematics of oceanic basalts: implications for mantle composition and processes; *in* Magmatism in the ocean basins, Geological Society Special Publication, no.42, p.313-345.
- Taylor, B. and Timbal, A. 1998. Regional stable isotope studies in the Clifford-Ben Nevis area; *in* The use of regional-scale alteration zones and subvolcanic intrusions in the exploration for volcanic-associated massive sulphide deposits; Canadian Mining Industry Research Organization (CAMIRO) - Exploration Division, Third Annual Report, 94E07, p.123-130.
- Thompson, P.H. 2005. A new metamorphic framework for gold exploration in the Timmins–Kirkland Lake area, western Abitibi greenstone belt: Discover Abitibi Initiative; Ontario Geological Survey, Open File Report 6162.
- Trudel, P. 1978. Géologie de la région de Cléricy, Abitibi-Ouest; Ministère des Ressources Naturelles du Québec, Rapport Final DP598, 150p.
- 1979. Le volcanisme archéen et la géologie structurale de a région de Cléricy, Abitibi, Québec; unpublished PhD thesis, École Polytechnique, Montréal, Québec, 307p.
- Vaillancourt, D. 1996. Âges U-Pb des minéralisations de type sulfures massifs volcanogènes dans le Groupe de Blake River de la Sous-province de l'Abitibi, Québec: Les sites d'Aldermac, Hébécourt et Millenbach; unpublished MSc thesis, Université du Québec à Montréal, Montréal, Québec, 32p.
- Watson, E.B. and Harrison, T.M. 1983. Zircon saturation revisited: temperature and composition effects in a variety of magma types; *Earth and Planetary Science Letters*, v.64, p.295-304.
- Williams, H. and McBirney, A.R. 1979. *Volcanology*; Freeman, Cooper and Co., San Francisco, 397 p.
- Wilson, W.J. 1901a. Western part of the Abitibi region; Geological Survey of Canada, Summary Report XIV, pt.A, p.117-130A.
- 1901b. Western part of the Abitibi region; Geological Survey of Canada, Map 760, scale 1 inch to 16 miles.

Wolfe, W.J. 1977. Geochemical exploration of early Precambrian volcanogenic sulphide mineralization in Ben Nevis township, District of Cochrane; Ontario Geological Survey, Study 19, 39p.

This page left blank intentionally.

Appendix 1

Major, Trace and Rare Earth Element Data for Ben Nevis and Katrine Townships

Abbreviations:

BRG	Blake River Group
OGL	Ontario Geoscience Laboratories (Geo Labs)
ActLab	Activation Laboratories
XRF	X-ray fluorescence
ICP-AES	inductively coupled plasma atomic emission spectroscopy
ICP-MS	inductively coupled plasma mass spectrometry
2003 d.l.	2003 detection limit
2004 d.l.	2004 detection limit

Note:

A minus sign in front of a value (e.g., -1000) indicates the value is either below or above the detection limit for that element.

Sample number	03ASP0142.1.1	03ASP0145.1.1	03ASP0137.1.1	03ASP0010.2.1
Township	Ben Nevis	Ben Nevis	Ben Nevis	Ben Nevis
Easting UTM NAD83	595486	595872	595218	598585
Northing UTM NAD83	5354252	5353798	5352837	5355697
Phase	BRG Volcanic	BRG Volcanic	BRG Volcanic	BRG Volcanic
Structural Block	Ben Nevis North	Ben Nevis North	Ben Nevis North	Ben Nevis North
Rock type	Andesite - Massive	Andesite - Massive	Andesite Massive	Andesite Pillows
Note	Poor Oxide Closure	Poor Oxide Closure		
	<i>laboratory</i>	OGL	OGL	OGL
	method	units	2003 d.l.	2004 d.l.
SiO2	XRF	wt%	0.01	0.01
TiO2	XRF	wt%	0.01	0.01
Al2O3	XRF	wt%	0.01	0.01
Fe2O3	XRF	wt%	0.01	0.01
MgO	XRF	wt%	0.01	0.01
CaO	XRF	wt%	0.01	0.01
Na2O	XRF	wt%	0.01	0.01
K2O	XRF	wt%	0.01	0.01
MnO	XRF	wt%	0.01	0.001
P2O5	XRF	wt%	0.01	0.01
Cr2O3	XRF	wt%	0.01	0.01
LOI	XRF	wt%	0.05	0.01
TOTAL			101.86	101.54
	<i>laboratory</i>	OGL	OGL	OGL
Cr	XRF	ppm	4	5
Ni	XRF	ppm		5
Nb	XRF	ppm	2	2
Y	XRF	ppm	1	2
Zr	XRF	ppm	3	5
V	XRF	ppm		5
	<i>laboratory</i>	OGL	OGL	OGL
Al	ICP-AES	ppm	100	100
Ba	ICP-AES	ppm	1	1
Be	ICP-AES	ppm	0.1	0
Ca	ICP-AES	ppm	50	50
Cd	ICP-AES	ppm	2	2
Co	ICP-AES	ppm	1	1
Cr	ICP-AES	ppm	6	1
Cu	ICP-AES	ppm	3	3
Fe	ICP-AES	ppm	100	100
K	ICP-AES	ppm	60	60
Li	ICP-AES	ppm	1	1
Mg	ICP-AES	ppm	70	70
Mn	ICP-AES	ppm	1	1
Mo	ICP-AES	ppm	8	8
Na	ICP-AES	ppm	150	150
Ni	ICP-AES	ppm	3	3
P	ICP-AES	ppm	10	10
S	ICP-AES	ppm	43	43
Sc	ICP-AES	ppm	3	0.3
Sr	ICP-AES	ppm	0.7	0.7
Ti	ICP-AES	ppm	10	10
V	ICP-AES	ppm	0.6	1
W	ICP-AES	ppm	2	2
Y	ICP-AES	ppm	0.2	0.2
Zn	ICP-AES	ppm	2	2
	<i>laboratory</i>	OGL	OGL	OGL
Ce	ICP-MS	ppm	0.07	0.07
Cs	ICP-MS	ppm	0.007	0.007
Dy	ICP-MS	ppm	0.008	0.008
Er	ICP-MS	ppm	0.008	0.008
Eu	ICP-MS	ppm	0.005	0.005
Gd	ICP-MS	ppm	0.009	0.009
Hf	ICP-MS	ppm	0.1	0.1
Ho	ICP-MS	ppm	0.003	0.003
La	ICP-MS	ppm	0.02	0.02
Lu	ICP-MS	ppm	0.003	0.003
Nb	ICP-MS	ppm	0.2	0.2
Nd	ICP-MS	ppm	0.03	0.03
Pr	ICP-MS	ppm	0.006	0.006
Rb	ICP-MS	ppm	0.05	0.05
Sm	ICP-MS	ppm	0.01	0.01
Sr	ICP-MS	ppm	0.5	0.5
Ta	ICP-MS	ppm	0.17	0.17
Tb	ICP-MS	ppm	0.003	0.003
Th	ICP-MS	ppm	0.06	0.06
Tm	ICP-MS	ppm	0.003	0.003
U	ICP-MS	ppm	0.007	0.007
Y	ICP-MS	ppm	0.02	0.02
Yb	ICP-MS	ppm	0.01	0.01
Zr	ICP-MS	ppm	4	4

Sample number	03ASP0143.1.1	03ASP0144.1.2	03ASP0135.1.2	03ASP0141.1.3	03ASP0071.1.1
Township	Ben Nevis	Ben Nevis	Ben Nevis	Ben Nevis	Ben Nevis
Easting UTM NAD83	595645	595551	595310	594806	599899
Northing UTM NAD83	5354339	5354159	5352465	5352965	5354039
Phase	BRG Volcanic	BRG Volcanic	BRG Volcanic	BRG Volcanic	BRG Volcanic
Structural Block	Ben Nevis North	Ben Nevis North	Ben Nevis North	Ben Nevis North	Ben Nevis Southeast
Rock type	Rhyolite Lapilli Tuff	Rhyolite Lapilli Tuff	Rhyolite Massive	Rhyolite Massive	Andesite
Note					

			OGL	OGL	OGL	OGL	OGL
<i>laboratory</i>			OGL	OGL	OGL	OGL	OGL
	method	units					
SiO2	XRF	wt%	74.25	69.2	72.06	68.7	55.85
TiO2	XRF	wt%	0.26	0.25	0.19	0.34	0.81
Al2O3	XRF	wt%	12.41	15.3	12.14	12.82	17.25
Fe2O3	XRF	wt%	3.33	2.9	3.19	3.68	7.22
MgO	XRF	wt%	0.58	0.77	0.4	0.6	4.64
CaO	XRF	wt%	1.59	3	2.85	3.49	6.82
Na2O	XRF	wt%	4.4	2.14	4.81	4.18	3.05
K2O	XRF	wt%	2.53	4.42	0.89	1.51	1.72
MnO	XRF	wt%	0.04	0.06	0.03	0.07	0.11
P2O5	XRF	wt%	0.05	0.05	0.04	0.07	0.14
Cr2O3	XRF	wt%					
LOI	XRF	wt%	0.89	1.95	3.08	4.37	3.18
TOTAL			100.32	100.05	99.69	99.83	100.8
<i>laboratory</i>			OGL	OGL	OGL	OGL	OGL
Cr	XRF	ppm	49	18	20	18	90
Ni	XRF	ppm					
Nb	XRF	ppm	6	8	4	6	3
Y	XRF	ppm	33	40	27	30	17
Zr	XRF	ppm	175	221	176	189	106
V	XRF	ppm					
<i>laboratory</i>			OGL	OGL	OGL	OGL	OGL
Al	ICP-AES	ppm	55619	72903	55518	59684	73550
Ba	ICP-AES	ppm	525	848	195	292	372
Be	ICP-AES	ppm	0.48	0.78	0.34	0.45	0.28
Ca	ICP-AES	ppm	9135	17874	15096	20644	31324
Cd	ICP-AES	ppm	0	0	0	0	0
Co	ICP-AES	ppm	3	2	1	3	26
Cr	ICP-AES	ppm	16.48	15.77	12.26	9.45	57.24
Cu	ICP-AES	ppm	0	0	15	3	10
Fe	ICP-AES	ppm	21345	19455	20241	23152	46828
K	ICP-AES	ppm	15283	29678	5787	9947	10567
Li	ICP-AES	ppm	3	8	16	7	9
Mg	ICP-AES	ppm	3180	4258	2388	3347	24996
Mn	ICP-AES	ppm	261	405	144	414	706
Mo	ICP-AES	ppm	0	0	0	0	0
Na	ICP-AES	ppm	27923	15210	32307	27624	19752
Ni	ICP-AES	ppm	6	4	3	3	88
P	ICP-AES	ppm	148	119	110	239	523
S	ICP-AES	ppm	48	59	102	66	-400
Sc	ICP-AES	ppm	4.8	5	3.6	4.9	9.9
Sr	ICP-AES	ppm	141.9	59.9	78.9	84.8	119.6
Ti	ICP-AES	ppm	1083	1214	801	1505	3362
V	ICP-AES	ppm	1	0	1	8	137.4
W	ICP-AES	ppm	0	0	0	0	0
Y	ICP-AES	ppm	24.3	27.5	18.8	22.8	8.5
Zn	ICP-AES	ppm	22	59	20	51	42
<i>laboratory</i>			OGL	OGL	OGL	OGL	OGL
Ce	ICP-MS	ppm	46.58	54.85	48.93	45.02	11.85
Cs	ICP-MS	ppm	0.691	2.215	1.201	1.521	1.332
Dy	ICP-MS	ppm	5.69	6.73	5.164	5.444	1.805
Er	ICP-MS	ppm	3.709	4.51	3.378	3.554	1.121
Eu	ICP-MS	ppm	1.033	1.049	1.013	1.218	0.497
Gd	ICP-MS	ppm	5.245	6.111	4.995	5.376	1.729
Hf	ICP-MS	ppm	5.1	6.5	5	5.4	2.9
Ho	ICP-MS	ppm	1.225	1.452	1.111	1.171	0.382
La	ICP-MS	ppm	22.84	25.93	23.54	20.13	5.79
Lu	ICP-MS	ppm	0.614	0.723	0.525	0.596	0.161
Nb	ICP-MS	ppm	8.1	10.3	6.3	8.4	4.3
Nd	ICP-MS	ppm	21.55	25.45	22.48	22.94	6.43
Pr	ICP-MS	ppm	5.551	6.622	5.853	5.568	1.544
Rb	ICP-MS	ppm	60.11	141.42	24.6	49.53	49.34
Sm	ICP-MS	ppm	4.89	5.81	4.85	5.51	1.59
Sr	ICP-MS	ppm	170.2	66.9	94.6	98.9	145.4
Ta	ICP-MS	ppm	0.8	1.04	0.64	0.72	0.34
Tb	ICP-MS	ppm	0.923	1.06	0.829	0.885	0.291
Th	ICP-MS	ppm	5.49	7.2	5.02	4.6	1.06
Tm	ICP-MS	ppm	0.573	0.695	0.508	0.555	0.165
U	ICP-MS	ppm	1.617	2.013	1.322	1.164	0.317
Y	ICP-MS	ppm	34.54	40.48	31.24	31.97	9.76
Yb	ICP-MS	ppm	3.9	4.68	3.36	3.75	1.08
Zr	ICP-MS	ppm	190.8	238.1	193.9	205.8	113.4

Sample number	03ASP0121.2.1	03ASP0003.1.1	03ASP0124.1.1	03ASP0087.1.1	03ASP0121.1.1
Township	Ben Nevis	Ben Nevis	Ben Nevis	Ben Nevis	Ben Nevis
Easting UTM NAD83	599532	601526	601016	600102	599532
Northing UTM NAD83	5353404	5355557	5351781	5353297	5353404
Phase	BRG Volcanic	BRG Volcanic	BRG Volcanic	BRG Volcanic	BRG Volcanic
Structural Block	Ben Nevis Southeast	Ben Nevis Southeast	Ben Nevis Southeast	Ben Nevis Southeast	Ben Nevis Southeast
Rock type	Andesite Massive	Andesite Pillows	Andesite Pillows	Rhyolite Lobe_Breccia	Rhyolite Lobe_Breccia
Note		Poor Oxide Closure	Poor Oxide Closure		

			OGL	OGL	OGL	OGL	OGL
<i>laboratory</i>			OGL	OGL	OGL	OGL	OGL
	method	units					
SiO2	XRF	wt%	59.44	53.34	49.51	75.06	75.22
TiO2	XRF	wt%	0.73	1.02	0.91	0.17	0.21
Al2O3	XRF	wt%	16.27	16.3	17.16	12.07	13.23
Fe2O3	XRF	wt%	6.81	8.73	8.69	2.48	1.89
MgO	XRF	wt%	3.76	4.74	5.92	0.53	0.56
CaO	XRF	wt%	3.05	8.46	13.06	1.07	0.47
Na2O	XRF	wt%	4.97	2.43	2.51	4.48	6.17
K2O	XRF	wt%	1.97	0.83	0.17	2.53	1.85
MnO	XRF	wt%	0.12	0.14	0.13	0.06	0.03
P2O5	XRF	wt%	0.1	0.13	0.16	0.04	0.04
Cr2O3	XRF	wt%					
LOI	XRF	wt%	3.44	5.4	3.79	1.64	0.85
TOTAL			100.66	101.53	102.01	100.12	100.53
<i>laboratory</i>			OGL	OGL	OGL	OGL	OGL
Cr	XRF	ppm	79	86	138	21	16
Ni	XRF	ppm					
Nb	XRF	ppm	4	4	4	6	7
Y	XRF	ppm	19	23	18	32	37
Zr	XRF	ppm	121	115	133	167	204
V	XRF	ppm					
<i>laboratory</i>			OGL	OGL	OGL	OGL	OGL
Al	ICP-AES	ppm	74367	66375	77938	57802	60872
Ba	ICP-AES	ppm	359	137	106	223	223
Be	ICP-AES	ppm	0.39	0.41	0.76	0.44	0.54
Ca	ICP-AES	ppm	11563	32577	75501	5454	2600
Cd	ICP-AES	ppm	0	0	0	0	0
Co	ICP-AES	ppm	21	26	27	2	2
Cr	ICP-AES	ppm	48.77	49.84	99.01	16.11	10.04
Cu	ICP-AES	ppm	43	12	63	0	0
Fe	ICP-AES	ppm	47744	56049	56137	16488	13375
K	ICP-AES	ppm	12342	5396	1097	15214	11542
Li	ICP-AES	ppm	20	10	13	7	5
Mg	ICP-AES	ppm	22246	24703	32437	3080	3359
Mn	ICP-AES	ppm	786	868	830	374	202
Mo	ICP-AES	ppm	0	0	0	0	0
Na	ICP-AES	ppm	30217	16785	15676	28602	38744
Ni	ICP-AES	ppm	70	76	140	6	4
P	ICP-AES	ppm	386	536	571	76	76
S	ICP-AES	ppm	129	79	104	52	45
Sc	ICP-AES	ppm	7.9	7.6	13.7	4	4.3
Sr	ICP-AES	ppm	147.5	186.8	286.6	25.8	48
Ti	ICP-AES	ppm	2969	4493	3678	708	808
V	ICP-AES	ppm	120.2	157.2	170.1	0	0
W	ICP-AES	ppm	0	3	0	4	0
Y	ICP-AES	ppm	7.6	10.8	14.7	22.2	22.8
Zn	ICP-AES	ppm	55	76	65	39	15
<i>laboratory</i>			OGL	OGL	OGL	OGL	OGL
Ce	ICP-MS	ppm	11.96	13.63	32.12	58.72	41.32
Cs	ICP-MS	ppm	0.637	0.875	0.122	0.846	0.356
Dy	ICP-MS	ppm	0.908	2.283	3.417	4.527	4.474
Er	ICP-MS	ppm	0.589	1.387	2.046	2.815	2.949
Eu	ICP-MS	ppm	0.241	0.594	1.4	0.862	0.748
Gd	ICP-MS	ppm	0.882	2.116	3.626	4.816	4.131
Hf	ICP-MS	ppm	3.4	3.2	3.4	4.8	6.2
Ho	ICP-MS	ppm	0.193	0.48	0.696	0.919	0.941
La	ICP-MS	ppm	7.27	6.39	15.47	29.32	20.41
Lu	ICP-MS	ppm	0.104	0.176	0.278	0.453	0.499
Nb	ICP-MS	ppm	5.2	5	5.4	7.7	9
Nd	ICP-MS	ppm	4.41	7.85	15.99	25.22	18.66
Pr	ICP-MS	ppm	1.24	1.817	3.97	6.823	4.86
Rb	ICP-MS	ppm	35.93	27.61	1.86	59.32	31.58
Sm	ICP-MS	ppm	0.86	1.89	3.48	5.21	3.97
Sr	ICP-MS	ppm	159.8	215.6	320.9	29.1	59.1
Ta	ICP-MS	ppm	0.5	0.38	0.42	0.81	0.97
Tb	ICP-MS	ppm	0.146	0.358	0.565	0.753	0.698
Th	ICP-MS	ppm	1.97	1.05	1.65	4.86	6.36
Tm	ICP-MS	ppm	0.093	0.203	0.289	0.434	0.457
U	ICP-MS	ppm	0.79	0.38	0.457	1.464	1.899
Y	ICP-MS	ppm	5.1	12.09	17.52	26.46	26.91
Yb	ICP-MS	ppm	0.65	1.25	1.87	2.91	3.16
Zr	ICP-MS	ppm	130.6	121.8	135.4	176.2	223.1

Sample number	03ASP0147.1.1	03ASP0075.1.1	03ASP0146.1.1	03ASP0170.1.1	03ASP0175.1.1
Township	Ben Nevis	Ben Nevis	Ben Nevis	Ben Nevis	Ben Nevis
Easting UTM NAD83	599365	599600	599323	599293	599463
Northing UTM NAD83	5352135	5353590	5352512	5353039	5353167
Phase	BRG Volcanic	BRG Volcanic	BRG Volcanic	BRG Volcanic	BRG Volcanic
Structural Block	Ben Nevis Southeast	Ben Nevis Southeast	Ben Nevis Southeast	Ben Nevis Southeast	Ben Nevis Southeast
Rock type	Rhyolite Lobe_Breccia	Rhyolite Massive	Rhyolite Massive	Rhyolite Massive	Rhyolite Massive
Note					

			OGL	OGL	OGL	OGL	OGL
<i>laboratory</i>			OGL	OGL	OGL	OGL	OGL
	method	units					
SiO2	XRF	wt%	72.88	72.29	69.22	74.42	70.74
TiO2	XRF	wt%	0.34	0.2	0.25	0.15	0.24
Al2O3	XRF	wt%	12.68	12.44	12.48	11.72	12.97
Fe2O3	XRF	wt%	6.25	2.3	3.16	2.23	2.84
MgO	XRF	wt%	3.11	0.27	1.56	0.43	0.3
CaO	XRF	wt%	0.09	2.68	4.35	2.56	3.58
Na2O	XRF	wt%	0.1	4.3	0.84	4.3	3.79
K2O	XRF	wt%	2.15	2.03	2.5	1.2	1.99
MnO	XRF	wt%	0.06	0.04	0.16	0.03	0.06
P2O5	XRF	wt%	0.07	0.04	0.05	0.03	0.05
Cr2O3	XRF	wt%					
LOI	XRF	wt%	3.17	2.91	5.79	2.82	3.92
TOTAL			100.89	99.5	100.36	99.89	100.46
<i>laboratory</i>			OGL	OGL	OGL	OGL	OGL
Cr	XRF	ppm	17	9	18	12	30
Ni	XRF	ppm					
Nb	XRF	ppm	6	7	4	6	7
Y	XRF	ppm	35	35	33	37	33
Zr	XRF	ppm	197	188	136	144	188
V	XRF	ppm					
<i>laboratory</i>			OGL	OGL	OGL	OGL	OGL
Al	ICP-AES	ppm	50671	56760	58860	54298	59291
Ba	ICP-AES	ppm	481	379	294	185	188
Be	ICP-AES	ppm	0.32	0.55	0.37	0.38	0.55
Ca	ICP-AES	ppm	556	15898	27312	15879	21501
Cd	ICP-AES	ppm	0	0	0	0	0
Co	ICP-AES	ppm	4	2	4	2	2
Cr	ICP-AES	ppm	9.22	10.42	9.44	10.14	8.82
Cu	ICP-AES	ppm	0	0	3	3	0
Fe	ICP-AES	ppm	43040	14717	21296	14539	18140
K	ICP-AES	ppm	12134	12219	16565	7483	12237
Li	ICP-AES	ppm	16	4	12	9	6
Mg	ICP-AES	ppm	12866	1568	8703	2522	1689
Mn	ICP-AES	ppm	370	252	1027	170	340
Mo	ICP-AES	ppm	0	0	0	0	0
Na	ICP-AES	ppm	1235	26691	6226	28870	25352
Ni	ICP-AES	ppm	8	0	7	3	0
P	ICP-AES	ppm	265	72	164	54	128
S	ICP-AES	ppm	0	132	-400	49	52
Sc	ICP-AES	ppm	3.7	4.4	5.9	3.8	4.9
Sr	ICP-AES	ppm	8.6	49.3	45	62.5	48.1
Ti	ICP-AES	ppm	1509	849	1095	640	1043
V	ICP-AES	ppm	6	0	4	3	0
W	ICP-AES	ppm	2	3	4	4	5
Y	ICP-AES	ppm	22.1	26.5	23.5	28.4	24.4
Zn	ICP-AES	ppm	172	38	91	24	47
<i>laboratory</i>			OGL	OGL	OGL	OGL	OGL
Ce	ICP-MS	ppm	38.5	63.85	37.94	47.87	50.34
Cs	ICP-MS	ppm	0.959	2.117	1.604	1.799	1.96
Dy	ICP-MS	ppm	5.17	6.417	5.779	6.582	5.907
Er	ICP-MS	ppm	3.409	4.062	3.913	4.358	3.818
Eu	ICP-MS	ppm	0.666	1.126	0.898	0.875	1.025
Gd	ICP-MS	ppm	4.885	6.37	5.317	5.877	5.598
Hf	ICP-MS	ppm	5.7	5.6	4.1	4.6	5.5
Ho	ICP-MS	ppm	1.123	1.32	1.259	1.406	1.233
La	ICP-MS	ppm	17.33	31.81	17.22	23.12	24.14
Lu	ICP-MS	ppm	0.567	0.653	0.647	0.733	0.619
Nb	ICP-MS	ppm	8.4	9.1	6.1	7.7	8.7
Nd	ICP-MS	ppm	19.45	28.88	19.03	23.32	24.06
Pr	ICP-MS	ppm	4.777	7.448	4.666	5.888	6.109
Rb	ICP-MS	ppm	27.54	74.48	78.44	41.7	66.07
Sm	ICP-MS	ppm	4.56	6.26	4.64	5.48	5.24
Sr	ICP-MS	ppm	10	59.4	51.6	74.2	55.9
Ta	ICP-MS	ppm	0.79	0.93	0.62	0.75	0.87
Tb	ICP-MS	ppm	0.824	1.061	0.917	1.017	0.925
Th	ICP-MS	ppm	3.2	6.66	4.88	5.23	6.05
Tm	ICP-MS	ppm	0.543	0.63	0.614	0.688	0.578
U	ICP-MS	ppm	1.21	1.751	1.268	1.474	1.716
Y	ICP-MS	ppm	28.68	37.98	36.13	39.97	34.56
Yb	ICP-MS	ppm	3.65	4.3	4.11	4.7	3.99
Zr	ICP-MS	ppm	211.7	207.9	147.5	159.3	203.1

Sample number	03ASP0176.1.1	03ASP0179.1.1	03ASP0109.1.1	03ASP0164.1.1	03ASP0209.1.1
Township	Ben Nevis	Ben Nevis	Ben Nevis	Ben Nevis	Ben Nevis
Easting UTM NAD83	599828	599636	597870	598893	597916
Northing UTM NAD83	5352946	5352799	5350474	5351361	5352132
Phase	BRG Volcanic	BRG Volcanic	BRG Volcanic	BRG Volcanic	BRG Volcanic
Structural Block	Ben Nevis Southeast	Ben Nevis Southeast	Ben Nevis Southwest	Ben Nevis Southwest	Ben Nevis Southwest
Rock type	Rhyolite Massive	Rhyolite Massive	Andesite	Andesite	Andesite
Note					

			OGL	OGL	OGL	OGL	OGL
<i>laboratory</i>			OGL	OGL	OGL	OGL	OGL
	method	units					
SiO2	XRF	wt%	72.36	72.97	70.85	53.53	54.73
TiO2	XRF	wt%	0.18	0.15	0.31	0.82	0.83
Al2O3	XRF	wt%	13.38	11.62	13.58	15.67	17.23
Fe2O3	XRF	wt%	2.38	1.93	3.82	7.91	8.15
MgO	XRF	wt%	0.28	0.52	0.81	5.26	5.61
CaO	XRF	wt%	1.22	3.39	2.48	5.85	5.9
Na2O	XRF	wt%	6.72	3.35	3.96	3.59	4.84
K2O	XRF	wt%	1.15	2.04	1.69	0.47	0.09
MnO	XRF	wt%	0.04	0.05	0.05	0.13	0.09
P2O5	XRF	wt%	0.03	0.03	0.08	0.1	0.1
Cr2O3	XRF	wt%					
LOI	XRF	wt%	2.06	3.6	3.14	7.34	3.55
TOTAL			99.81	99.64	100.76	100.67	101.12
<i>laboratory</i>			OGL	OGL	OGL	OGL	OGL
Cr	XRF	ppm	8	16	22	161	135
Ni	XRF	ppm					
Nb	XRF	ppm	6	6	5	3	3
Y	XRF	ppm	42	40	29	13	16
Zr	XRF	ppm	164	146	168	98	105
V	XRF	ppm					
<i>laboratory</i>			OGL	OGL	OGL	OGL	OGL
Al	ICP-AES	ppm	65100	52843	55996	69350	83746
Ba	ICP-AES	ppm	316	291	184	486	52
Be	ICP-AES	ppm	0.53	0.53	0.39	0.23	0.46
Ca	ICP-AES	ppm	8215	19224	7368	33328	36705
Cd	ICP-AES	ppm	0	0	0	0	0
Co	ICP-AES	ppm	2	2	5	20	26
Cr	ICP-AES	ppm	16.16	10.59	5.05	114.01	84.41
Cu	ICP-AES	ppm	0	0	0	20	60
Fe	ICP-AES	ppm	16351	12791	27008	47381	49695
K	ICP-AES	ppm	8025	12661	9949	2907	649
Li	ICP-AES	ppm	3	5	10	49	24
Mg	ICP-AES	ppm	1988	2955	3863	27708	29973
Mn	ICP-AES	ppm	290	293	308	763	508
Mo	ICP-AES	ppm	0	0	0	0	0
Na	ICP-AES	ppm	44165	21808	24800	23216	33628
Ni	ICP-AES	ppm	0	0	7	124	119
P	ICP-AES	ppm	64	55	251	352	359
S	ICP-AES	ppm	44	0	44	-400	90
Sc	ICP-AES	ppm	4.2	3	3.5	12.2	13.4
Sr	ICP-AES	ppm	79.4	63.2	49.9	82.1	293.3
Ti	ICP-AES	ppm	783	645	1200	3479	3784
V	ICP-AES	ppm	3	3	6.5	140	165
W	ICP-AES	ppm	3	3	0	4	0
Y	ICP-AES	ppm	32.8	27.9	9.4	10.5	13.5
Zn	ICP-AES	ppm	27	23	27	171	66
<i>laboratory</i>			OGL	OGL	OGL	OGL	OGL
Ce	ICP-MS	ppm	51.64	44.32	29.85	23.61	25.9
Cs	ICP-MS	ppm	0.874	1.847	3.03	1.248	0.279
Dy	ICP-MS	ppm	7.359	6.7	1.516	2.631	3.113
Er	ICP-MS	ppm	4.946	4.42	0.932	1.653	1.951
Eu	ICP-MS	ppm	0.988	0.837	0.733	0.879	1
Gd	ICP-MS	ppm	6.597	5.985	2.473	2.66	2.984
Hf	ICP-MS	ppm	5.3	4.8	5.1	2.6	2.8
Ho	ICP-MS	ppm	1.549	1.425	0.304	0.547	0.635
La	ICP-MS	ppm	24.84	20.77	14.42	11.31	12.57
Lu	ICP-MS	ppm	0.811	0.692	0.17	0.243	0.296
Nb	ICP-MS	ppm	8.8	7.8	6.5	4.3	4.5
Nd	ICP-MS	ppm	25.09	21.91	14.66	11.65	12.38
Pr	ICP-MS	ppm	6.294	5.459	3.672	2.883	3.117
Rb	ICP-MS	ppm	39.82	63.02	51.54	17.98	1.53
Sm	ICP-MS	ppm	5.93	5.15	3.21	2.61	2.84
Sr	ICP-MS	ppm	90.3	75.4	60.9	102.8	336.9
Ta	ICP-MS	ppm	0.86	0.77	0.59	0.36	0.4
Tb	ICP-MS	ppm	1.148	1.064	0.29	0.436	0.489
Th	ICP-MS	ppm	5.91	5.18	1.81	1.97	2.16
Tm	ICP-MS	ppm	0.764	0.667	0.147	0.245	0.282
U	ICP-MS	ppm	1.568	1.402	0.893	0.509	0.579
Y	ICP-MS	ppm	45.08	40.56	8.44	14.81	17.52
Yb	ICP-MS	ppm	5.2	4.46	1.06	1.6	1.91
Zr	ICP-MS	ppm	184.7	169	183.8	107.8	111.3

Sample number	03ASP0210.1.1	03ASP0163.3.1	03ASP0028.3.1	03ASP0016.1.1	03ASP0020.1.1
Township	Ben Nevis	Ben Nevis	Ben Nevis	Ben Nevis	Ben Nevis
Easting UTM NAD83	597964	599061	594701	596388	596754
Northing UTM NAD83	5352187	5351237	5349004	5348979	5348631
Phase	BRG Volcanic	BRG Volcanic	BRG Volcanic	BRG Volcanic	BRG Volcanic
Structural Block	Ben Nevis Southwest	Ben Nevis Southwest	Ben Nevis Southwest	Ben Nevis Southwest	Ben Nevis Southwest
Rock type	Andesite	Andesite Dyke- altered	Andesite Massive	Andesite Pillows	Andesite Pillows
Note					

			OGL	OGL	OGL	OGL	OGL
<i>laboratory</i>			OGL	OGL	OGL	OGL	OGL
	method	units					
SiO2	XRF	wt%	53.65	58.41	48.53	55.34	56.93
TiO2	XRF	wt%	0.88	0.68	1.69	0.89	0.78
Al2O3	XRF	wt%	16.26	16.52	16.65	17.36	14.97
Fe2O3	XRF	wt%	8.08	4.61	12.16	7.08	6.57
MgO	XRF	wt%	5.36	1.99	6.17	4.64	3.99
CaO	XRF	wt%	5.79	5.89	7.8	8.18	8.3
Na2O	XRF	wt%	4.72	2.59	2.86	2.83	3.51
K2O	XRF	wt%	0.11	2.76	0.14	0.91	0.26
MnO	XRF	wt%	0.11	0.11	0.19	0.09	0.1
P2O5	XRF	wt%	0.1	0.15	0.33	0.09	0.1
Cr2O3	XRF	wt%					
LOI	XRF	wt%	4.94	6.9	4.73	3.45	5.18
TOTAL			99.99	100.6	101.24	100.87	100.69
<i>laboratory</i>			OGL	OGL	OGL	OGL	OGL
Cr	XRF	ppm	141	28	197	75	170
Ni	XRF	ppm					
Nb	XRF	ppm	3	3	6	3	3
Y	XRF	ppm	15	7	29	13	13
Zr	XRF	ppm	110	92	143	103	96
V	XRF	ppm					
<i>laboratory</i>			OGL	OGL	OGL	OGL	OGL
Al	ICP-AES	ppm	80971	74322	80573	72784	64487
Ba	ICP-AES	ppm	64	472	69	165	81
Be	ICP-AES	ppm	0.38	0.45	0.39	0.28	0.24
Ca	ICP-AES	ppm	35561	35934	45132	29099	34864
Cd	ICP-AES	ppm	0	0	0	0	0
Co	ICP-AES	ppm	27	12	33	24	25
Cr	ICP-AES	ppm	92.39	17.48	131.99	46.97	102.57
Cu	ICP-AES	ppm	196	21	38	33	42
Fe	ICP-AES	ppm	51199	29308	78737	47393	42387
K	ICP-AES	ppm	798	17884	916	5971	1749
Li	ICP-AES	ppm	29	24	22	13	10
Mg	ICP-AES	ppm	30721	10459	36617	27412	22401
Mn	ICP-AES	ppm	674	699	1171	554	642
Mo	ICP-AES	ppm	0	0	0	0	0
Na	ICP-AES	ppm	33791	16697	17754	18532	23264
Ni	ICP-AES	ppm	127	22	120	93	132
P	ICP-AES	ppm	392	538	1348	341	370
S	ICP-AES	ppm	185	251	97	86	-400
Sc	ICP-AES	ppm	14.3	4.1	18.3	6.3	7
Sr	ICP-AES	ppm	252.6	64.6	267.9	113	105.9
Ti	ICP-AES	ppm	4085	3010	7403	3788	3296
V	ICP-AES	ppm	157	75	163.8	153.6	130.5
W	ICP-AES	ppm	0	0	0	2	3
Y	ICP-AES	ppm	13.4	5.6	21.7	6.4	8
Zn	ICP-AES	ppm	79	89	86	62	57
<i>laboratory</i>			OGL	OGL	OGL	OGL	OGL
Ce	ICP-MS	ppm	27.07	21.29	50.17	7.25	9.88
Cs	ICP-MS	ppm	0.343	1.181	0.208	0.956	0.41
Dy	ICP-MS	ppm	3.126	1.586	5.508	1.008	1.478
Er	ICP-MS	ppm	1.961	0.729	3.185	0.63	0.861
Eu	ICP-MS	ppm	0.944	0.796	2.03	0.284	0.426
Gd	ICP-MS	ppm	3.125	2.198	6.228	0.98	1.441
Hf	ICP-MS	ppm	3	2.7	3.8	2.8	2.6
Ho	ICP-MS	ppm	0.653	0.275	1.115	0.207	0.306
La	ICP-MS	ppm	13.28	9.62	19.4	4.03	5.02
Lu	ICP-MS	ppm	0.291	0.09	0.444	0.091	0.119
Nb	ICP-MS	ppm	4.8	4.9	7.9	4.2	3.8
Nd	ICP-MS	ppm	13.25	12.02	31.15	3.69	5.23
Pr	ICP-MS	ppm	3.285	2.767	7.116	0.89	1.264
Rb	ICP-MS	ppm	2.1	87.92	4.02	25.81	8.59
Sm	ICP-MS	ppm	2.97	2.55	6.61	0.88	1.25
Sr	ICP-MS	ppm	295.3	80.3	303.9	128.6	124.4
Ta	ICP-MS	ppm	0.42	0.34	0.54	0.4	0.36
Tb	ICP-MS	ppm	0.513	0.307	0.927	0.16	0.229
Th	ICP-MS	ppm	2.29	1.19	1.65	1.55	1.48
Tm	ICP-MS	ppm	0.288	0.101	0.458	0.093	0.128
U	ICP-MS	ppm	0.605	0.418	0.486	0.566	0.47
Y	ICP-MS	ppm	17.98	7.67	28.55	5.8	8.15
Yb	ICP-MS	ppm	1.9	0.62	2.95	0.61	0.83
Zr	ICP-MS	ppm	120.9	99.4	146.4	108.5	99.3

Sample number	03ASP0164.4.1	03ASP0027.1.1	03ASP0028.1.1	03ASP0059.2.1	03ASP0133.1.1
Township	Ben Nevis	Ben Nevis	Ben Nevis	Ben Nevis	Ben Nevis
Easting UTM NAD83	598893	594816	594701	596399	593276
Northing UTM NAD83	5351361	5349260	5349004	5350739	5350764
Phase	BRG Volcanic	BRG Volcanic	BRG Volcanic	BRG Volcanic	BRG Volcanic
Structural Block	Ben Nevis Southwest	Ben Nevis Southwest	Ben Nevis Southwest	Ben Nevis Southwest	Clifford South
Rock type	Andesite Pillows	Rhyolite Breccia	Rhyolite Breccia	Rhyolite Massive	Rhyolite Massive
Note					

			OGL	OGL	OGL	OGL	OGL
<i>laboratory</i>			OGL	OGL	OGL	OGL	OGL
	method	units					
SiO2	XRF	wt%	55.95	80.51	78.26	75.66	71.54
TiO2	XRF	wt%	0.84	0.29	0.31	0.35	0.37
Al2O3	XRF	wt%	15.6	10.15	11.2	12.56	13.46
Fe2O3	XRF	wt%	9.91	0.96	1.24	2.48	4.65
MgO	XRF	wt%	6	0.13	0.25	0.47	0.52
CaO	XRF	wt%	2.79	1.26	3.01	1.09	1.46
Na2O	XRF	wt%	2.67	4.23	4.49	5.53	5.97
K2O	XRF	wt%	0.25	1.65	0.7	1.09	0.81
MnO	XRF	wt%	0.15	0.02	0.02	0.04	0.1
P2O5	XRF	wt%	0.1	0.08	0.08	0.08	0.08
Cr2O3	XRF	wt%					
LOI	XRF	wt%	5.87	0.81	0.92	1.15	1.15
TOTAL			100.13	100.09	100.49	100.51	100.1
<i>laboratory</i>			OGL	OGL	OGL	OGL	OGL
Cr	XRF	ppm	224	31	17	12	16
Ni	XRF	ppm					
Nb	XRF	ppm	3	4	6	6	8
Y	XRF	ppm	13	24	33	31	37
Zr	XRF	ppm	94	139	175	161	215
V	XRF	ppm					
<i>laboratory</i>			OGL	OGL	OGL	OGL	OGL
Al	ICP-AES	ppm	69046	47919	49650	60120	61338
Ba	ICP-AES	ppm	59	260	201	79	202
Be	ICP-AES	ppm	0.26	0.44	0.44	0.3	0.48
Ca	ICP-AES	ppm	15960	6208	9498	6243	8440
Cd	ICP-AES	ppm	0	0	0	0	0
Co	ICP-AES	ppm	31	2	2	4	3
Cr	ICP-AES	ppm	128.05	20.99	31.83	8.71	23.35
Cu	ICP-AES	ppm	174	8	0	13	96
Fe	ICP-AES	ppm	59649	6763	9045	18358	28422
K	ICP-AES	ppm	1464	9916	4949	6950	5194
Li	ICP-AES	ppm	55	1	3	5	6
Mg	ICP-AES	ppm	31103	961	1574	2935	2956
Mn	ICP-AES	ppm	892	140	131	282	593
Mo	ICP-AES	ppm	0	0	0	0	0
Na	ICP-AES	ppm	17657	26156	28974	35208	39642
Ni	ICP-AES	ppm	131	4	5	5	3
P	ICP-AES	ppm	384	251	281	309	266
S	ICP-AES	ppm	-400	187	89	-400	237
Sc	ICP-AES	ppm	12.6	3.9	3.6	6.8	5.6
Sr	ICP-AES	ppm	40.1	63	170.2	43.4	85.9
Ti	ICP-AES	ppm	3491	1165	1303	1379	1586
V	ICP-AES	ppm	143	3	3.1	2.8	4
W	ICP-AES	ppm	0	6	6	2	0
Y	ICP-AES	ppm	10.4	15.2	14.9	19.5	27.7
Zn	ICP-AES	ppm	127	10	13	34	73
<i>laboratory</i>			OGL	OGL	OGL	OGL	OGL
Ce	ICP-MS	ppm	25.32	20.24	16.28	21.52	50.02
Cs	ICP-MS	ppm	1.07	0.483	0.534	0.659	0.225
Dy	ICP-MS	ppm	2.567	2.812	1.934	3.04	6.659
Er	ICP-MS	ppm	1.548	1.699	1.297	2.049	4.335
Eu	ICP-MS	ppm	0.797	0.475	0.375	0.531	1.103
Gd	ICP-MS	ppm	2.685	2.678	1.809	2.758	6.258
Hf	ICP-MS	ppm	2.6	4.2	5.1	4.9	6.2
Ho	ICP-MS	ppm	0.535	0.577	0.42	0.653	1.424
La	ICP-MS	ppm	12.24	9.58	8.45	9.72	24
Lu	ICP-MS	ppm	0.245	0.245	0.21	0.336	0.696
Nb	ICP-MS	ppm	4.1	5.8	7.6	6.8	9.1
Nd	ICP-MS	ppm	12.45	9.98	7.44	10.86	24.64
Pr	ICP-MS	ppm	3.089	2.47	1.908	2.664	5.966
Rb	ICP-MS	ppm	7.74	36.78	28.36	32.1	11.63
Sm	ICP-MS	ppm	2.71	2.46	1.68	2.55	5.62
Sr	ICP-MS	ppm	50.1	73.7	196.6	51.4	101
Ta	ICP-MS	ppm	0.34	0.53	0.66	0.61	0.79
Tb	ICP-MS	ppm	0.427	0.433	0.295	0.468	1.035
Th	ICP-MS	ppm	1.88	2.92	1.96	3.01	4.83
Tm	ICP-MS	ppm	0.232	0.249	0.2	0.313	0.66
U	ICP-MS	ppm	0.491	0.908	0.931	1.016	1.319
Y	ICP-MS	ppm	14.26	15.82	12.01	17.48	38.23
Yb	ICP-MS	ppm	1.55	1.65	1.32	2.18	4.41
Zr	ICP-MS	ppm	104.9	150.6	188.2	175.3	232.8

Sample number	03ASP0100.1.1	03ASP0201.1.1	03ASP0205.1.1	03ASP0043.1.1	03ASP0104.1.1
Township	Katrine	Katrine	Katrine	Katrine	Katrine
Easting UTM NAD83	597287	598292	598034	599285	597415
Northing UTM NAD83	5347195	5346311	5345624	5345294	5347463
Phase	BRG Volcanic	BRG Volcanic	BRG Volcanic	BRG Volcanic	BRG Volcanic
Structural Block	Katrine North	Katrine North	Katrine North	Katrine North	Katrine North
Rock type	Andesite Massive	Andesite Massive	Andesite Massive	Andesite Pillow Breccia	Andesite Porphyritic
Note					

			OGL	OGL	OGL	OGL	OGL
<i>laboratory</i>			OGL	OGL	OGL	OGL	OGL
	method	units					
SiO2	XRF	wt%	59	53.78	55.96	52.22	59.24
TiO2	XRF	wt%	0.84	0.89	0.72	0.93	0.71
Al2O3	XRF	wt%	14.97	17.95	17.86	18.73	16.23
Fe2O3	XRF	wt%	7.02	9.17	7.12	8.8	5.55
MgO	XRF	wt%	5.85	3.18	3.89	3.89	3.59
CaO	XRF	wt%	5.48	7.89	6.76	9.62	6.82
Na2O	XRF	wt%	3.77	2.87	3.1	2.33	4.59
K2O	XRF	wt%	0.23	1.08	1.22	0.91	0.71
MnO	XRF	wt%	0.11	0.13	0.11	0.15	0.09
P2O5	XRF	wt%	0.1	0.11	0.11	0.11	0.1
Cr2O3	XRF	wt%					
LOI	XRF	wt%	3.49	3.74	3.81	3.53	3.13
TOTAL			100.85	100.8	100.66	101.24	100.76
<i>laboratory</i>			OGL	OGL	OGL	OGL	OGL
Cr	XRF	ppm	206	53	135	118	79
Ni	XRF	ppm					
Nb	XRF	ppm	3	2	4	3	3
Y	XRF	ppm	12	19	13	13	15
Zr	XRF	ppm	96	73	124	82	107
V	XRF	ppm					
<i>laboratory</i>			OGL	OGL	OGL	OGL	OGL
Al	ICP-AES	ppm	68353	79859	80795	72253	74687
Ba	ICP-AES	ppm	87	194	224	175	203
Be	ICP-AES	ppm	0.28	0.25	0.41	0.32	0.32
Ca	ICP-AES	ppm	28398	46073	39170	24348	40271
Cd	ICP-AES	ppm	0	0	0	0	0
Co	ICP-AES	ppm	26	17	20	35	19
Cr	ICP-AES	ppm	145.64	13.18	69.96	69.23	58.99
Cu	ICP-AES	ppm	27	67	36	55	35
Fe	ICP-AES	ppm	46486	55410	42735	60004	33334
K	ICP-AES	ppm	1427	7135	8532	6108	4778
Li	ICP-AES	ppm	14	29	22	13	11
Mg	ICP-AES	ppm	31466	16481	20438	24323	19059
Mn	ICP-AES	ppm	670	789	659	1051	496
Mo	ICP-AES	ppm	0	0	0	0	0
Na	ICP-AES	ppm	24368	18933	21913	15379	30734
Ni	ICP-AES	ppm	150	11	61	71	78
P	ICP-AES	ppm	373	415	353	446	325
S	ICP-AES	ppm	223	182	120	109	342
Sc	ICP-AES	ppm	11.4	22.6	11.2	8.2	11.5
Sr	ICP-AES	ppm	89.3	208.1	89.3	660.4	143.7
Ti	ICP-AES	ppm	3335	4001	3182	4086	3049
V	ICP-AES	ppm	139	192	139	180.2	121
W	ICP-AES	ppm	0	0	0	0	0
Y	ICP-AES	ppm	8.6	14	9.9	5.8	12
Zn	ICP-AES	ppm	56	87	67	64	207
<i>laboratory</i>			OGL	OGL	OGL	OGL	OGL
Ce	ICP-MS	ppm	19.16	15.83	30.39	3.57	25.71
Cs	ICP-MS	ppm	0.187	1.154	1.297	0.566	0.468
Dy	ICP-MS	ppm	2.033	3.542	2.493	0.691	2.855
Er	ICP-MS	ppm	1.207	2.308	1.518	0.429	1.773
Eu	ICP-MS	ppm	0.599	0.947	1.007	0.199	0.72
Gd	ICP-MS	ppm	2.095	3.205	2.762	0.635	2.851
Hf	ICP-MS	ppm	2.7	2.1	3.3	2.1	2.9
Ho	ICP-MS	ppm	0.413	0.759	0.505	0.141	0.602
La	ICP-MS	ppm	9.35	6.95	15.21	1.9	12.4
Lu	ICP-MS	ppm	0.169	0.359	0.223	0.065	0.274
Nb	ICP-MS	ppm	4.1	3.4	5.1	4.6	4.7
Nd	ICP-MS	ppm	9.24	9.69	13.77	2.08	12.07
Pr	ICP-MS	ppm	2.289	2.164	3.609	0.467	3.061
Rb	ICP-MS	ppm	3.87	31.53	51.21	36.09	15.38
Sm	ICP-MS	ppm	2.04	2.71	2.78	0.57	2.68
Sr	ICP-MS	ppm	99.3	259.7	110.4	728.5	172.2
Ta	ICP-MS	ppm	0.37	0.25	0.46	0.37	0.4
Tb	ICP-MS	ppm	0.325	0.559	0.424	0.108	0.465
Th	ICP-MS	ppm	1.62	1.16	2.39	0.65	2.61
Tm	ICP-MS	ppm	0.175	0.342	0.222	0.064	0.269
U	ICP-MS	ppm	0.48	0.334	0.6	0.367	0.699
Y	ICP-MS	ppm	9.73	20.4	14.22	3.51	16.22
Yb	ICP-MS	ppm	1.11	2.31	1.48	0.42	1.74
Zr	ICP-MS	ppm	105.5	78.4	136.4	77.1	114.7

Sample number	03ASP0107.1.1	03ASP0083.1.1	03ASP0157.1.1	03ASP0030.1.1	03ASP0050.1.1	03ASP0149.1.1
Township	Katrine	Katrine	Katrine	Katrine	Katrine	Katrine
Easting UTM NAD83	597406	600061	599296	600235	597477	599882
Northing UTM NAD83	5346947	5344582	5343755	5339147	5340148	5341795
Phase	BRG Volcanic	BRG Volcanic	BRG Volcanic	BRG Volcanic	BRG Volcanic	BRG Volcanic
Structural Block	Katrine North	Katrine South	Katrine South	Katrine South	Katrine South	Katrine South
Rock type	Andesite Porphyritic	Andesite Lapilli Tuff	Andesite Massive	Andesite Pillows	Andesite Pillows	Andesite Pillows
Note						

			OGL	OGL	OGL	OGL	OGL	OGL
<i>laboratory</i>			OGL	OGL	OGL	OGL	OGL	OGL
	method	units						
SiO2	XRF	wt%	59.55	56.5	57.66	52.2	55.5	61.34
TiO2	XRF	wt%	0.57	1.29	0.74	1.25	1.1	0.69
Al2O3	XRF	wt%	18.75	15.28	16	17.19	15.97	14.34
Fe2O3	XRF	wt%	5.5	10.99	7.72	10.01	8.15	6.7
MgO	XRF	wt%	1.82	4.18	4.57	5.7	4.08	5.41
CaO	XRF	wt%	4.8	3.64	7.06	8.68	6.83	4.25
Na2O	XRF	wt%	5.7	4.97	2.79	3.59	3.79	3.51
K2O	XRF	wt%	1.87	0.26	1.05	0.44	1.21	1.09
MnO	XRF	wt%	0.08	0.17	0.1	0.22	0.12	0.09
P2O5	XRF	wt%	0.13	0.19	0.14	0.13	0.16	0.09
Cr2O3	XRF	wt%						
LOI	XRF	wt%	1.99	3.1	3.32	2.05	4.17	3.38
TOTAL			100.76	100.56	101.15	101.46	101.07	100.9
<i>laboratory</i>			OGL	OGL	OGL	OGL	OGL	OGL
Cr	XRF	ppm	40	32	124	264	116	138
Ni	XRF	ppm						
Nb	XRF	ppm	8	6	4	4	4	3
Y	XRF	ppm	56	31	23	19	16	12
Zr	XRF	ppm	192	139	142	104	106	95
V	XRF	ppm						
<i>laboratory</i>			OGL	OGL	OGL	OGL	OGL	OGL
Al	ICP-AES	ppm	84615	71632	74545	83488	67614	66415
Ba	ICP-AES	ppm	425	103	220	110	335	344
Be	ICP-AES	ppm	0.56	0.43	0.38	0.23	0.24	0.2
Ca	ICP-AES	ppm	24374	22079	42117	51097	26244	24756
Cd	ICP-AES	ppm	0	0	0	0	0	0
Co	ICP-AES	ppm	7	25	24	41	23	25
Cr	ICP-AES	ppm	15.11	16.32	77.12	189.09	79.73	101.28
Cu	ICP-AES	ppm	0	65	17	38	43	41
Fe	ICP-AES	ppm	35450	69390	48395	67136	56468	41196
K	ICP-AES	ppm	13194	1652	6776	2742	7934	6800
Li	ICP-AES	ppm	16	10	18	14	13	15
Mg	ICP-AES	ppm	10027	22959	25159	33877	23708	29080
Mn	ICP-AES	ppm	479	1051	635	1443	800	552
Mo	ICP-AES	ppm	0	0	0	0	0	0
Na	ICP-AES	ppm	37182	32098	18666	23008	24279	23908
Ni	ICP-AES	ppm	10	31	100	130	49	104
P	ICP-AES	ppm	487	782	546	485	646	351
S	ICP-AES	ppm	61	-400	80	117	-400	-400
Sc	ICP-AES	ppm	6.8	21	13.1	22	8.8	12.6
Sr	ICP-AES	ppm	194.2	64.1	166.9	105.6	238.9	168.8
Ti	ICP-AES	ppm	2481	5879	3299	5349	4857	2954
V	ICP-AES	ppm	46	212	120	215.8	177.5	129
W	ICP-AES	ppm	0	0	0	0	0	0
Y	ICP-AES	ppm	33	25	18.3	14.8	8.3	10.3
Zn	ICP-AES	ppm	32	172	82	77	63	68
<i>laboratory</i>			OGL	OGL	OGL	OGL	OGL	OGL
Ce	ICP-MS	ppm	62.4	31.52	30.65	21.48	11.78	23.77
Cs	ICP-MS	ppm	0.649	0.412	0.927	1.001	0.759	0.807
Dy	ICP-MS	ppm	10.181	5.841	4.364	3.409	1.457	2.491
Er	ICP-MS	ppm	6.562	3.688	2.735	2.217	0.849	1.583
Eu	ICP-MS	ppm	1.587	1.434	1.13	0.878	0.429	0.586
Gd	ICP-MS	ppm	9.473	5.535	4.307	3.232	1.461	2.528
Hf	ICP-MS	ppm	6.1	3.9	3.8	2.9	2.8	2.6
Ho	ICP-MS	ppm	2.18	1.253	0.93	0.731	0.301	0.521
La	ICP-MS	ppm	28.63	13.63	13.66	9.45	5.67	11.29
Lu	ICP-MS	ppm	1.057	0.58	0.405	0.329	0.12	0.233
Nb	ICP-MS	ppm	11.1	7.1	6.2	4.9	4.8	4
Nd	ICP-MS	ppm	33.05	18.72	16.5	12.08	6.4	11.15
Pr	ICP-MS	ppm	7.814	4.289	3.908	2.823	1.525	2.825
Rb	ICP-MS	ppm	42.44	3.67	35.69	16.05	37.56	28.82
Sm	ICP-MS	ppm	8.36	4.77	3.87	2.94	1.36	2.39
Sr	ICP-MS	ppm	236.7	75.6	201.9	123.9	282.8	212.6
Ta	ICP-MS	ppm	1	0.48	0.45	0.36	0.37	0.34
Tb	ICP-MS	ppm	1.62	0.91	0.708	0.54	0.231	0.399
Th	ICP-MS	ppm	6.17	1.59	1.56	1.19	0.9	1.86
Tm	ICP-MS	ppm	1.006	0.56	0.401	0.326	0.124	0.226
U	ICP-MS	ppm	1.689	0.423	0.421	0.313	0.326	0.491
Y	ICP-MS	ppm	60.37	33.2	24.8	19.19	7.73	14.16
Yb	ICP-MS	ppm	6.71	3.7	2.7	2.15	0.8	1.52
Zr	ICP-MS	ppm	216.4	148.3	157.8	112.2	111.8	107.9

Sample number	03ASP0152.1.1	03ASP0093.1.1	03ASP0212.1.1	03ASP0048.1.1
Township	Katrine	Katrine	Katrine	Katrine
Easting UTM NAD83	599694	600078	596846	596789
Northing UTM NAD83	5342260	5340761	5340279	5340101
Phase	BRG Volcanic	BRG Volcanic	BRG Volcanic	BRG Volcanic
Structural Block	Katrine South	Katrine South	Katrine South_Garrison	Katrine South_Garrison
Rock type	Andesite Pillows	Andesite Pillows - spherulitic	Andesite	Andesite Pillows
Note	Poor Oxide Closure			

			OGL	OGL	OGL	OGL
<i>laboratory</i>			OGL	OGL	OGL	OGL
	method	units				
SiO2	XRF	wt%	52.18	51.76	54.84	57.47
TiO2	XRF	wt%	1.08	0.76	0.89	0.92
Al2O3	XRF	wt%	16.2	14.01	13.51	14.91
Fe2O3	XRF	wt%	9.14	8.84	8.59	7.12
MgO	XRF	wt%	2.63	4.6	4.38	3.75
CaO	XRF	wt%	11.52	18.06	8.38	8.27
Na2O	XRF	wt%	2.8	0.33	3.98	4.69
K2O	XRF	wt%	0.21	0.68	0.38	0.14
MnO	XRF	wt%	0.22	0.12	0.16	0.13
P2O5	XRF	wt%	0.11	0.13	0.13	0.14
Cr2O3	XRF	wt%				
LOI	XRF	wt%	5.32	2.37	5.7	3.93
TOTAL			101.41	101.66	100.96	101.47
<i>laboratory</i>			OGL	OGL	OGL	OGL
Cr	XRF	ppm	292	189	240	219
Ni	XRF	ppm				
Nb	XRF	ppm	0	3	3	3
Y	XRF	ppm	16	13	13	13
Zr	XRF	ppm	50	96	90	86
V	XRF	ppm				
<i>laboratory</i>			OGL	OGL	OGL	OGL
Al	ICP-AES	ppm	72031	64293	63777	67726
Ba	ICP-AES	ppm	105	73	98	53
Be	ICP-AES	ppm	0.26	0.28	0.37	0.38
Ca	ICP-AES	ppm	67163	94962	49843	46624
Cd	ICP-AES	ppm	0	0	0	0
Co	ICP-AES	ppm	37	28	27	26
Cr	ICP-AES	ppm	191.08	168.99	165.84	152.91
Cu	ICP-AES	ppm	74	3	60	36
Fe	ICP-AES	ppm	55871	55055	53074	42120
K	ICP-AES	ppm	1425	4043	2712	888
Li	ICP-AES	ppm	16	3	8	6
Mg	ICP-AES	ppm	14166	17749	24144	19854
Mn	ICP-AES	ppm	1302	757	978	753
Mo	ICP-AES	ppm	0	0	0	0
Na	ICP-AES	ppm	19359	2154	26678	30199
Ni	ICP-AES	ppm	125	144	121	166
P	ICP-AES	ppm	459	493	504	531
S	ICP-AES	ppm	-400	90	111	-400
Sc	ICP-AES	ppm	23.1	12.8	15.8	15.5
Sr	ICP-AES	ppm	166.5	184.7	53.5	85.4
Ti	ICP-AES	ppm	4904	3351	4053	4097
V	ICP-AES	ppm	210	126	138	142
W	ICP-AES	ppm	0	0	0	0
Y	ICP-AES	ppm	12.9	10.9	11.2	11
Zn	ICP-AES	ppm	75	55	75	65
<i>laboratory</i>			OGL	OGL	OGL	OGL
Ce	ICP-MS	ppm	12.26	21.89	20.54	21.5
Cs	ICP-MS	ppm	0.517	0.473	0.427	0.451
Dy	ICP-MS	ppm	3.106	2.582	2.714	2.705
Er	ICP-MS	ppm	1.933	1.513	1.681	1.56
Eu	ICP-MS	ppm	0.875	0.876	0.818	0.801
Gd	ICP-MS	ppm	2.917	2.739	2.802	2.798
Hf	ICP-MS	ppm	1.5	2.5	2.4	2.5
Ho	ICP-MS	ppm	0.668	0.527	0.566	0.546
La	ICP-MS	ppm	5.03	9.78	8.98	9.37
Lu	ICP-MS	ppm	0.284	0.224	0.248	0.22
Nb	ICP-MS	ppm	3	4.5	4.4	4.3
Nd	ICP-MS	ppm	8.61	11.62	11.32	11.88
Pr	ICP-MS	ppm	1.807	2.846	2.694	2.8
Rb	ICP-MS	ppm	5.43	20.96	9.95	3.34
Sm	ICP-MS	ppm	2.33	2.66	2.65	2.67
Sr	ICP-MS	ppm	206.3	221.7	64.4	102.5
Ta	ICP-MS	ppm	0.21	0.33	0.3	0.29
Tb	ICP-MS	ppm	0.49	0.425	0.438	0.436
Th	ICP-MS	ppm	0.31	0.99	1	0.92
Tm	ICP-MS	ppm	0.284	0.224	0.245	0.226
U	ICP-MS	ppm	0.079	0.257	0.258	0.247
Y	ICP-MS	ppm	18.21	13.59	14.85	14.34
Yb	ICP-MS	ppm	1.84	1.44	1.61	1.51
Zr	ICP-MS	ppm	55.1	100.5	98.7	102.3

Sample number	04ASP514-1.1	04ASP512-1.1	03ASP0146.3.1
Township	Ben Nevis	Ben Nevis	Ben Nevis
Easting UTM NAD83	599534	599554	599323
Northing UTM NAD83	5347875	5348303	5352512
Phase	BRG High-level Synvolc Intrusion	BRG High-level Synvolc Intrusion	BRG High-level Synvolc Intrusion
Structural Block	Ben Nevis South	Ben Nevis South	Ben Nevis Southeast
Rock type	Diorite -synvolcanic	QFP -synvolcanic	Andesite Dyke
Note			

<i>laboratory</i>			ActLab	ActLab	OGL
	method	units			
SiO2	XRF	wt%	54.98	67.96	51.66
TiO2	XRF	wt%	1.06	0.42	1
Al2O3	XRF	wt%	16.68	15.21	16.32
Fe2O3	XRF	wt%	10.02	4.46	9.85
MgO	XRF	wt%	6.4	1.87	5.66
CaO	XRF	wt%	2.11	2.35	4.84
Na2O	XRF	wt%	4.23	2.48	4.1
K2O	XRF	wt%	0.17	2.32	0.43
MnO	XRF	wt%	0.185	0.073	0.13
P2O5	XRF	wt%	0.17	0.11	0.14
Cr2O3	XRF	wt%	0.02	-0.01	
LOI	XRF	wt%	4.2195	2.0098	6.92
TOTAL			100.2445	99.2528	101.05
<i>laboratory</i>			ActLabs	ActLabs	OGL
Cr	XRF	ppm	147	13	173
Ni	XRF	ppm	137	-4	
Nb	XRF	ppm	5	5	3
Y	XRF	ppm	21	39	18
Zr	XRF	ppm	125	135	91
V	XRF	ppm	227	54	
<i>laboratory</i>			OGL	OGL	OGL
Al	ICP-AES	ppm	60786	74115	79756
Ba	ICP-AES	ppm	63	594	84
Be	ICP-AES	ppm	0	1	0.26
Ca	ICP-AES	ppm	15023	16762	31729
Cd	ICP-AES	ppm	0	0	0
Co	ICP-AES	ppm	26	6	28
Cr	ICP-AES	ppm	114	31	114.09
Cu	ICP-AES	ppm	30	4	71
Fe	ICP-AES	ppm	66178	30412	64183
K	ICP-AES	ppm	1222	17688	2939
Li	ICP-AES	ppm	17	10	52
Mg	ICP-AES	ppm	26934	10290	32477
Mn	ICP-AES	ppm	1204	502	834
Mo	ICP-AES	ppm	0	0	0
Na	ICP-AES	ppm	29400	17970	29281
Ni	ICP-AES	ppm	143	12	69
P	ICP-AES	ppm	682	361	570
S	ICP-AES	ppm	-400	0	193
Sc	ICP-AES	ppm	8.3	7.6	20.5
Sr	ICP-AES	ppm	174.1	82.3	108.4
Ti	ICP-AES	ppm	6004	2275	4446
V	ICP-AES	ppm	167	45	187
W	ICP-AES	ppm	0	4	0
Y	ICP-AES	ppm	9.5	32.3	14.4
Zn	ICP-AES	ppm	161	46	115
<i>laboratory</i>			OGL	OGL	OGL
Ce	ICP-MS	ppm	13.66	40.44	22.13
Cs	ICP-MS	ppm	0.273	1.876	0.628
Dy	ICP-MS	ppm	1.761	6.423	3.658
Er	ICP-MS	ppm	1.13	4.165	2.276
Eu	ICP-MS	ppm	0.424	1.087	1.059
Gd	ICP-MS	ppm	1.561	5.986	3.573
Hf	ICP-MS	ppm	3.3	4.4	2.6
Ho	ICP-MS	ppm	0.377	1.352	0.77
La	ICP-MS	ppm	6.3	18.48	9.59
Lu	ICP-MS	ppm	0.17	0.687	0.332
Nb	ICP-MS	ppm	5.2	7.6	4.5
Nd	ICP-MS	ppm	6.77	21.45	12.67
Pr	ICP-MS	ppm	1.674	5.133	2.901
Rb	ICP-MS	ppm	3.22	66.93	14.79
Sm	ICP-MS	ppm	1.48	5.36	3.14
Sr	ICP-MS	ppm	170.2	81.8	129.9
Ta	ICP-MS	ppm	0	1	0.31
Tb	ICP-MS	ppm	0.274	1.018	0.599
Th	ICP-MS	ppm	1	4	0.94
Tm	ICP-MS	ppm	0.174	0.64	0.336
U	ICP-MS	ppm	0.418	1.183	0.249
Y	ICP-MS	ppm	10.03	38.44	20.22
Yb	ICP-MS	ppm	1.14	4.36	2.17
Zr	ICP-MS	ppm	132	155.9	105.2

Sample number	03ASP0147.2.1	03ASP0183.2.1	03ASP0126.2.1
Township	Ben Nevis	Ben Nevis	Ben Nevis
Easting UTM NAD83	599365	599419	600515
Northing UTM NAD83	5352135	5351732	5351813
Phase	BRG High-level Synvolc Intrusion	BRG High-level Synvolc Intrusion	BRG High-level Synvolc Intrusion
Structural Block	Ben Nevis Southeast	Ben Nevis Southeast	Ben Nevis Southeast
Rock type	Andesite Dyke	Andesite Dyke	Rhyolite Dyke
Note			

	<i>laboratory</i>		OGL	OGL	OGL
	method	units			
SiO2	XRF	wt%	56.69	47.36	74.9
TiO2	XRF	wt%	0.92	0.87	0.33
Al2O3	XRF	wt%	17.44	13.94	12.36
Fe2O3	XRF	wt%	12.02	9.88	3.1
MgO	XRF	wt%	6.15	7.82	0.37
CaO	XRF	wt%	0.16	8.46	1.34
Na2O	XRF	wt%	0.1	2.48	6.22
K2O	XRF	wt%	2.37	0.36	0.09
MnO	XRF	wt%	0.08	0.13	0.05
P2O5	XRF	wt%	0.09	0.11	0.07
Cr2O3	XRF	wt%			
LOI	XRF	wt%	4.98	10.03	0.74
TOTAL			101.01	101.44	99.56
	<i>laboratory</i>		OGL	OGL	OGL
Cr	XRF	ppm	74	156	23
Ni	XRF	ppm			
Nb	XRF	ppm	3	3	6
Y	XRF	ppm	16	31	32
Zr	XRF	ppm	109	82	192
V	XRF	ppm			
	<i>laboratory</i>		OGL	OGL	OGL
Al	ICP-AES	ppm	58679	63400	56421
Ba	ICP-AES	ppm	375	41	75
Be	ICP-AES	ppm	0.32	0.21	0.47
Ca	ICP-AES	ppm	882	48937	5313
Cd	ICP-AES	ppm	0	0	0
Co	ICP-AES	ppm	13	21	4
Cr	ICP-AES	ppm	33.31	96.01	37.02
Cu	ICP-AES	ppm	0	0	0
Fe	ICP-AES	ppm	75821	58685	21432
K	ICP-AES	ppm	12499	2167	566
Li	ICP-AES	ppm	31	47	2
Mg	ICP-AES	ppm	22290	41786	2404
Mn	ICP-AES	ppm	501	741	354
Mo	ICP-AES	ppm	0	0	0
Na	ICP-AES	ppm	1027	15341	40475
Ni	ICP-AES	ppm	78	78	7
P	ICP-AES	ppm	394	419	214
S	ICP-AES	ppm	62	391	0
Sc	ICP-AES	ppm	9.7	18.1	3.7
Sr	ICP-AES	ppm	5.3	66.6	86.1
Ti	ICP-AES	ppm	4176	3755	1272
V	ICP-AES	ppm	157	162	6.1
W	ICP-AES	ppm	0	0	0
Y	ICP-AES	ppm	12.1	24.1	14.4
Zn	ICP-AES	ppm	400	93	37
	<i>laboratory</i>		OGL	OGL	OGL
Ce	ICP-MS	ppm	28.31	30.61	34.86
Cs	ICP-MS	ppm	1.529	0.563	0.277
Dy	ICP-MS	ppm	3.116	5.858	2.484
Er	ICP-MS	ppm	1.876	3.813	1.631
Eu	ICP-MS	ppm	0.628	0.888	0.481
Gd	ICP-MS	ppm	3.241	4.596	2.458
Hf	ICP-MS	ppm	3	2.3	5.7
Ho	ICP-MS	ppm	0.635	1.257	0.522
La	ICP-MS	ppm	14.05	13.54	18.23
Lu	ICP-MS	ppm	0.271	0.488	0.292
Nb	ICP-MS	ppm	4.9	5	8
Nd	ICP-MS	ppm	13	15.16	14.03
Pb	ICP-MS	ppm	3.326	3.747	3.885
Rb	ICP-MS	ppm	53.9	16.2	2.06
Sm	ICP-MS	ppm	2.85	3.74	2.6
Sr	ICP-MS	ppm	6.4	82.3	103.5
Ta	ICP-MS	ppm	0.44	0.27	0.76
Tb	ICP-MS	ppm	0.516	0.846	0.394
Th	ICP-MS	ppm	2.36	1	4.19
Tm	ICP-MS	ppm	0.273	0.548	0.256
U	ICP-MS	ppm	0.726	0.156	1.22
Y	ICP-MS	ppm	16.99	32.94	14.3
Yb	ICP-MS	ppm	1.78	3.41	1.78
Zr	ICP-MS	ppm	116.2	89.8	209.7

Sample number	03ASP0162.2.1	03ASP0207.2.1	03ASP0115.1.1
Township	Ben Nevis	Ben Nevis	Ben Nevis
Easting UTM NAD83	599091	598826	598428
Northing UTM NAD83	5351293	5351143	5350747
Phase	BRG High-level Synvolc Intrusion	BRG High-level Synvolc Intrusion	BRG High-level Synvolc Intrusion
Structural Block	Ben Nevis Southwest	Ben Nevis Southwest	Ben Nevis Southwest
Rock type	Rhyolite Dyke	Rhyolite Dyke	Rhyolite Dyke- altered
Note			

<i>laboratory</i>			OGL	OGL	OGL
	method	units			
SiO2	XRF	wt%	70.48	72.05	69.68
TiO2	XRF	wt%	0.32	0.3	0.32
Al2O3	XRF	wt%	11.77	11.47	13.62
Fe2O3	XRF	wt%	3.45	3.76	3.68
MgO	XRF	wt%	1.06	2.45	1.04
CaO	XRF	wt%	3.35	2.94	3.8
Na2O	XRF	wt%	2.2	1.54	1.58
K2O	XRF	wt%	1.77	0.85	3.03
MnO	XRF	wt%	0.08	0.1	0.07
P2O5	XRF	wt%	0.06	0.07	0.09
Cr2O3	XRF	wt%			
LOI	XRF	wt%	4.08	4.58	4.13
TOTAL			98.62	100.11	101.02
<i>laboratory</i>			OGL	OGL	OGL
Cr	XRF	ppm	4	23	11
Ni	XRF	ppm			
Nb	XRF	ppm	7	5	6
Y	XRF	ppm	37	40	40
Zr	XRF	ppm	202	186	160
V	XRF	ppm			
<i>laboratory</i>			OGL	OGL	OGL
Al	ICP-AES	ppm	54592	53433	52368
Ba	ICP-AES	ppm	329	273	385
Be	ICP-AES	ppm	0.37	0.45	0.45
Ca	ICP-AES	ppm	19799	17195	10709
Cd	ICP-AES	ppm	0	0	0
Co	ICP-AES	ppm	1	4	7
Cr	ICP-AES	ppm	9.63	8.42	6.98
Cu	ICP-AES	ppm	0	24	4
Fe	ICP-AES	ppm	23143	23993	25555
K	ICP-AES	ppm	10444	5232	17898
Li	ICP-AES	ppm	15	27	6
Mg	ICP-AES	ppm	5996	13003	5445
Mn	ICP-AES	ppm	525	602	455
Mo	ICP-AES	ppm	0	0	0
Na	ICP-AES	ppm	15201	10836	10549
Ni	ICP-AES	ppm	4	6	9
P	ICP-AES	ppm	242	220	302
S	ICP-AES	ppm	111	57	-400
Sc	ICP-AES	ppm	5.3	4.5	2.8
Sr	ICP-AES	ppm	44.1	47.9	28.9
Ti	ICP-AES	ppm	1464	1280	1308
V	ICP-AES	ppm	1	5	19.8
W	ICP-AES	ppm	4	0	3
Y	ICP-AES	ppm	26.3	30.3	10.7
Zn	ICP-AES	ppm	53	260	32
<i>laboratory</i>			OGL	OGL	OGL
Ce	ICP-MS	ppm	47.87	58.16	13.56
Cs	ICP-MS	ppm	0.747	1.17	2.613
Dy	ICP-MS	ppm	6.423	7.29	1.749
Er	ICP-MS	ppm	4.154	4.602	1.132
Eu	ICP-MS	ppm	1.135	1.188	0.291
Gd	ICP-MS	ppm	6.006	6.959	1.62
Hf	ICP-MS	ppm	5.9	5.5	4.9
Ho	ICP-MS	ppm	1.37	1.54	0.377
La	ICP-MS	ppm	22.14	28.23	6.53
Lu	ICP-MS	ppm	0.642	0.655	0.206
Nb	ICP-MS	ppm	9	7.6	7.3
Nd	ICP-MS	ppm	23.47	28.97	6.66
Pb	ICP-MS	ppm	5.846	7.1	1.652
Rb	ICP-MS	ppm	51.14	24.79	79.68
Sm	ICP-MS	ppm	5.46	6.5	1.5
Sr	ICP-MS	ppm	53.3	55.1	33.7
Ta	ICP-MS	ppm	0.76	0.74	0.68
Tb	ICP-MS	ppm	1.024	1.164	0.268
Th	ICP-MS	ppm	4.33	4.32	1.72
Tm	ICP-MS	ppm	0.632	0.68	0.179
U	ICP-MS	ppm	1.188	1.17	0.931
Y	ICP-MS	ppm	38.07	41.85	10.6
Yb	ICP-MS	ppm	4.18	4.36	1.26
Zr	ICP-MS	ppm	225.6	201	172.8

Sample number	03ASP0130.3.1	03ASP0130.1.2	03ASP0198.2.1
Township	Ben Nevis	Ben Nevis	Katrine
Easting UTM NAD83	593446	593446	596765
Northing UTM NAD83	5350654	5350654	5345233
Phase	BRG High-level Synvolc Intrusion	BRG High-level Synvolc Intrusion	BRG High-level Synvolc Intrusion
Structural Block	Clifford South	Clifford South	Katrine North
Rock type	Diorite -synvolcanic	QFP -synvolcanic	Rhyolite Dyke
Note			

	laboratory		OGL	OGL	OGL
	method	units			
SiO2	XRF	wt%	60.49	64.79	70.1
TiO2	XRF	wt%	0.65	0.49	0.36
Al2O3	XRF	wt%	15.43	14.02	14.33
Fe2O3	XRF	wt%	6.87	4.95	3.92
MgO	XRF	wt%	4.11	2.54	0.74
CaO	XRF	wt%	5.9	4.28	2.09
Na2O	XRF	wt%	3.52	3.04	5.72
K2O	XRF	wt%	0.7	1.76	1.51
MnO	XRF	wt%	0.1	0.07	0.06
P2O5	XRF	wt%	0.13	0.11	0.08
Cr2O3	XRF	wt%			
LOI	XRF	wt%	3.21	4.37	1.31
TOTAL			101.1	100.42	100.23
	laboratory		OGL	OGL	OGL
Cr	XRF	ppm	104	89	20
Ni	XRF	ppm			
Nb	XRF	ppm	5	7	6
Y	XRF	ppm	24	35	33
Zr	XRF	ppm	147	130	154
V	XRF	ppm			
	laboratory		OGL	OGL	OGL
Al	ICP-AES	ppm	63141	65969	65941
Ba	ICP-AES	ppm	150	362	294
Be	ICP-AES	ppm	0.4	0.51	0.38
Ca	ICP-AES	ppm	26212	26955	12244
Cd	ICP-AES	ppm	0	0	0
Co	ICP-AES	ppm	19	12	6
Cr	ICP-AES	ppm	69.91	57.51	12.01
Cu	ICP-AES	ppm	4	7	0
Fe	ICP-AES	ppm	40057	31974	24250
K	ICP-AES	ppm	4308	11705	9702
Li	ICP-AES	ppm	11	24	5
Mg	ICP-AES	ppm	20193	13966	3965
Mn	ICP-AES	ppm	542	434	357
Mo	ICP-AES	ppm	0	0	0
Na	ICP-AES	ppm	23933	21310	37281
Ni	ICP-AES	ppm	80	56	5
P	ICP-AES	ppm	481	409	264
S	ICP-AES	ppm	103	-400	76
Sc	ICP-AES	ppm	5.4	8	6.2
Sr	ICP-AES	ppm	162.3	82.3	107.9
Ti	ICP-AES	ppm	2611	2195	1640
V	ICP-AES	ppm	90.3	60	28
W	ICP-AES	ppm	0	0	3
Y	ICP-AES	ppm	10.6	25.8	25.3
Zn	ICP-AES	ppm	56	75	22
	laboratory		OGL	OGL	OGL
Ce	ICP-MS	ppm	14.06	40.06	40.92
Cs	ICP-MS	ppm	0.343	0.831	0.532
Dy	ICP-MS	ppm	2.435	6.072	5.98
Er	ICP-MS	ppm	1.529	4.085	4.096
Eu	ICP-MS	ppm	0.532	1.436	0.991
Gd	ICP-MS	ppm	2.216	5.692	5.528
Hf	ICP-MS	ppm	4.2	4.2	4.7
Ho	ICP-MS	ppm	0.517	1.321	1.262
La	ICP-MS	ppm	6.99	17.28	19.26
Lu	ICP-MS	ppm	0.228	0.692	0.698
Nb	ICP-MS	ppm	6.3	8.4	7.8
Nd	ICP-MS	ppm	7.68	20.57	20.61
Pr	ICP-MS	ppm	1.783	5.053	5.122
Rb	ICP-MS	ppm	18.41	51.14	36.82
Sm	ICP-MS	ppm	1.9	5.14	5
Sr	ICP-MS	ppm	197.5	94.8	132.3
Ta	ICP-MS	ppm	0.53	0.83	0.7
Tb	ICP-MS	ppm	0.379	0.987	0.941
Th	ICP-MS	ppm	1.82	5.3	4.52
Tm	ICP-MS	ppm	0.228	0.632	0.638
U	ICP-MS	ppm	0.588	1.587	1.181
Y	ICP-MS	ppm	13.7	36.62	36.51
Yb	ICP-MS	ppm	1.5	4.33	4.42
Zr	ICP-MS	ppm	162	152.2	172.9

Sample number	03ASP0083.3.1	03ASP0048.3.1	03ASP0015.2.1	03ASP0015.1.1
Township	Katrine	Katrine	Ben Nevis	Ben Nevis
Easting UTM NAD83	600061	596789	599179	599179
Northing UTM NAD83	5344582	5340101	5354866	5354866
Phase	BRG High-level Synvolc Intrusion	BRG High-level Synvolc Intrusion	BRG Intrusion	BRG Intrusion
Structural Block	Katrine South	Katrine South_Garrison	Ben Nevis North	Ben Nevis North
Rock type	Andesite Dyke	Andesite Dyke	Diorite	Gabbro
Note				

			OGL	OGL	OGL	OGL
<i>laboratory</i>			OGL	OGL	OGL	OGL
	method	units				
SiO2	XRF	wt%	46.28	51.68	54.79	47.32
TiO2	XRF	wt%	1.24	1.07	0.79	1.29
Al2O3	XRF	wt%	17.22	17.36	16.27	16.02
Fe2O3	XRF	wt%	14.35	10	8.73	12.42
MgO	XRF	wt%	7.87	5.72	5.63	8.63
CaO	XRF	wt%	4.89	8.15	7.79	8.34
Na2O	XRF	wt%	2.54	2.2	3.9	2.94
K2O	XRF	wt%	2.14	1.57	0.25	0.15
MnO	XRF	wt%	0.26	0.13	0.12	0.18
P2O5	XRF	wt%	0.14	0.12	0.12	0.19
Cr2O3	XRF	wt%				
LOI	XRF	wt%	4.48	3.31	2.98	3.91
TOTAL			101.41	101.32	101.37	101.39
<i>laboratory</i>			OGL	OGL	OGL	OGL
Cr	XRF	ppm	149	163	156	276
Ni	XRF	ppm				
Nb	XRF	ppm	0	3	3	4
Y	XRF	ppm	14	19	19	20
Zr	XRF	ppm	53	100	103	92
V	XRF	ppm				
<i>laboratory</i>			OGL	OGL	OGL	OGL
Al	ICP-AES	ppm	84731	78108	74024	68551
Ba	ICP-AES	ppm	700	216	69	58
Be	ICP-AES	ppm	0.2	0.27	0.23	0.26
Ca	ICP-AES	ppm	26486	41054	36959	44197
Cd	ICP-AES	ppm	0	0	0	0
Co	ICP-AES	ppm	47	32	35	42
Cr	ICP-AES	ppm	101.74	112.94	107.75	181.74
Cu	ICP-AES	ppm	182	47	274	81
Fe	ICP-AES	ppm	-100000	66573	60608	77576
K	ICP-AES	ppm	13512	9444	1731	944
Li	ICP-AES	ppm	18	17	11	13
Mg	ICP-AES	ppm	45997	32303	34034	38336
Mn	ICP-AES	ppm	1822	847	822	1071
Mo	ICP-AES	ppm	0	0	0	0
Na	ICP-AES	ppm	16983	13954	26542	18450
Ni	ICP-AES	ppm	115	64	95	168
P	ICP-AES	ppm	572	454	499	748
S	ICP-AES	ppm	295	101	-400	147
Sc	ICP-AES	ppm	22.1	14.5	12.5	16.9
Sr	ICP-AES	ppm	123.9	317.2	181.3	143.6
Ti	ICP-AES	ppm	5464	4525	3290	5897
V	ICP-AES	ppm	198.9	193.8	145.5	197.8
W	ICP-AES	ppm	0	0	5	4
Y	ICP-AES	ppm	11.4	12.5	10.9	13.9
Zn	ICP-AES	ppm	110	77	49	83
<i>laboratory</i>			OGL	OGL	OGL	OGL
Ce	ICP-MS	ppm	8.88	13.51	12.57	18.16
Cs	ICP-MS	ppm	0.556	0.7	0.29	0.164
Dy	ICP-MS	ppm	2.596	2.668	2.274	3.564
Er	ICP-MS	ppm	1.517	1.689	1.471	2.051
Eu	ICP-MS	ppm	0.733	0.702	0.594	1.066
Gd	ICP-MS	ppm	2.487	2.474	2.049	3.603
Hf	ICP-MS	ppm	1.5	2.6	2.8	2.5
Ho	ICP-MS	ppm	0.521	0.57	0.488	0.72
La	ICP-MS	ppm	3.5	6.19	6.17	6.8
Lu	ICP-MS	ppm	0.209	0.242	0.216	0.284
Nb	ICP-MS	ppm	2.6	4.4	4.5	5.5
Nd	ICP-MS	ppm	6.64	8.02	6.91	12.45
Pr	ICP-MS	ppm	1.348	1.818	1.645	2.665
Rb	ICP-MS	ppm	29.32	49.44	5.96	2.1
Sm	ICP-MS	ppm	2.05	2.1	1.78	3.29
Sr	ICP-MS	ppm	132.2	354.5	217.3	163.6
Ta	ICP-MS	ppm	0.19	0.33	0.36	0.36
Tb	ICP-MS	ppm	0.411	0.417	0.348	0.582
Th	ICP-MS	ppm	0.27	0.9	1	0.42
Tm	ICP-MS	ppm	0.215	0.248	0.216	0.295
U	ICP-MS	ppm	0.078	0.262	0.265	0.128
Y	ICP-MS	ppm	11.79	14.24	12.73	17.2
Yb	ICP-MS	ppm	1.38	1.59	1.43	1.91
Zr	ICP-MS	ppm	55.7	100	108.7	97.2

Sample number	03ASP0068.1.1		03ASP0125.1.1		03ASP0166.1.1		03ASP0134.1.1		03ASP0130.2.1	
Township	Ben Nevis		Ben Nevis		Ben Nevis		Ben Nevis		Ben Nevis	
Easting UTM NAD83	600548		600509		599046		593510		593446	
Northing UTM NAD83	5354770		5351760		5352817		5350992		5350654	
Phase	BRG Intrusion		BRG Intrusion		BRG Intrusion		BRG Intrusion		BRG Intrusion	
Structural Block	Ben Nevis Southeast		Ben Nevis Southeast		Ben Nevis Southeast		Clifford South		Clifford South	
Rock type	Dacite		Diorite		Diorite		Diorite		Diorite - porphyritic	
Note	Poor Oxide Closure									
<i>laboratory</i>			OGL	OGL	OGL	OGL	OGL	OGL	OGL	OGL
	method	units								
SiO2	XRF	wt%	63.74	51.97	50.58	55.75	59.87			
TiO2	XRF	wt%	0.64	1	0.99	1.03	0.68			
Al2O3	XRF	wt%	13.27	16.63	18.13	16.97	15.69			
Fe2O3	XRF	wt%	5.01	9.65	10.8	7.78	7.12			
MgO	XRF	wt%	0.99	6.7	6.96	4.17	4.43			
CaO	XRF	wt%	5.76	6.66	3.13	7.28	6.6			
Na2O	XRF	wt%	3.73	4.86	4.4	3.65	3.29			
K2O	XRF	wt%	1.32	0.15	0.35	0.35	0.55			
MnO	XRF	wt%	0.16	0.11	0.13	0.15	0.1			
P2O5	XRF	wt%	0.15	0.13	0.13	0.1	0.13			
Cr2O3	XRF	wt%								
LOI	XRF	wt%	5.48	3.28	5.22	3.67	3.1			
TOTAL			100.26	101.12	100.83	100.9	101.56			
<i>laboratory</i>			OGL	OGL	OGL	OGL	OGL	OGL	OGL	OGL
Cr	XRF	ppm	30	163	202	65	113			
Ni	XRF	ppm								
Nb	XRF	ppm	7	3	4	3	5			
Y	XRF	ppm	53	16	19	14	23			
Zr	XRF	ppm	221	92	100	102	146			
V	XRF	ppm								
<i>laboratory</i>			OGL	OGL	OGL	OGL	OGL	OGL	OGL	OGL
Al	ICP-AES	ppm	62390	72393	79671	77013	73901			
Ba	ICP-AES	ppm	265	101	83	133	163			
Be	ICP-AES	ppm	0.5	0.28	0.33	0.44	0.39			
Ca	ICP-AES	ppm	33270	32646	18338	42525	35037			
Cd	ICP-AES	ppm	0	0	0	0	0			
Co	ICP-AES	ppm	8	30	32	23	26			
Cr	ICP-AES	ppm	14	113.65	131.44	34.61	102.9			
Cu	ICP-AES	ppm	10	10	19	60	0			
Fe	ICP-AES	ppm	32386	63623	61149	46802	49860			
K	ICP-AES	ppm	8662	952	2173	2410	3688			
Li	ICP-AES	ppm	9	20	91	20	19			
Mg	ICP-AES	ppm	5626	31417	34196	22113	27983			
Mn	ICP-AES	ppm	972	683	713	913	673			
Mo	ICP-AES	ppm	0	0	0	0	0			
Na	ICP-AES	ppm	24683	29852	29492	24444	20926			
Ni	ICP-AES	ppm	8	80	90	71	109			
P	ICP-AES	ppm	592	519	523	308	507			
S	ICP-AES	ppm	306	47	85	176	88			
Sc	ICP-AES	ppm	8.7	16.6	21.2	14.1	9.5			
Sr	ICP-AES	ppm	99.8	156.5	88.9	73.2	171.9			
Ti	ICP-AES	ppm	3041	4112	4583	4570	2837			
V	ICP-AES	ppm	38	182.3	186	196	95.8			
W	ICP-AES	ppm	0	0	4	0	0			
Y	ICP-AES	ppm	40.8	11.6	14.6	10.6	16.8			
Zn	ICP-AES	ppm	75	45	86	83	62			
<i>laboratory</i>			OGL	OGL	OGL	OGL	OGL	OGL	OGL	OGL
Ce	ICP-MS	ppm	46.87	18.73	23.32	23.52	24.94			
Cs	ICP-MS	ppm	1.229	0.301	1.009	0.535	0.306			
Dy	ICP-MS	ppm	9.634	2.886	3.916	2.61	3.696			
Er	ICP-MS	ppm	6.234	1.683	2.444	1.653	2.309			
Eu	ICP-MS	ppm	1.72	0.87	1.176	0.786	0.853			
Gd	ICP-MS	ppm	8.796	2.903	3.667	2.63	3.471			
Hf	ICP-MS	ppm	6.3	2.6	2.8	2.8	4.2			
Ho	ICP-MS	ppm	2.064	0.586	0.821	0.542	0.777			
La	ICP-MS	ppm	20.3	8.15	10.38	11.65	11.71			
Lu	ICP-MS	ppm	0.94	0.233	0.336	0.25	0.335			
Nb	ICP-MS	ppm	9.6	4.1	4.9	4.4	6.6			
Nd	ICP-MS	ppm	28.38	10.65	12.98	11	13.32			
Pr	ICP-MS	ppm	6.359	2.455	3.073	2.805	3.121			
Rb	ICP-MS	ppm	41.99	2.42	12.52	7.24	15.37			
Sm	ICP-MS	ppm	7.48	2.61	3.26	2.4	3.17			
Sr	ICP-MS	ppm	117.5	172.8	112.4	87.9	198.6			
Ta	ICP-MS	ppm	0.66	0.32	0.34	0.38	0.54			
Tb	ICP-MS	ppm	1.512	0.465	0.615	0.426	0.582			
Th	ICP-MS	ppm	2.79	0.72	1.09	2.42	1.96			
Tm	ICP-MS	ppm	0.932	0.242	0.357	0.245	0.344			
U	ICP-MS	ppm	0.729	0.222	0.288	0.632	0.55			
Y	ICP-MS	ppm	55.72	12.94	20.93	14.84	20.26			
Yb	ICP-MS	ppm	6.1	1.56	2.29	1.61	2.25			
Zr	ICP-MS	ppm	236.6	100.1	109.8	111.8	161			

Sample number	03ASP0045.1.1	03ASP0044.1.1	03ASP0064.2.1	03ASP0078.1.1	03ASP0052.1.1
Township	Katrine	Katrine	Katrine	Katrine	Katrine
Easting UTM NAD83	599477	599340	600144	599967	597117
Northing UTM NAD83	5345342	5345293	5340608	5344587	5339960
Phase	BRG Intrusion	BRG Intrusion	BRG Intrusion	BRG Intrusion	BRG Intrusion
Structural Block	Katrine North	Katrine North	Katrine South	Katrine South	Katrine South_Garrison
Rock type	Granodiorite	Granodiorite-porphyrific	Basalt	Gabbro	Leucogabbro
Note					

	laboratory		OGL	OGL	OGL	OGL	OGL
	method	units					
SiO2	XRF	wt%	64.19	62.52	54	47.71	54.43
TiO2	XRF	wt%	0.58	0	0.87	0.93	0.75
Al2O3	XRF	wt%	15.24	15.87	15.92	17.81	15.37
Fe2O3	XRF	wt%	5.62	6.71	8.76	11.37	8.37
MgO	XRF	wt%	2.12	2.71	6.72	8.41	7.16
CaO	XRF	wt%	6.1	4.51	7.42	7.25	7.66
Na2O	XRF	wt%	4.46	5.02	4.16	2	2.98
K2O	XRF	wt%	0.34	0.7	0.51	0.68	0.67
MnO	XRF	wt%	0.08	0.13	0.14	0.2	0.1
P2O5	XRF	wt%	0.1	0.11	0.14	0.12	0.12
Cr2O3	XRF	wt%					
LOI	XRF	wt%	2.52	2.36	2.17	5.01	3.67
TOTAL			101.37	100.64	100.81	101.49	101.3
	laboratory		OGL	OGL	OGL	OGL	OGL
Cr	XRF	ppm	16	18	195	126	240
Ni	XRF	ppm					
Nb	XRF	ppm	4	4	4	0	3
Y	XRF	ppm	24	26	18	9	15
Zr	XRF	ppm	120	117	118	34	99
V	XRF	ppm					
	laboratory		OGL	OGL	OGL	OGL	OGL
Al	ICP-AES	ppm	55688	65909	72151	82366	75632
Ba	ICP-AES	ppm	80	153	362	141	135
Be	ICP-AES	ppm	0.38	0.35	0.28	0.17	0.29
Ca	ICP-AES	ppm	13877	13245	40025	45503	43939
Cd	ICP-AES	ppm	0	0	0	0	0
Co	ICP-AES	ppm	11	13	32	37	33
Cr	ICP-AES	ppm	7.39	8.84	124.45	70.74	153.47
Cu	ICP-AES	ppm	12	17	30	10	0
Fe	ICP-AES	ppm	35485	44360	55982	73106	55908
K	ICP-AES	ppm	2014	4593	3157	4026	4203
Li	ICP-AES	ppm	6	10	14	26	16
Mg	ICP-AES	ppm	10906	14816	34747	43562	41447
Mn	ICP-AES	ppm	519	818	851	1236	664
Mo	ICP-AES	ppm	0	0	0	0	0
Na	ICP-AES	ppm	28217	32482	26326	12246	19780
Ni	ICP-AES	ppm	10	12	174	82	174
P	ICP-AES	ppm	356	396	534	423	448
S	ICP-AES	ppm	67	71	-400	74	97
Sc	ICP-AES	ppm	4.2	6.7	14.7	20.3	15.8
Sr	ICP-AES	ppm	87.2	114.7	119.4	130.4	146.9
Ti	ICP-AES	ppm	2428	2708	3488	3602	3100
V	ICP-AES	ppm	87.5	105.8	123.8	177.7	128.3
W	ICP-AES	ppm	0	5	0	0	0
Y	ICP-AES	ppm	7.5	7.4	13.2	7.1	12.3
Zn	ICP-AES	ppm	31	44	74	60	48
	laboratory		OGL	OGL	OGL	OGL	OGL
Ce	ICP-MS	ppm	6.27	7.6	25.04	6.29	22.43
Cs	ICP-MS	ppm	0.246	0.402	1.048	0.535	0.629
Dy	ICP-MS	ppm	0.828	1.019	3.116	1.628	2.761
Er	ICP-MS	ppm	0.566	0.701	1.877	1.028	1.66
Eu	ICP-MS	ppm	0.183	0.216	0.922	0.613	0.861
Gd	ICP-MS	ppm	0.767	0.886	3.158	1.523	2.733
Hf	ICP-MS	ppm	3.6	3.6	3.1	0.9	2.8
Ho	ICP-MS	ppm	0.18	0.224	0.636	0.347	0.573
La	ICP-MS	ppm	3.54	4.26	10.86	2.76	10.3
Lu	ICP-MS	ppm	0.092	0.137	0.265	0.157	0.253
Nb	ICP-MS	ppm	5.7	5.6	5.2	1.8	4.5
Nd	ICP-MS	ppm	2.88	3.38	13.34	4.4	11.51
Pr	ICP-MS	ppm	0.732	0.859	3.234	0.896	2.838
Rb	ICP-MS	ppm	7.1	15.87	14.13	14.03	16.62
Sm	ICP-MS	ppm	0.69	0.82	3.07	1.26	2.68
Sr	ICP-MS	ppm	104.7	139	139.3	151.3	168.5
Ta	ICP-MS	ppm	0.48	0.47	0.41	0	0.35
Tb	ICP-MS	ppm	0.129	0.152	0.495	0.251	0.453
Th	ICP-MS	ppm	1.49	1.26	1.39	0.24	1.3
Tm	ICP-MS	ppm	0.085	0.112	0.267	0.15	0.246
U	ICP-MS	ppm	0.707	0.701	0.394	0.069	0.353
Y	ICP-MS	ppm	5	6.27	15.71	8.51	15
Yb	ICP-MS	ppm	0.59	0.81	1.76	1.01	1.64
Zr	ICP-MS	ppm	131.4	129.3	124.5	33.4	107.8

Sample number	03ASP0053.2.1	03ASP0041.1.1	03ASP0040.1.1	03ASP0094.1.1
Township	Katrine	Ben Nevis	Ben Nevis	Katrine
Easting UTM NAD83	597210	596858	596611	600639
Northing UTM NAD83	5340023	5350588	5350634	5341436
Phase	BRG Intrusion	Late Intrusion?	Late Intrusion?	Late Intrusion
Structural Block	Katrine South_Garrison	Ben Nevis Southwest	Ben Nevis Southwest	Katrine South
Rock type	Melanogabbro	Diorite-porphyrific	QFP	Alkalic Intrusion-multiphase
Note	Poor Oxide Closure			

			OGL	OGL	OGL	OGL
<i>laboratory</i>			OGL	OGL	OGL	OGL
	method	units				
SiO2	XRF	wt%	57.33	58.49	62.81	52.95
TiO2	XRF	wt%	0.96	0.78	0.4	0.75
Al2O3	XRF	wt%	14.07	17.29	16.27	13.61
Fe2O3	XRF	wt%	8.03	5.99	3.16	8.61
MgO	XRF	wt%	3.88	3.18	1.43	6.82
CaO	XRF	wt%	7.51	6.42	5.13	7.5
Na2O	XRF	wt%	4.55	4.32	8.29	3.41
K2O	XRF	wt%	0.12	0.93	0.06	3.51
MnO	XRF	wt%	0.14	0.08	0.04	0.15
P2O5	XRF	wt%	0.14	0.22	0.11	0.41
Cr2O3	XRF	wt%				
LOI	XRF	wt%	4.82	2.75	2.54	3.04
TOTAL			101.55	100.44	100.24	100.76
<i>laboratory</i>			OGL	OGL	OGL	OGL
Cr	XRF	ppm	209	72	25	444
Ni	XRF	ppm				
Nb	XRF	ppm	3	6	7	4
Y	XRF	ppm	14	8	8	25
Zr	XRF	ppm	87	115	96	123
V	XRF	ppm				
<i>laboratory</i>			OGL	OGL	OGL	OGL
Al	ICP-AES	ppm	61369	72680	65820	62728
Ba	ICP-AES	ppm	74	149	37	1302
Be	ICP-AES	ppm	0.25	0.37	0.23	1.32
Ca	ICP-AES	ppm	35301	11741	11848	41745
Cd	ICP-AES	ppm	0	0	0	0
Co	ICP-AES	ppm	29	20	10	31
Cr	ICP-AES	ppm	153.63	33.24	20.02	344.02
Cu	ICP-AES	ppm	37	3	74	11
Fe	ICP-AES	ppm	52058	41278	21312	58285
K	ICP-AES	ppm	789	6512	463	21736
Li	ICP-AES	ppm	7	18	5	5
Mg	ICP-AES	ppm	21628	19869	8447	38033
Mn	ICP-AES	ppm	903	530	218	989
Mo	ICP-AES	ppm	0	0	0	0
Na	ICP-AES	ppm	29114	27176	51123	20964
Ni	ICP-AES	ppm	154	44	19	87
P	ICP-AES	ppm	505	927	436	1691
S	ICP-AES	ppm	149	68	296	73
Sc	ICP-AES	ppm	11.2	3.9	2.3	17.3
Sr	ICP-AES	ppm	107.1	323	126.1	638.5
Ti	ICP-AES	ppm	3937	3442	1597	3155
V	ICP-AES	ppm	131	96.1	53.7	139.2
W	ICP-AES	ppm	0	0	0	0
Y	ICP-AES	ppm	10.4	3.2	3.6	19.7
Zn	ICP-AES	ppm	69	66	29	84
<i>laboratory</i>			OGL	OGL	OGL	OGL
Ce	ICP-MS	ppm	11.57	5.3	7.75	86.63
Cs	ICP-MS	ppm	0.408	0.653	0.113	0.987
Dy	ICP-MS	ppm	2.113	0.288	0.432	4.897
Er	ICP-MS	ppm	1.319	0.156	0.244	2.694
Eu	ICP-MS	ppm	0.585	0.139	0.158	2.134
Gd	ICP-MS	ppm	2.054	0.375	0.496	6.647
Hf	ICP-MS	ppm	2.4	3.2	3	4
Ho	ICP-MS	ppm	0.44	0.053	0.082	0.959
La	ICP-MS	ppm	5.21	2.94	4.38	40.79
Lu	ICP-MS	ppm	0.177	0.021	0.037	0.385
Nb	ICP-MS	ppm	4	7.5	8	6.4
Nd	ICP-MS	ppm	7.32	2.33	3.17	43.52
Pr	ICP-MS	ppm	1.606	0.62	0.859	10.75
Rb	ICP-MS	ppm	2.78	24.46	0.75	93.47
Sm	ICP-MS	ppm	1.86	0.44	0.62	8.3
Sr	ICP-MS	ppm	128.8	309.6	147.6	771.4
Ta	ICP-MS	ppm	0.29	0.49	0.62	0.4
Tb	ICP-MS	ppm	0.336	0.05	0.075	0.884
Th	ICP-MS	ppm	0.84	0.47	0.87	6.01
Tm	ICP-MS	ppm	0.185	0.021	0.036	0.391
U	ICP-MS	ppm	0.229	0.441	0.701	1.587
Y	ICP-MS	ppm	11.13	1.28	2.32	24.92
Yb	ICP-MS	ppm	1.16	0.15	0.23	2.54
Zr	ICP-MS	ppm	92	121	108.2	146.6

Sample number 03ASP0033.1.1
 Township Katrine
 Easting UTM NAD83 600175
 Northing UTM NAD83 5339597
 Phase Late Intrusion
 Structural Block Katrine South
 Rock type Alkalic porphyry dyke
 Note

<i>laboratory</i>			OGL
	method	units	
SiO2	XRF	wt%	58.87
TiO2	XRF	wt%	0.5
Al2O3	XRF	wt%	15.18
Fe2O3	XRF	wt%	5.42
MgO	XRF	wt%	3.62
CaO	XRF	wt%	5.72
Na2O	XRF	wt%	4.66
K2O	XRF	wt%	3.69
MnO	XRF	wt%	0.11
P2O5	XRF	wt%	0.29
Cr2O3	XRF	wt%	
LOI	XRF	wt%	1.71
TOTAL			99.77
<i>laboratory</i>			OGL
Cr	XRF	ppm	160
Ni	XRF	ppm	
Nb	XRF	ppm	7
Y	XRF	ppm	28
Zr	XRF	ppm	221
V	XRF	ppm	
<i>laboratory</i>			OGL
Al	ICP-AES	ppm	66472
Ba	ICP-AES	ppm	1319
Be	ICP-AES	ppm	1.79
Ca	ICP-AES	ppm	17301
Cd	ICP-AES	ppm	0
Co	ICP-AES	ppm	17
Cr	ICP-AES	ppm	113.37
Cu	ICP-AES	ppm	24
Fe	ICP-AES	ppm	37222
K	ICP-AES	ppm	23942
Li	ICP-AES	ppm	6
Mg	ICP-AES	ppm	20486
Mn	ICP-AES	ppm	789
Mo	ICP-AES	ppm	0
Na	ICP-AES	ppm	30804
Ni	ICP-AES	ppm	35
P	ICP-AES	ppm	1209
S	ICP-AES	ppm	-400
Sc	ICP-AES	ppm	5.6
Sr	ICP-AES	ppm	872
Ti	ICP-AES	ppm	2129
V	ICP-AES	ppm	79
W	ICP-AES	ppm	5
Y	ICP-AES	ppm	12.4
Zn	ICP-AES	ppm	70
<i>laboratory</i>			OGL
Ce	ICP-MS	ppm	72.11
Cs	ICP-MS	ppm	0.889
Dy	ICP-MS	ppm	1.632
Er	ICP-MS	ppm	0.965
Eu	ICP-MS	ppm	0.854
Gd	ICP-MS	ppm	2.456
Hf	ICP-MS	ppm	5.8
Ho	ICP-MS	ppm	0.328
La	ICP-MS	ppm	40.54
Lu	ICP-MS	ppm	0.168
Nb	ICP-MS	ppm	8.6
Nd	ICP-MS	ppm	26.93
Pr	ICP-MS	ppm	7.685
Rb	ICP-MS	ppm	84.27
Sm	ICP-MS	ppm	3.7
Sr	ICP-MS	ppm	1022.5
Ta	ICP-MS	ppm	0.5
Tb	ICP-MS	ppm	0.296
Th	ICP-MS	ppm	8.51
Tm	ICP-MS	ppm	0.143
U	ICP-MS	ppm	3.13
Y	ICP-MS	ppm	9.11
Yb	ICP-MS	ppm	1.05
Zr	ICP-MS	ppm	222.5

Appendix 2

Major, Trace and Rare Earth Element Data for Clifford Township

(Selected data from MacDonald et al. 2005)

Abbreviations:

BRG	Blake River Group
XRF	X-ray fluorescence

Note:

A minus sign in front of a value (e.g., -1000) indicates the value is either below or above the detection limit for that element.

Sample number	P03-005	03SJP017-1	03SJP027-1	03SJP096-1-1	03SJP047-1-1	03SJP019	
Township	Clifford	Clifford	Clifford	Clifford	Clifford	Clifford	
Easting UTM NAD83	591250	588861	588900	591934	590849	589121	
Northing UTM NAD83	5350623	5349923	5350525	5351663	5351742	5350008	
Phase	BRG Volcanic	BRG Volcanic	BRG Volcanic	BRG Volcanic	BRG Volcanic	BRG Volcanic	
Structural Block	Clifford North	Clifford North	Clifford North	Clifford North	Clifford North	Clifford North	
Rock type	Andesite	Andesite Pillows	Andesite Pillows	Andesite- Porphyritic	Basalt Pillows	Basaltic Andesite	
Notes							
	units						
SiO2	wt %	55.9	61.31	56.09	50.37	54.5	49.8
TiO2	wt %	0.97	0.63	0.71	1.16	1.13	1.42
Al2O3	wt %	16.01	16.25	16.45	16.22	15.61	17.61
Fe2O3	wt %	8.73	5.52	7.26	10.98	8.64	10.76
MnO	wt %	0.16	0.11	0.14	0.19	0.23	0.2
MgO	wt %	6.25	4.33	5.54	7.8	5.08	6.87
CaO	wt %	6.9	6.52	7.58	8.61	9.42	6.45
Na2O	wt %	2.62	3.43	3.58	2.67	3.2	2.43
K2O	wt %	0.76	0.86	0.93	0.75	0.85	1.39
P2O5	wt %	0.17	0.11	0.14	0.18	0.18	0.21
LOI	wt %	2.67	1.77	2.39	2.4	1.77	3.13
Total		101.15	100.85	100.8	101.33	100.6	100.27
Ni	ppm	139	108	152	165	116	176
Cr	ppm	120.98	91.39	128.11	158.04	139.94	150.97
Co	ppm	29	21	25	39	28	45
V	ppm	131.2	100.9	124.7	131.8	131.1	172.3
Sc	ppm	15.1	10.6	13.6	17.8	16.4	20.4
Cu	ppm	31	78	110	119	552	70
Pb	ppm						
Zn	ppm	100	67	96	110	192	115
Cd	ppm	0	0	0	0	0	0
Mo	ppm	0	0	0	0	0	0
W	ppm	0	4	10	0	4	5
S	ppm	128	188	145	-400	-400	243
Nb (XRF)	ppm	7	6	6	7	8	9
Y (XRF)	ppm	28	20	20	21	26	29
Zr (XRF)	ppm	150	128	150	149	140	164
Zr	ppm	153.1	137.5	149.2	157.6	131.1	177.3
Hf	ppm	3.9	3.6	3.9	4.2	3.4	4.6
Nb	ppm	6.9	5.7	6	7	5.9	8.4
Ta	ppm	0.51	0.49	0.52	0.53	0.42	0.58
Y	ppm	24.41	18.86	21.02	28.76	24.58	29.82
Be	ppm	0.52	0.45	0.43	0.6	0.44	0.61
Li	ppm	12	7	6	17	19	16
Cs	ppm	0.802	0.732	0.765	1.403	0.725	1.755
Rb	ppm	23.24	24.16	29.87	25.67	26.63	52.72
Ba	ppm	155	210	196	180	220	333
Sr	ppm	167.2	206.3	199.2	195.1	197.7	182.9
Th	ppm	1.15	1.5	1.66	1.06	0.8	0.78
U	ppm	0.335	0.395	0.513	0.303	0.227	0.224
La	ppm	10.94	10.21	13.6	13.5	11.06	11.92
Ce	ppm	26.61	22.3	28.73	32.66	27.57	29.46
Pr	ppm	3.591	2.857	3.399	4.547	3.766	4.156
Nd	ppm	15.82	12.3	13.73	20.98	17.13	18.82
Sm	ppm	3.92	2.99	3.2	5.11	4.28	4.8
Eu	ppm	1.137	0.9	0.938	0.795	1.4	1.385
Gd	ppm	4.385	3.304	3.57	5.378	4.641	5.465
Tb	ppm	0.698	0.545	0.591	0.885	0.74	0.879
Dy	ppm	4.393	3.385	3.762	5.395	4.674	5.504
Ho	ppm	0.931	0.727	0.801	1.146	0.954	1.17
Er	ppm	2.729	2.175	2.363	3.316	2.768	3.381
Tm	ppm	0.399	0.314	0.355	0.486	0.403	0.493
Yb	ppm	2.65	2.05	2.34	3.26	2.61	3.14
Lu	ppm	0.415	0.313	0.361	0.497	0.396	0.479

Sample number	03SJP095-1	03SJP046-2	03SJP046-1	03SJP052-1	03SJP055-1	03SJP056-1	
Township	Clifford	Clifford	Clifford	Clifford	Clifford	Clifford	
Easting UTM NAD83	591979	591080	591080	590119	590175	590216	
Northing UTM NAD83	5351476	5351814	5351814	5348846	5349090	5349027	
Phase	BRG Volcanic	BRG Volcanic	BRG Volcanic	BRG Volcanic	BRG Volcanic	BRG Volcanic	
Structural Block	Clifford North	Clifford North	Clifford North	Clifford South	Clifford South	Clifford South	
Rock type	Basaltic Andesite	Basaltic Andesite Hornfelsed	Basaltic Andesite Pillows	Andesite	Andesite	Andesite	
Notes							
units							
SiO2	wt %	56.07	49.58	50.48	57.29	52.49	63.96
TiO2	wt %	0.92	1.26	1.29	0.94	1.25	0.56
Al2O3	wt %	15.4	15.9	16.21	16.44	16.91	13.72
Fe2O3	wt %	7.01	11.13	10.01	8.38	10.05	7.72
MnO	wt %	0.11	0.26	0.26	0.09	0.22	0.08
MgO	wt %	6.45	4.68	5.04	3.93	6.27	3.93
CaO	wt %	7.57	12.82	11.1	5.93	7.62	2.93
Na2O	wt %	2.54	2.52	3.14	3.32	2.44	2.29
K2O	wt %	1.3	0.48	0.67	1.45	1.05	1.7
P2O5	wt %	0.17	0.16	0.16	0.11	0.24	0.06
LOI	wt %	2.4	1.65	1.73	2.43	1.78	3.52
Total		99.93	100.44	100.1	100.31	100.32	100.47
Ni	ppm	181	122	120	51	109	89
Cr	ppm	142.8	123.61	148.67	12.39	132.79	27.63
Co	ppm	54	32	35	27	19	50
V	ppm	138.1	161.4	170.7	174.5	162.7	106.5
Sc	ppm	15.9	18.8	19.9	17.4	18.9	9.4
Cu	ppm	1067	138	290	330	222	275
Pb	ppm						
Zn	ppm	118	107	118	72	78	77
Cd	ppm	0	0	0	0	0	0
Mo	ppm	0	0	0	0	0	0
W	ppm	2	7	8	8	5	6
S	ppm	-400	121	97	-400	-400	-400
Nb (XRF)	ppm	7	6	6	7	8	5
Y (XRF)	ppm	24	28	28	25	28	15
Zr (XRF)	ppm	155	121	124	138	152	128
Zr	ppm	154.3	122.8	127.3	136.2	147.3	129.7
Hf	ppm	3.9	3.4	3.5	3.7	3.9	3.5
Nb	ppm	6.7	5.6	5.6	6	7	4.6
Ta	ppm	0.5	0.41	0.42	0.49	0.5	0.51
Y	ppm	22.12	28.63	28.37	24.75	27.51	14.88
Be	ppm	0.43	0.38	0.38	0.41	0.47	0.44
Li	ppm	13	13	16	6	4	14
Cs	ppm	1.263	0.529	0.635	0.871	0.956	1.408
Rb	ppm	54.32	15.96	23.5	54.36	38.96	63.99
Ba	ppm	182	98	132	230	122	386
Sr	ppm	167.8	203.9	184	141.9	176.7	138.3
Th	ppm	1.22	0.65	0.65	1.6	0.84	2.89
U	ppm	0.378	0.176	0.182	0.392	0.243	0.758
La	ppm	6.66	8.89	9.01	13.21	12.06	8.46
Ce	ppm	14.46	22.58	23.51	28.56	30.24	19.47
Pr	ppm	1.884	3.298	3.485	3.622	4.163	2.406
Nd	ppm	8.75	15.84	16.37	15.37	18.74	9.53
Sm	ppm	2.56	4.38	4.47	3.65	4.54	2.33
Eu	ppm	1.263	1.378	1.526	1.042	1.415	0.64
Gd	ppm	3.271	5.135	5.32	4.182	5.036	2.499
Tb	ppm	0.56	0.84	0.879	0.693	0.813	0.425
Dy	ppm	3.634	5.203	5.476	4.403	5.098	2.658
Ho	ppm	0.803	1.114	1.161	0.945	1.065	0.572
Er	ppm	2.35	3.293	3.349	2.81	3.151	1.766
Tm	ppm	0.363	0.466	0.48	0.423	0.461	0.27
Yb	ppm	2.46	3.02	3.15	2.79	2.98	1.8
Lu	ppm	0.392	0.462	0.472	0.426	0.453	0.289

Sample number	03SJP070-2-1	WC04-08, 64.53-64.69	03SJP011-1	WC04-08, 25.05-25.18	WC04-08, 26.81-26.97	
Township	Clifford	Clifford	Clifford	Clifford	Clifford	
Easting UTM NAD83	591805	591510	590898	591510	591510	
Northing UTM NAD83	5349956	5350267	5349546	5350267	5350267	
Phase	BRG Volcanic	BRG Volcanic	BRG Volcanic	BRG Volcanic	BRG Volcanic	
Structural Block	Clifford South	Clifford South	Clifford South	Clifford South	Clifford South	
Rock type	Andesite	Andesite	Andesite- Porphyritic	Andesitic Tuff	Andesitic Tuff	
Notes						
units						
SiO2	wt %	50.44	60.37	53.75	59.51	59.47
TiO2	wt %	1.12	0.74	1.3	0.72	0.76
Al2O3	wt %	15.24	15.54	15.12	15.56	15.52
Fe2O3	wt %	11.7	6.85	10.82	6.74	6.88
MnO	wt %	0.2	0.115	0.19	0.076	0.075
MgO	wt %	8.91	4.01	6.74	4.69	4.94
CaO	wt %	6.49	6.14	5.21	5.73	4.81
Na2O	wt %	1.87	3.03	2.96	3.03	4.79
K2O	wt %	0.8	1.54	0.95	1.75	1.12
P2O5	wt %	0.18	0.16	0.18	0.15	0.15
LOI	wt %	2.34	1.8	4.04	2.21	2.04
Total		99.29	100.295	101.25	100.166	100.555
Ni	ppm	246	87	128	111	110
Cr	ppm	209.64	66	164.39	117	103
Co	ppm	38	18	26	23	24
V	ppm	155.8	116	157.6	122	132
Sc	ppm	18.4	13.6	19.4	15	15
Cu	ppm	4977	19	68	0	0
Pb	ppm					
Zn	ppm	386	85	182	128	57
Cd	ppm	0	0	0	0	0
Mo	ppm	0	0	0	0	0
W	ppm	2	2	3	0	0
S	ppm	-400	183	-400	134	279
Nb (XRF)	ppm	6	5	7	4	5
Y (XRF)	ppm	25	28	29	28	29
Zr (XRF)	ppm	122	183	133	158	148
Zr	ppm	126.4	191.2	131.4	169.6	160.7
Hf	ppm	3.2	4.8	3.4	4.3	4.1
Nb	ppm	6	7.6	6.2	7.1	6.9
Ta	ppm	0.43	0.54	0.46	0.53	0.5
Y	ppm	25.85	27.38	28.36	28.74	31.15
Be	ppm	0.38	0.56	0.38	0.62	0.51
Li	ppm	10	8	14	12	12
Cs	ppm	1.102	1.005	0.28	1.397	0.876
Rb	ppm	27.48	56.87	16.48	72.46	38.34
Ba	ppm	96	251	178	237	196
Sr	ppm	128.2	149.6	247.4	134.1	126.4
Th	ppm	0.75	2.09	0.86	2.19	1.92
U	ppm	0.253	0.614	0.287	0.675	0.653
La	ppm	8.24	14.4	15.28	11.88	12.56
Ce	ppm	20.74	32.34	38.7	27.09	27.95
Pr	ppm	2.969	4.108	5.368	3.524	3.617
Nd	ppm	13.95	17.29	23.68	15.03	15.26
Sm	ppm	3.82	3.99	5.78	3.77	4.09
Eu	ppm	1.141	1.084	1.354	1.039	0.989
Gd	ppm	4.388	4.424	5.744	4.449	4.946
Tb	ppm	0.747	0.732	0.898	0.754	0.851
Dy	ppm	4.691	4.703	5.512	4.833	5.397
Ho	ppm	0.988	1.019	1.154	1.038	1.17
Er	ppm	2.892	3.071	3.286	3.196	3.504
Tm	ppm	0.42	0.462	0.473	0.487	0.522
Yb	ppm	2.79	3.08	3.01	3.32	3.4
Lu	ppm	0.429	0.477	0.449	0.507	0.527

Sample number	WC04-03, 150.63-150.79	WC04-03, 79.43-79.57	03SJP065-1	03SJP065-1-2	03SJP090-1	WC04-08, 13.10-13.20	
Township	Clifford	Clifford	Clifford	Clifford	Clifford	Clifford	
Easting UTM NAD83	591513	591513	590904	590904	591996	591510	
Northing UTM NAD83	5350066	5350066	5349046	5349046	5350686	5350267	
Phase	BRG Volcanic	BRG Volcanic	BRG Volcanic	BRG Volcanic	BRG Volcanic	BRG Volcanic	
Structural Block	Clifford South	Clifford South	Clifford South	Clifford South	Clifford South	Clifford South	
Rock type	Basalt Lapilli Tuff	Basalt Lapilli Tuff	Basaltic Andesite	Basaltic Andesite	Basaltic Andesite	Basaltic Andesite	
Notes							
	units						
SiO2	wt %	48.68	43.43	56.61	58.29	52.49	58.62
TiO2	wt %	0.58	0.62	0.96	1.04	0.88	0.72
Al2O3	wt %	17.41	16.17	16.69	16.87	15.76	14.92
Fe2O3	wt %	12.31	17.57	7.41	7.16	8.98	6.68
MnO	wt %	0.029	0.032	0.1	0.11	0.15	0.066
MgO	wt %	0.79	1.29	4.42	4.74	6.76	5.26
CaO	wt %	6.23	4.61	5.31	4.36	8.61	5.23
Na2O	wt %	3.64	5.29	4.61	3.88	2.33	3.18
K2O	wt %	2.2	1.1	1.13	1	1.12	1.6
P2O5	wt %	0.12	0.14	0.11	0.12	0.14	0.16
LOI	wt %	6.66	9.39	2.44	2.96	2.85	2.68
Total		98.649	99.642	99.78	100.53	100.07	99.116
Ni	ppm	15	19	68	54	66	114
Cr	ppm	18	53	13.42	11.24	186.33	107
Co	ppm	22	17	36	28	35	46
V	ppm	60	96	193.6	189.3	73.9	103
Sc	ppm	7.5	6.4	17.3	17.3	16.9	13.8
Cu	ppm	841	63	847	491	458	10
Pb	ppm						
Zn	ppm	30	45	144	122	129	85
Cd	ppm	0	0	0	0	0	0
Mo	ppm	0	0	0	0	0	0
W	ppm	11	5	8	5	0	0
S	ppm	-400	-400	-400	-400	88	-400
Nb (XRF)	ppm	9	6	6	7	9	6
Y (XRF)	ppm	32	29	25	26	35	27
Zr (XRF)	ppm	169	171	138	148	152	138
Zr	ppm	182.7	179.1	139.2	147.4	162.7	152.9
Hf	ppm	5.1	4.8	3.9	4	4.1	3.8
Nb	ppm	10	8.1	6	6.4	6.9	6.7
Ta	ppm	1.05	0.86	0.53	0.53	0.52	0.49
Y	ppm	33.49	28.76	24.02	23.51	25.75	28.1
Be	ppm	0.58	0.31	0.55	0.53	0.44	0.48
Li	ppm	4	7	7	12	14	15
Cs	ppm	1.36	0.672	1.003	0.798	1.34	1.001
Rb	ppm	78.72	38.75	40.84	35.69	43.08	57.75
Ba	ppm	247	98	174	163	187	216
Sr	ppm	301.5	141.3	164.9	169.6	236.9	132.2
Th	ppm	6.16	5.99	1.6	1.68	1.3	2.52
U	ppm	2.312	1.264	0.445	0.431	0.35	0.659
La	ppm	21.07	24.23	15.76	12.25	12.98	23.35
Ce	ppm	46.65	50.18	33.36	26.29	29.77	53.01
Pr	ppm	5.508	6.241	4.177	3.4	3.963	6.502
Nd	ppm	21.05	24.3	17.34	14.71	17.33	26.97
Sm	ppm	4.82	5.5	4.12	3.53	4	5.62
Eu	ppm	1.306	1.44	1.282	1.127	1.148	1.134
Gd	ppm	5.103	5.593	4.337	4.033	4.458	5.361
Tb	ppm	0.875	0.892	0.704	0.683	0.726	0.818
Dy	ppm	5.724	5.142	4.445	4.272	4.523	4.996
Ho	ppm	1.262	1.024	0.938	0.915	0.962	1.042
Er	ppm	3.887	2.942	2.793	2.765	2.872	3.079
Tm	ppm	0.587	0.445	0.412	0.416	0.42	0.46
Yb	ppm	4.02	3.09	2.69	2.74	2.76	3.09
Lu	ppm	0.675	0.526	0.41	0.422	0.428	0.477

Sample number	WC04-08, 134.45-134.61	WC04-08, 168.34-168.52	WC04-08, 171.03-171.26	03SJP031-1-1	03SJP053-1	03SJP088-1	
Township	Clifford	Clifford	Clifford	Clifford	Clifford	Clifford	
Easting UTM NAD83	591510	591510	591510	591846	590153	591815	
Northing UTM NAD83	5350267	5350267	5350267	5349969	5348894	5350056	
Phase	BRG Volcanic	BRG Volcanic	BRG Volcanic	BRG Volcanic	BRG Volcanic	BRG Volcanic	
Structural Block	Clifford South	Clifford South	Clifford South	Clifford South	Clifford South	Clifford South	
Rock type	Basaltic Andesite	Basaltic Andesite	Basaltic Andesite	Dacite	Dacite	Dacite- Porphyritic	
Notes	Poor Oxide Closure						
units							
SiO2	wt %	62.44	52.56	53.19	64.44	64.24	65.05
TiO2	wt %	0.43	1.17	1.18	0.49	0.61	0.65
Al2O3	wt %	13.49	15.68	15.08	13.92	15.92	14.73
Fe2O3	wt %	3.32	10.24	11.08	4.76	4.78	6.36
MnO	wt %	0.04	0.12	0.1	0.12	0.04	0.06
MgO	wt %	1.54	6.32	6.53	2.6	1.75	3.39
CaO	wt %	9.16	6.5	5.74	3.93	3.28	2.8
Na2O	wt %	0.31	2.85	3.2	1.02	2.75	3.59
K2O	wt %	3.16	0.87	0.86	3.4	2.76	1.23
P2O5	wt %	0.11	0.21	0.2	0.1	0.11	0.13
LOI	wt %	8.76	2.51	2.69	5.27	3.35	2.55
Total		102.76	99.03	99.85	100.05	99.59	100.54
Ni	ppm	39	121	109	55	11	128
Cr	ppm	28	145	175	45.14	9.62	55.88
Co	ppm	4	23	29	12	6	17
V	ppm	49	175	169	60	68	148.8
Sc	ppm	7.5	18.6	18.1	8.5	8.6	10.2
Cu	ppm	0	15	55	383	33	298
Pb	ppm						
Zn	ppm	27	77	53	145	53	148
Cd	ppm	0	0	0	0	0	0
Mo	ppm	0	0	0	0	0	0
W	ppm	0	0	0	8	9	0
S	ppm	156	-400	-400	-400	-400	-400
Nb (XRF)	ppm	6	5	4	8	9	6
Y (XRF)	ppm	27	25	26	35	36	29
Zr (XRF)	ppm	121	123	115	135	197	133
Zr	ppm	137	132.9	123.7	142.7	198.8	166.3
Hf	ppm	4	3.4	3.2	4.3	5.6	4.6
Nb	ppm	8	6.3	5.9	8	9	8.5
Ta	ppm	0.81	0.38	0.36	0.9	0.91	0.86
Y	ppm	28.95	27.25	25.94	35.33	35.56	35.84
Be	ppm	0.43	0.39	0.39	0.57	0.59	0.7
Li	ppm	15	13	13	16	11	17
Cs	ppm	1.861	0.883	1.315	2.018	1.899	1.013
Rb	ppm	117.27	26.95	20.35	113.24	87.6	48.3
Ba	ppm	419	290	273	210	545	180
Sr	ppm	19.6	178.7	138.2	24.8	94.8	162.1
Th	ppm	5.44	0.84	0.68	5.41	5.39	4.52
U	ppm	1.453	0.222	0.225	1.514	1.476	1.325
La	ppm	2.68	10.29	10.53	20.21	20.23	19.2
Ce	ppm	6.48	25.74	25.32	44.2	43.04	42.58
Pr	ppm	0.887	3.65	3.549	5.496	5.264	5.448
Nd	ppm	4.02	16.6	16.38	22.52	20.75	22.85
Sm	ppm	1.51	4.27	4.06	5.5	4.92	5.27
Eu	ppm	0.377	1.293	1.36	1.219	1.182	1.422
Gd	ppm	2.682	4.786	4.72	5.874	5.277	5.732
Tb	ppm	0.573	0.789	0.776	0.991	0.943	0.96
Dy	ppm	4.136	4.847	4.855	6.148	6.015	6.176
Ho	ppm	0.977	1.03	1.017	1.321	1.309	1.285
Er	ppm	3.171	2.995	2.994	4.037	3.993	3.853
Tm	ppm	0.504	0.443	0.431	0.608	0.606	0.593
Yb	ppm	3.74	2.92	2.84	4.16	4.14	4.08
Lu	ppm	0.623	0.443	0.424	0.665	0.642	0.659

Sample number	P03-001	P03-003	WC04-03, 131.59-131.7	WC04-03, 146.0-146.16	WC04-03, 154.75-154.90	WC04-03, 62.65-62.79	
Township	Clifford	Clifford	Clifford	Clifford	Clifford	Clifford	
Easting UTM NAD83	591319	591335	591513	591513	591513	591513	
Northing UTM NAD83	5349924	5350300	5350066	5350066	5350066	5350066	
Phase	BRG Volcanic	BRG Volcanic	BRG Volcanic	BRG Volcanic	BRG Volcanic	BRG Volcanic	
Structural Block	Clifford South	Clifford South	Clifford South	Clifford South	Clifford South	Clifford South	
Rock type	Dacite- Porphyritic	Dacite- Porphyritic	Dacite Tuff	Dacite Tuff	Dacite Tuff	Dacite Tuff	
Notes							
units							
SiO2	wt %	62.16	65.86	66.18	68.32	69.62	61.38
TiO2	wt %	0.7	0.52	0.6	0.57	0.42	0.62
Al2O3	wt %	15.03	14.3	14.47	14.23	13.1	14.48
Fe2O3	wt %	6.79	5.2	4.63	5.01	3.69	6.28
MnO	wt %	0.05	0.06	0.045	0.041	0.033	0.081
MgO	wt %	3.98	2.56	2.34	2.16	1.59	3.67
CaO	wt %	4.68	4.62	3.56	3.51	4	4.68
Na2O	wt %	4	4.21	4.96	4.26	3.77	3.74
K2O	wt %	1.5	1.35	0.75	0.75	1.1	1.05
P2O5	wt %	0.14	0.11	0.15	0.14	0.11	0.14
LOI	wt %	2.34	1.77	2.44	2	1.99	3.43
Total		101.38	100.56	100.125	100.991	99.423	99.551
Ni	ppm	97	64	33	23	23	87
Cr	ppm	88.57	52.55	29	23	23	162
Co	ppm	14	15	8	8	14	22
V	ppm	99	61.5	58	46	39	95
Sc	ppm	11.9	8.5	10.4	9.4	8.2	11.7
Cu	ppm	777	681	38	34	46	12
Pb	ppm						
Zn	ppm	90	99	71	72	51	88
Cd	ppm	0	0	0	0	0	0
Mo	ppm	0	0	0	0	0	0
W	ppm	0	0	6	3	4	5
S	ppm	-400	59	-400	144	-400	-400
Nb (XRF)	ppm	8	9	6	7	7	5
Y (XRF)	ppm	33	38	36	38	37	30
Zr (XRF)	ppm	152	141	156	143	123	137
Zr	ppm	160.6	147.5	162.6	168.1	144.3	144.3
Hf	ppm	4.2	4.3	4.6	4.7	4.1	3.9
Nb	ppm	7.8	8.6	8.7	8.9	8.5	7.3
Ta	ppm	0.73	0.94	0.81	0.84	0.83	0.63
Y	ppm	32.89	36.23	37.7	39.32	38.68	30.75
Be	ppm	0.68	0.68	0.55	0.58	0.51	0.56
Li	ppm	10	9	11	10	6	14
Cs	ppm	0.916	0.607	0.539	0.608	0.732	0.697
Rb	ppm	69.49	45.97	24.79	28.05	36.44	32.67
Ba	ppm	205	247	101	132	189	227
Sr	ppm	126	133.2	102	130.7	136.6	151.7
Th	ppm	3.36	5.63	4.88	5.3	5.06	3.4
U	ppm	1.035	1.714	1.411	1.536	1.74	0.985
La	ppm	16.53	19.76	15.39	18.69	15.19	17.68
Ce	ppm	36.43	42.06	35.38	42.3	34.02	38.46
Pr	ppm	4.661	5.196	4.569	5.358	4.283	4.892
Nd	ppm	20.02	21.62	19.28	21.96	17.36	20.66
Sm	ppm	4.85	5.17	4.97	5.56	4.51	4.84
Eu	ppm	1.139	1.086	1.124	1.182	1.045	1.125
Gd	ppm	5.229	5.703	5.664	6.237	5.313	5.279
Tb	ppm	0.876	0.96	1.004	1.059	0.974	0.85
Dy	ppm	5.546	6.158	6.454	6.596	6.493	5.37
Ho	ppm	1.18	1.329	1.402	1.426	1.388	1.154
Er	ppm	3.518	4.048	4.32	4.384	4.412	3.452
Tm	ppm	0.541	0.636	0.664	0.682	0.679	0.526
Yb	ppm	3.64	4.4	4.55	4.67	4.62	3.56
Lu	ppm	0.578	0.695	0.716	0.742	0.718	0.559

Sample number	WC04-03, 68.12-68.25	WC04-03, 76.27-76.41	WC04-08, 123.7-123.9	WC04-08, 132.4-132.55	WC04-08, 158.61-158.94	03SJP068-1-1	
Township	Clifford	Clifford	Clifford	Clifford	Clifford	Clifford	
Easting UTM NAD83	591513	591513	591510	591510	591510	591261	
Northing UTM NAD83	5350066	5350066	5350267	5350267	5350267	5348588	
Phase	BRG Volcanic	BRG Volcanic	BRG Volcanic	BRG Volcanic	BRG Volcanic	BRG Volcanic	
Structural Block	Clifford South	Clifford South	Clifford South	Clifford South	Clifford South	Clifford South	
Rock type	Dacite Tuff	Dacite Tuff	Lapilli Tuff	Lapilli Tuff	Lapillistone	Rhyolite	
Notes							
	units						
SiO2	wt %	65.77	62.5	67.15	66.69	67	75.04
TiO2	wt %	0.56	0.62	0.59	0.47	0.51	0.17
Al2O3	wt %	13.31	14.75	14.06	13.97	16.11	12.91
Fe2O3	wt %	6.11	6.89	5.92	4.08	4.85	1.35
MnO	wt %	0.047	0.058	0.051	0.04	0.034	0.03
MgO	wt %	2.25	2.97	1.94	1.95	1.03	0.52
CaO	wt %	3.19	5.58	4.84	3.83	3.23	1.81
Na2O	wt %	3.88	3.49	3.9	3.83	4.9	4.29
K2O	wt %	1.18	0.56	0.53	1.5	1.22	1.67
P2O5	wt %	0.13	0.14	0.14	0.11	0.11	0.06
LOI	wt %	2.88	2.62	1.68	3.77	1.82	2.18
Total		99.307	100.178	100.801	100.24	100.814	100.04
Ni	ppm	41	54	24	32	-4	6
Cr	ppm	48	102	22	27	-8	9.32
Co	ppm	23	22	8	6	6	2
V	ppm	68	78	55	48	-5	4.7
Sc	ppm	10	11.3	9.6	7.7	10.1	2
Cu	ppm	30	8	0	4	0	185
Pb	ppm						
Zn	ppm	63	69	43	35	39	40
Cd	ppm	0	0	0	0	0	0
Mo	ppm	0	0	0	0	0	0
W	ppm	4	3	0	0	0	3
S	ppm	-400	-400	69	165	-400	-400
Nb (XRF)	ppm	7	7	7	7	8	11
Y (XRF)	ppm	34	37	34	42	43	10
Zr (XRF)	ppm	142	153	150	129	280	94
Zr	ppm	154.7	167.6	166.3	152.9	297.8	100.8
Hf	ppm	4.3	4.5	4.7	4.4	8	3
Nb	ppm	8	8.4	8.9	8.6	12.3	11.5
Ta	ppm	0.75	0.74	0.84	0.86	0.96	0.96
Y	ppm	34.41	39.83	36.07	44.64	45.35	10.28
Be	ppm	0.46	0.59	0.56	0.51	0.78	0.59
Li	ppm	9	13	9	14	6	7
Cs	ppm	0.523	0.393	0.41	0.958	0.666	0.756
Rb	ppm	38.57	20.14	18.28	52.65	34.02	57.87
Ba	ppm	141	82	66	262	520	449
Sr	ppm	124	261	189.2	68	178.4	95.1
Th	ppm	4.4	4.28	5.18	5.58	5.37	3.71
U	ppm	1.326	1.373	1.447	1.661	1.37	1.063
La	ppm	13.05	20.52	14.31	25.83	25.66	16.54
Ce	ppm	30.4	45.5	33.22	55.48	56.3	33.58
Pr	ppm	3.894	5.743	4.217	7.052	7.11	3.852
Nd	ppm	15.84	23.65	17.24	29.65	29.69	14
Sm	ppm	4.2	5.72	4.41	7.52	6.99	2.49
Eu	ppm	1.074	1.232	0.965	1.733	1.731	0.549
Gd	ppm	4.903	6.338	5.155	8.33	7.645	2.127
Tb	ppm	0.897	1.083	0.915	1.333	1.263	0.319
Dy	ppm	5.84	6.846	6.091	7.871	8.044	1.796
Ho	ppm	1.261	1.447	1.344	1.602	1.713	0.355
Er	ppm	3.916	4.414	4.204	4.631	5.288	1.098
Tm	ppm	0.607	0.675	0.663	0.7	0.815	0.166
Yb	ppm	4.13	4.55	4.55	4.8	5.51	1.15
Lu	ppm	0.647	0.714	0.709	0.718	0.865	0.178

Sample number	03SJP068-36	03SJP112-1	03SJP84-1	03SJP037-1	03SJP109-2-1	03SJP080-1-1	03SJP110-2	
Township	Clifford	Ben Nevis	Ben Nevis	Ben Nevis	Ben Nevis	Ben Nevis	Ben Nevis	
Easting UTM NAD83	591261	593182	592470	592278	593437	592497	593171	
Northing UTM NAD83	5348588	5350691	5350306	5350685	5350948	5349867	5350838	
Phase	BRG Volcanic	BRG High-level Synvolc Intrusion	BRG Intrusion	BRG Intrusion	BRG Intrusion	BRG Intrusion	BRG Intrusion	
Structural Block	Clifford South	Clifford South	Clifford South	Clifford South	Clifford South	Clifford South	Clifford South	
Rock type	Rhyolite	Diabase/Diorite	Diabase- synvolcanic	Granodiorite	Granodiorite	Leucogabbro	Leucogabbro	
Notes								
units								
SiO2	wt %	70.4	49.92	51.05	71.32	65.54	52.67	51.52
TiO2	wt %	0.4	1.16	1.24	0.43	0.5	0.56	1.21
Al2O3	wt %	14.93	14.88	15.92	13.63	15.42	9.23	15.5
Fe2O3	wt %	1.89	11.77	11.8	3.98	5.37	10.92	11.39
MnO	wt %	0.02	0.16	0.19	0.05	0.09	0.16	0.17
MgO	wt %	0.35	7.65	6.42	0.4	2.3	14.67	6.51
CaO	wt %	2.15	7.45	7.51	1.55	2.83	4.44	8.01
Na2O	wt %	6.27	1.87	1.7	4.88	5.32	1.65	2.02
K2O	wt %	1.85	0.28	0.38	2.76	1.1	0.32	0.69
P2O5	wt %	0.07	0.14	0.18	0.09	0.1	0.09	0.18
LOI	wt %	1.11	5.77	4.3	1.18	2.09	4.22	3.62
Total		99.45	101.05	100.69	100.27	100.66	98.93	100.8
Ni	ppm	5	167	179	7	67	463	36
Cr	ppm	9.04	172.69	147.02	10.23	37.41	-400	167.24
Co	ppm	2	43	38	4	17	56	43
V	ppm	4	150.3	172.2	0	105.5	113.4	64.7
Sc	ppm	6.4	18.7	18.7	8.4	8.9	18.3	20.1
Cu	ppm	89	110	442	34	490	167	114
Pb	ppm							
Zn	ppm	22	130	103	33	210	112	86
Cd	ppm	0	0	0	0	0	0	0
Mo	ppm	0	0	0	0	0	0	0
W	ppm	0	5	0	8	3	0	0
S	ppm	-400	92	191	45	53	58	126
Nb (XRF)	ppm	10	6	5	10	8	5	8
Y (XRF)	ppm	39	27	23	39	8	16	30
Zr (XRF)	ppm	247	117	105	237	120	93	170
Zr	ppm	250.8	108.9	142.6	245.7	175.4	97.4	122.6
Hf	ppm	7.1	2.9	3.7	6.8	5	2.5	3.2
Nb	ppm	9.9	4.9	6.4	10.2	7.4	3.9	5.8
Ta	ppm	0.96	0.36	0.45	0.88	0.75	0.34	0.41
Y	ppm	38.67	23.24	30.11	39.35	30.6	15.99	27.27
Be	ppm	0.78	0.36	0.4	0.71	0.66	0.28	0.55
Li	ppm	3	20	19	4	17	14	25
Cs	ppm	0.489	0.61	0.783	0.483	0.393	2.418	0.589
Rb	ppm	32.28	8.56	11.96	44.69	25.93	13.02	19.07
Ba	ppm	795	76	101	796	327	99	244
Sr	ppm	72.3	161.7	173.1	99	173.6	95.7	218.1
Th	ppm	5.62	0.58	0.79	4.54	4.21	0.85	0.7
U	ppm	1.362	0.163	0.216	1.168	1.105	0.228	0.194
La	ppm	25.73	7.77	10.26	22.66	21.2	8.25	9.21
Ce	ppm	54.4	19.79	25.84	49.43	44.91	18.49	23.86
Pr	ppm	6.595	2.962	3.743	6.191	5.413	2.411	3.453
Nd	ppm	26.86	13.85	17.47	25.78	22.36	10.22	16.36
Sm	ppm	6.23	3.53	4.68	6.28	5.02	2.51	4.27
Eu	ppm	1.336	1.297	1.151	1.363	0.85	0.707	1.069
Gd	ppm	6.7	4.24	5.305	6.744	5.39	2.783	4.919
Tb	ppm	1.105	0.678	0.87	1.148	0.886	0.456	0.808
Dy	ppm	7.012	4.27	5.456	7.127	5.53	2.847	4.957
Ho	ppm	1.491	0.896	1.133	1.508	1.163	0.618	1.065
Er	ppm	4.463	2.577	3.23	4.527	3.494	1.843	3.049
Tm	ppm	0.69	0.379	0.475	0.684	0.534	0.273	0.438
Yb	ppm	4.84	2.48	3.14	4.61	3.6	1.89	2.84
Lu	ppm	0.744	0.378	0.478	0.705	0.561	0.303	0.436

Sample number	WC04-03, 212.49-212.63	WC04-08, 176.74-176.96	WC04-04, 166.52-166.67	WC04-04, 130.88-131.04	WC04-04, 51.62-51.92	
Township	Clifford	Clifford	Clifford	Clifford	Clifford	
Easting UTM NAD83	591513	591510	591517	591517	591517	
Northing UTM NAD83	5350066	5350267	5349643	5349643	5349643	
Phase	BRG Intrusion	BRG Intrusion	BRG Intrusion	BRG Intrusion	BRG Intrusion	
Structural Block	Clifford South	Clifford South	Clifford South	Clifford South	Clifford South	
Rock type	Diorite	Diorite	Granodiorite	Leucogabbro	Leucogabbro	
Notes						
	units					
SiO2	wt %	57.74	58.74	65.14	53.28	53.47
TiO2	wt %	0.95	0.78	0.67	1.24	1.17
Al2O3	wt %	12.19	16.19	11.48	15.94	15.69
Fe2O3	wt %	10.09	7.36	6.41	9.13	10.04
MnO	wt %	0.112	0.119	0.059	0.092	0.09
MgO	wt %	6.15	4.58	5.06	6.96	7.2
CaO	wt %	5.87	5.64	4.22	4.92	3.5
Na2O	wt %	0.98	3.66	2.04	3.22	3.08
K2O	wt %	0.4	0.84	0.81	1.33	0.85
P2O5	wt %	0.19	0.17	0.15	0.22	0.2
LOI	wt %	4.95	1.67	3.37	3.11	4.88
Total		99.622	99.749	99.409	99.442	100.17
Ni	ppm	160	98	120	125	108
Cr	ppm	190	90	177	181	154
Co	ppm	31	20	21	29	30
V	ppm	152	136	88	156	191
Sc	ppm	16.3	12.9	12	18.4	14.7
Cu	ppm	583	33	509	654	844
Pb	ppm					
Zn	ppm	204	63	140	88	106
Cd	ppm	0	0	0	0	0
Mo	ppm	0	0	0	13	0
W	ppm	2	0	4	6	9
S	ppm	-400	203	-400	-400	-400
Nb (XRF)	ppm	5	5	5	6	5
Y (XRF)	ppm	22	25	18	25	29
Zr (XRF)	ppm	102	159	99	136	123
Zr	ppm	110.5	163	107.3	145.6	127.8
Hf	ppm	2.8	4.1	2.8	3.7	3.3
Nb	ppm	5.2	6.6	5.2	6.8	6.2
Ta	ppm	0.32	0.48	0.32	0.42	0.38
Y	ppm	22.53	24.8	17.03	25.82	24.9
Be	ppm	0.58	0.43	0.46	0.51	0.52
Li	ppm	32	9	22	23	34
Cs	ppm	0.527	0.96	0.509	1.641	1.403
Rb	ppm	14.76	23.29	22.29	55.62	31
Ba	ppm	47	138	62	156	115
Sr	ppm	268.2	167.2	233	220.8	215.8
Th	ppm	0.65	1.85	0.94	0.89	0.78
U	ppm	0.258	0.487	0.457	0.625	0.564
La	ppm	10.94	14.66	9.83	11.08	8.79
Ce	ppm	26.8	32.85	24.39	27.36	22.64
Pr	ppm	3.719	4.128	3.381	3.915	3.354
Nd	ppm	16.67	17.42	14.8	18.11	15.7
Sm	ppm	4.07	4.05	3.52	4.61	4.21
Eu	ppm	1.2	1.118	0.862	1.288	1.058
Gd	ppm	4.331	4.38	3.538	5.065	4.847
Tb	ppm	0.665	0.701	0.553	0.812	0.795
Dy	ppm	4.094	4.269	3.173	4.823	4.82
Ho	ppm	0.84	0.911	0.642	0.999	1.015
Er	ppm	2.457	2.697	1.858	2.905	2.956
Tm	ppm	0.355	0.41	0.264	0.427	0.434
Yb	ppm	2.35	2.71	1.72	2.83	2.83
Lu	ppm	0.366	0.421	0.262	0.436	0.417

Sample number	WC04-04, 70.65-70.84	WC04-08, 227.76-227.93	WC04-08, 236.47-236.52	
Township	Clifford	Clifford	Clifford	
Easting UTM NAD83	591517	591510	591510	
Northing UTM NAD83	5349643	5350267	5350267	
Phase	BRG Intrusion	BRG Intrusion	BRG Intrusion	
Structural Block	Clifford South	Clifford South	Clifford South	
Rock type	Leucogabbro	Leucogabbro	Leucogabbro	
Notes				
	units			
SiO2	wt %	52.67	51.84	54.2
TiO2	wt %	1.14	1.25	1.17
Al2O3	wt %	15.76	16.17	14.94
Fe2O3	wt %	9.14	10.7	9.08
MnO	wt %	0.109	0.097	0.095
MgO	wt %	6.95	6.31	6.16
CaO	wt %	6.48	8.36	7.87
Na2O	wt %	2.23	2.41	3.76
K2O	wt %	2.19	1.28	0.63
P2O5	wt %	0.18	0.21	0.2
LOI	wt %	2.64	2.14	1.83
Total		99.489	100.767	99.935
Ni	ppm	136	99	91
Cr	ppm	189	135	158
Co	ppm	31	21	16
V	ppm	162	167	177
Sc	ppm	18.5	19	18.3
Cu	ppm	271	41	0
Pb	ppm			
Zn	ppm	70	62	61
Cd	ppm	0	0	0
Mo	ppm	0	0	0
W	ppm	5	0	0
S	ppm	-400	155	111
Nb (XRF)	ppm	5	6	5
Y (XRF)	ppm	26	27	28
Zr (XRF)	ppm	124	127	120
Zr	ppm	130.8	138.9	129
Hf	ppm	3.2	3.5	3.3
Nb	ppm	6	6.4	6.2
Ta	ppm	0.38	0.38	0.37
Y	ppm	26.05	28.31	29
Be	ppm	0.48	0.39	0.48
Li	ppm	10	13	6
Cs	ppm	1.872	1.816	0.922
Rb	ppm	99.64	61.62	22.25
Ba	ppm	225	153	69
Sr	ppm	159.1	170.6	225
Th	ppm	0.78	0.79	0.83
U	ppm	0.303	0.194	0.624
La	ppm	10.47	9.1	7.42
Ce	ppm	25.87	24.14	18.11
Pr	ppm	3.722	3.506	2.674
Nd	ppm	17.03	16.54	13.06
Sm	ppm	4.31	4.25	4.02
Eu	ppm	1.274	1.048	1.141
Gd	ppm	4.755	4.719	4.967
Tb	ppm	0.78	0.783	0.858
Dy	ppm	4.769	4.926	5.418
Ho	ppm	0.999	1.058	1.152
Er	ppm	2.94	3.153	3.367
Tm	ppm	0.424	0.465	0.493
Yb	ppm	2.8	3.07	3.22
Lu	ppm	0.424	0.467	0.486

Metric Conversion Table

Conversion from SI to Imperial			Conversion from Imperial to SI		
<i>SI Unit</i>	<i>Multiplied by</i>	<i>Gives</i>	<i>Imperial Unit</i>	<i>Multiplied by</i>	<i>Gives</i>
LENGTH					
1 mm	0.039 37	inches	1 inch	25.4	mm
1 cm	0.393 70	inches	1 inch	2.54	cm
1 m	3.280 84	feet	1 foot	0.304 8	m
1 m	0.049 709	chains	1 chain	20.116 8	m
1 km	0.621 371	miles (statute)	1 mile (statute)	1.609 344	km
AREA					
1 cm ²	0.155 0	square inches	1 square inch	6.451 6	cm ²
1 m ²	10.763 9	square feet	1 square foot	0.092 903 04	m ²
1 km ²	0.386 10	square miles	1 square mile	2.589 988	km ²
1 ha	2.471 054	acres	1 acre	0.404 685 6	ha
VOLUME					
1 cm ³	0.061 023	cubic inches	1 cubic inch	16.387 064	cm ³
1 m ³	35.314 7	cubic feet	1 cubic foot	0.028 316 85	m ³
1 m ³	1.307 951	cubic yards	1 cubic yard	0.764 554 86	m ³
CAPACITY					
1 L	1.759 755	pints	1 pint	0.568 261	L
1 L	0.879 877	quarts	1 quart	1.136 522	L
1 L	0.219 969	gallons	1 gallon	4.546 090	L
MASS					
1 g	0.035 273 962	ounces (avdp)	1 ounce (avdp)	28.349 523	g
1 g	0.032 150 747	ounces (troy)	1 ounce (troy)	31.103 476 8	g
1 kg	2.204 622 6	pounds (avdp)	1 pound (avdp)	0.453 592 37	kg
1 kg	0.001 102 3	tons (short)	1 ton (short)	907.184 74	kg
1 t	1.102 311 3	tons (short)	1 ton (short)	0.907 184 74	t
1 kg	0.000 984 21	tons (long)	1 ton (long)	1016.046 908 8	kg
1 t	0.984 206 5	tons (long)	1 ton (long)	1.016 046 90	t
CONCENTRATION					
1 g/t	0.029 166 6	ounce (troy)/ ton (short)	1 ounce (troy)/ ton (short)	34.285 714 2	g/t
1 g/t	0.583 333 33	pennyweights/ ton (short)	1 pennyweight/ ton (short)	1.714 285 7	g/t

OTHER USEFUL CONVERSION FACTORS

	<i>Multiplied by</i>	
1 ounce (troy) per ton (short)	31.103 477	grams per ton (short)
1 gram per ton (short)	0.032 151	ounces (troy) per ton (short)
1 ounce (troy) per ton (short)	20.0	pennyweights per ton (short)
1 pennyweight per ton (short)	0.05	ounces (troy) per ton (short)

Note: Conversion factors which are in bold type are exact. The conversion factors have been taken from or have been derived from factors given in the Metric Practice Guide for the Canadian Mining and Metallurgical Industries, published by the Mining Association of Canada in co-operation with the Coal Association of Canada.

ISSN 0826-9580
ISBN 0-7794-7793-6

